A Comparison between the Mechanical Behaviors of Different Equine Articular Cartilage Surfaces

by

Hyeon Lee

A thesis submitted to the Graduate Faculty of
Auburn University
in partial fulfillment of the
requirements for the Degree of
Master of Science

Auburn, Alabama
August 3, 2013

Keywords: articular cartilage, stiffness, thickness, equine joint

Approved by

Robert L. Jackson, Chair, Associate Professor of Mechanical Engineering
R. Reid Hanson, Professor of Clinical Sciences
Nels H. Madsen, Professor of Mechanical Engineering and Associate Dean for Assessment & Special Programs

Abstract

In order to determine the stiffness and thickness of the equine articular cartilage, an indentation test and needle probe test were performed on fresh equine articular cartilage surfaces from the fetlock, carpal, and stifle joints. The results demonstrated that the stiffness and thickness vary on different joints showing different mechanical behavior.

120 and 87 samples were used in the stiffness and thickness measurement. They were cultivated from fetlock, carpal, and stifle joints of 24 deceased, half of which were measured within 20 hours of death. After approximately three minutes of exposure to air during dissecting, all cartilage samples were preserved in a saline solution to keep the articular cartilage hydrated for testing.

In the indentation test, a flat-ended cylindrical indenter is lowered at a constant rate for 20 seconds until the indentation depth reaches 0.2mm (velocity of 10μm/s). The test was performed on three different locations on the same sample. The stiffness of the cartilage was determined by fitting cubic equations to the force versus indentation depth curves obtained from the tests. Afterwards, the stiffness values of the fetlock, carpal, and stifle joints were compared in magnitude throughout the test. Four different surfaces in the fetlock and four in the carpal joint were also compared. It was shown that the articular cartilage of the fetlock is stiffer than the carpal and stifle joint. The average stiffness of the fetlock, carpal, and stifle joint are 46.1N/mm, 20.5N/mm, and 2.73N/mm, respectively. The coefficients of the cubic equations for the joints

were statistically compared as well using the student *t*-test. The differences of some coefficients between the fetlock, carpus, and stifle were "very highly significant" ($p<0.001$). Four different surfaces in the fetlock and four in carpal joint were compared as well. The front lateral, front medial, rear lateral, and rear medial cartilage surfaces in the fetlock were not significantly different in stiffness. In the carpus, the distal radius and proximal radial carpal bone articular cartilage surfaces showed visually different stiffness from the others, while the distal radial carpal bone and proximal third carpal bone articular cartilage surfaces possessed similar stiffness values. The cartilage surfaces from the radiocarpal joint were stiffer than the midcarpal joint. Clear trends in the correlations between stiffness and weight as well as stiffness and age of the horse were not observed.

The needle probe test and analysis of the test data were implemented based on the established methodology from existing literature. The thickness of the articular cartilages from the fetlock, carpal, and stifle joints were measured. The needle is lowered at a velocity of 20μm/s until the measured force exceeds 2.5N. The thickness was measured on five different spots on the same sample. In the same manner as the stiffness measurement, the thicknesses of the fetlock, carpus, and stifle were compared. The articular cartilage of the stifle was thicker than the fetlock and carpus, while the fetlock and the carpus had similar thickness values. The average thickness of the fetlock, carpal, and stifle joint are 0.86mm, 0.87mm, and 2.1mm, respectively. They were statistically compared using the student t-test as well. The differences on the articular cartilage thicknesses between the fetlock and stifle, and carpus and stifle were "very highly significant" ($p<0.001$). This indicates that the articular cartilage thickness of the stifle is significantly different from that of the fetlock and carpus. Four different surfaces in the fetlock and four in carpal joint were also compared. The front lateral, front medial, rear lateral, and rear medial

fetlock cartilage surfaces possessed thicknesses on 0.87mm, 0.81mm, 0.89mm, and 0.87mm, respectively. Significant difference between the four surfaces was not observed. In the carpus, the difference in thickness between the distal radius and proximal third carpal bone articular cartilage surfaces as well as the proximal radial carpal bone and distal radial carpal bone articular cartilage surfaces were statistically significant. The difference between the proximal radial carpal bone (the thickest in the carpus) and proximal third carpal bone articular cartilage surfaces (the thinnest in the carpus) was highly significant. The cartilage thicknesses of the distal radius, proximal radial carpal bone, distal radial carpal bone, and proximal third carpal bone articular cartilage surfaces were 0.92mm, 0.99mm, 0.80mm, and 0.76mm, respectively. It is demonstrated that cartilage surfaces from the radiocarpal joint were thicker than the midcarpal joint.

It is believed that the different mechanisms between various joints cause the different mechanical properties. Various factors were considered as the possible reasons for the different mechanism in different joints, such as: joint type, pressure distribution in the forelimb and hindlimb, composition of the articular cartilage, proximity to the body, and different geometries such as size and shape of the surface.

Acknowledgements

The author would like to acknowledge the priceless support and guidance of Dr. Robert Jackson and Dr. Reid Hanson whose exceptional expertise made this project possible. Gratitude must also be extended to our cartilage research team members from Mechanical Engineering and the College of Veterinary Medicine, namely Grant Kirkland, Ryan Whitmore, Will Campbell, Colton Stinson, Hamed Ghaednia, Hannah Young, Kelcie Theis, Chad Malpass, Joy Waldrop, Dayton Schleicher, and Ashton Richardson. Thanks to their exceptional efforts, this research was possible. The author would also like to acknowledge the financial support of the Auburn University Intramural Grant Program, the Auburn University Undergraduate Research Fellowship Program, and the Merial-NIH Veterinary Scholar Program. The author is grateful for the love and support of his parents, Youngchun and Youngran Lee, as well as his brother Hyunho in Korea. This achievement would be impossible without their trust and ceaseless encouragement. The author would like to extend thanks to all his friends for their constant support and encouragement. Finally, the author would like to thank Matthew Nichols for his editorial assistance to the author.

Table of Contents

List of Figures

List of Tables

List of Terms

Abbreviations and Acronyms

PG	proteoglycan
GAG	glycosaminoglycan
GalNAc	N-acetylgalactosamine
FCD	fixed charge density
PRG4	proteoglycan 4
EHL	elastohydrodynamic lubrication
PMT	proximal medial trochlear
LT	lateral trochlear
DMT	distal medial trochlear
PMC	proximal medial condyle
DMC	distal medial condyle
C1	distal radius articular cartilage surface
C2	proximal radial carpal bone articular cartilage surface

C3	distal radial carpal bone articular cartilage surface
C4	proximal third carpal bone articular cartilage surface

Equation Symbols

F	force
d	displacement
k	stiffness
d_{max}	designated indentation depth, 0.2mm

1. Introduction

1.1 Motivation

The reliability and efficiency of the various joints in human and animal anatomy are affected by friction, wear, and lubrication of articular cartilage surfaces [1-14]. Excessive friction, wear, and poor lubrication play a major role in the development and progression of osteoarthritis leading to the development of severe joint pain, immobility, and loss of function for the patient. Surgical replacement of the joint or joints is a common palliative procedure performed to return the patient to a productive life style.

Rates of primary and revision hip and knee arthroplasties have increased from 1996 to 2005 [15, 16]. For the primary knee replacement, the rate of increase for the last three years had become steeper. Still the rates are constantly increasing as aging of the population has accelerated. According to a survey by Kurtz et al. [17], the median and average rates of total (primary and revision) knee replacement were 149 and 175 procedures/100,000 population around the world, respectively. The rates are believed to be greater considering the patients who are out of medical coverage. Furthermore, the total cost to be paid individually for a total knee replacement is approximately 22,000 dollars [18]. The annual direct and indirect costs for bone and joint health are 950 billion dollars, or 7.4% of the gross domestic product [18]. Much work has been directed toward studying the tribological performance of artificial joints [2, 6, 9, 12, 19, 20] to increase their life span. However, the materials (metals, ceramics, and polymers) currently used in artificial joints are still mechanically different from the actual biomaterials in a human joint.

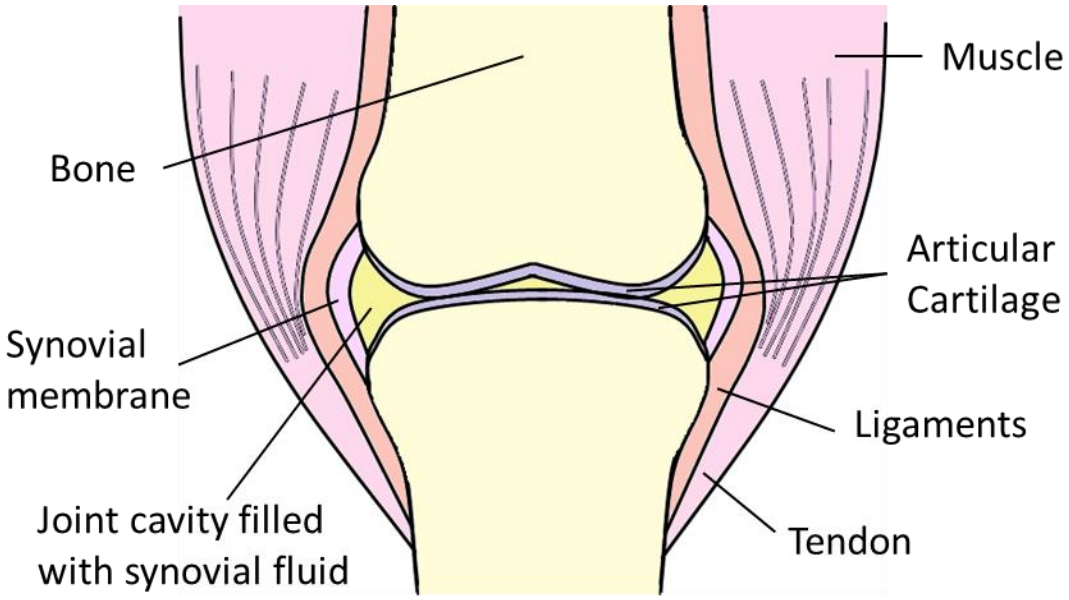

Figure 1.1: Normal synovial joint

Currently, most artificial joints are designed by choosing a combination of hard surfaces that reduce the amount of wear [1, 12, 14]. In contrast, as shown in Figure 1.1, a typical joint usually has a softer layer of cartilage and other materials separating the hard bone on opposite sides of the joint. Recent approaches to the design of joints use softer materials such as hydrogels [14, 21-27]. Other approaches include living articular cartilage transplants [28] that are more similar to the mechanical properties of articular cartilage to replace joint surfaces. These techniques still require significant advancements to become viable options for joint replacement.

1.2 Hypothesis and Objectives

A thorough understanding of the surface interactions of articular cartilage that will allow quantitative predictions and optimal design is lacking because we do not quantitatively understand the mechanics of articular cartilage joint surfaces. By measuring the properties of

normal articular cartilage under different loads and motions, the findings from this study will be helpful to create new biomimetic self-adapting artificial joint surfaces. As the first step of the quantitative understanding, the objective of this work is to determine the stiffness and thickness of equine articular cartilage in different joints. The hypothesis is that equine articular cartilage properties vary on different joints in relation to loading and motion.

2. Background

A detailed study of the material handled in research must precede testing, as in any scientific field; but this step is even more significant in tribology because friction, wear and lubrication depend critically on the materials of the interacting surfaces. Hence, the literature concerning the articular cartilage itself was scrupulously reviewed from the various perspectives of biology, chemistry, etc. because of its complexity as a biomaterial. This chapter will also introduce articular cartilage and various studies about it, such as its structure and composition, popular theories accounting for its system and mechanism, and both previous and current scientists' efforts to understand its behavior.

2.1 What is articular cartilage?

2.1.1 Articular Cartilage

Cartilage is a supple connective tissue found in various body parts of humans and animals such as the knees, ears, nose, and rib cage. Specifically, articular cartilage is located at the end of the bone in a synovial joint capsule (Figure 2.1). It is a thin layer whose color is opaque white, although it appears somewhat pink because of the penetrating color from the vessels in subchondral bone. The thickness of the articular cartilage varies depending on the animal species and the specific joint from which it was extracted. Thickness measurements of the equine articular cartilage on several joints are described in this work.

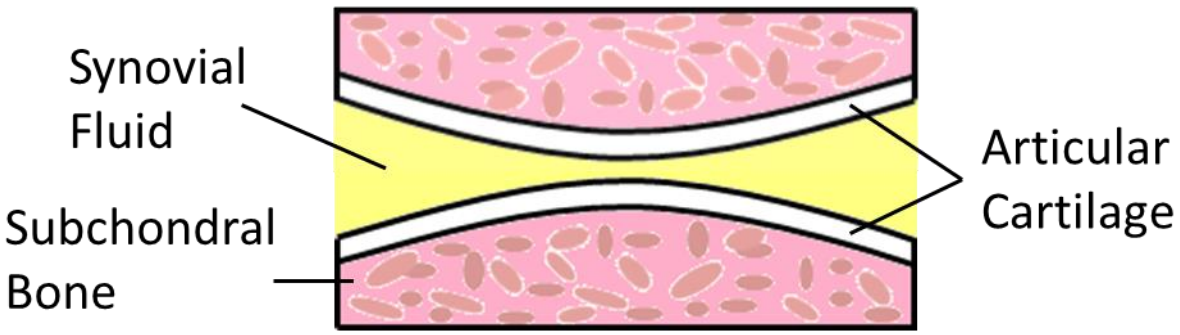

Figure 2.1: Articular cartilage and synovial fluid

Although there are other components of a joint, the condition of the articular cartilage surface generally defines the overall health of the joint because it plays a critical role in joint performance. It enables the synovial structures of the joint to move in a nearly frictionless condition. Moreover, it is the central structure associated with various mechanical, physiological, and biochemical functions of the synovial joint essential to maintenance of this exquisite system's unique structure and composition [29-31].

2.1.2 Cartilage structure and components

The cartilage extracellular matrix provides the basic foundation of cartilage (Figure 2.2) and consists of a variety of components. Collagens, proteoglycan (PG), and water are the three principal components (in terms of volume) among others that constitute the sophisticated extracellular matrix [32].

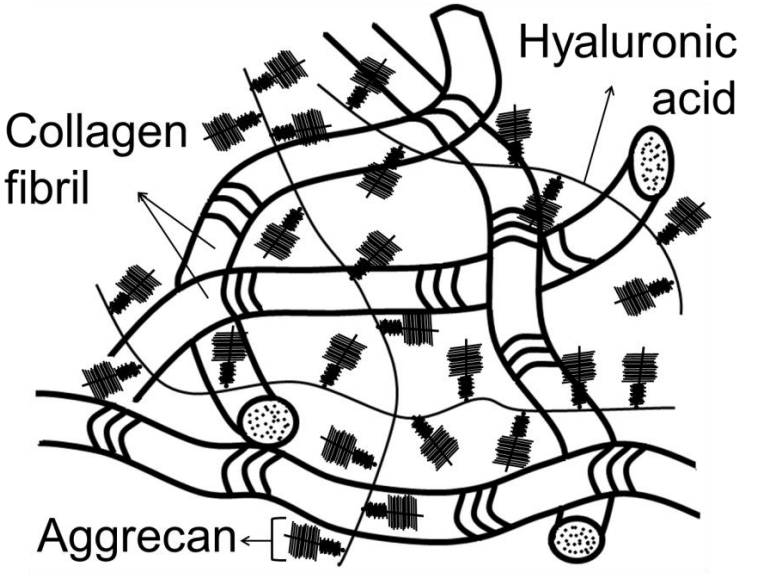

Figure 2.2: Organization of the articular cartilage matrix components

Water accounts for approximately 75% of the wet weight, while collagen (mainly type II) and proteoglycan are responsible for 50% and 35% of the dry weight, respectively [30]. Water is also the most dominant ingredient of synovial fluid produced by the synovial membrane (Figure 1.2). The synoviocytes from an intimal layer of the synovial membrane are believed to produce the synovial fluid components. As a lubricant, the synovial fluid with the cartilage reduces friction and wear between two ends of the bones to almost zero. It also supplies nutrients to cartilage and carries detritus in the joint capsule. The collagens function as the basic framework around which other components are settled, much like a tree trunk as shown in Figure 2.2. In addition, the collagen network plays a major role among solid components of the matrix in supporting external loads. It counteracts the compressive and shear stresses generated by the external loads.

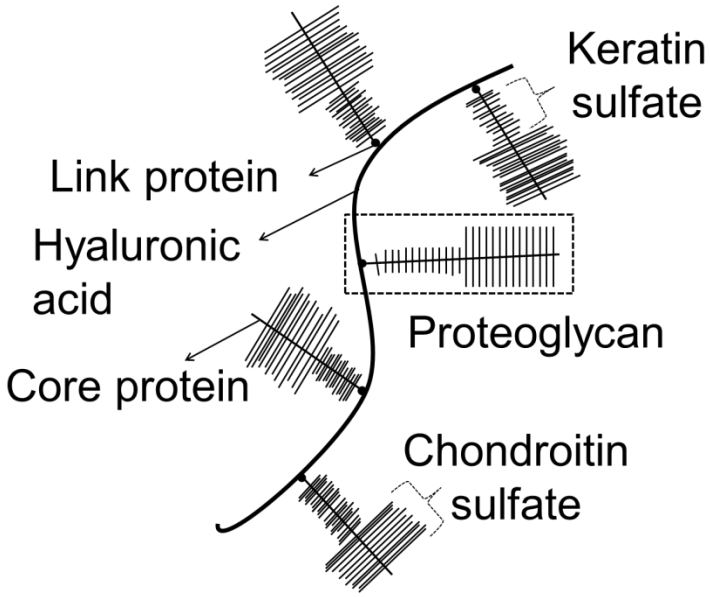

Figure 2.3: An aggrecan

Besides these main components, the extracellular matrix is composed of various other substances such as hyaluronic acid (hyaluronan or sodium hyaluronate), chondroitin sulfate, keratin sulfate, as well as core and link proteins. The hyaluronic acid that is connected to the collagen trunk by a link protein is spread out like a limb for many branches as shown in Figure 2.2. On the base of the hyaluronic acid, the core protein is like a branch with many leaves, a series of generally one hundred or more chondroitin and keratin sulfate chains as shown in Figure 2.3. The complex assembly of a core protein and the surrounding glycosaminoglycan (GAGs) (made up of three main molecules: chondroitin-4-sulfate, chondroitin-6-sulfate, and keratin sulfate), is called a proteoglycan (PG), which is responsible for approximately 35% on a dry weight [30]. The chondroitin and keratin sulfates in PG that are highly negatively charged repel each other, generating positive pressure (called Donnan osmotic pressure) against loading with interacting mobile ions around it in the interstitial fluid [33]. According to previous research, this high pressure supports 50% ~ 85% of the external force [34-36]. Also it is considered that initial load application is supported by only the fluid pressure without support of the solid matrix

[37]. Furthermore, these sulfates attract water, retaining hydration and the stiffness of the cartilage. The chondroitin sulfate consists of a chain of sugars that are glucuronic acid and N-acetylgalactosamine (GalNAc).

There are cells called chondrocytes found in only healthy cartilage as shown in Figure 2.4. They produce various substances which form and maintain the cartilage matrix. The volumetric ratio of the cells to the cartilage is 1% to 12% [29, 30] which is a smaller proportion than other tissues. However, the chondrocyte manufactures most components of the cartilage mentioned above: the hyaluronic acid, PG, chondroitin and keratin sulfates, and the link and core proteins. If the number of chondrocytes decrease or their function deteriorates, it influences other components, leading to destruction of the aggrecan (Figure 2.3) complex resulting in the inability of the matrix to retain water that results in the malfunction of the cartilage and finally the whole joint. In other words, the properties and function of the cartilage matrix rely primarily on the activities of the chondrocytes.

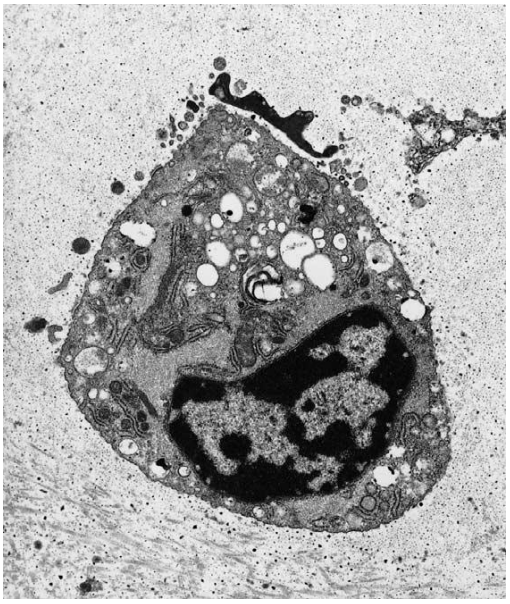

Figure 2.4: A normal chondrocyte [38]

The articular cartilage is often compared to sponge because of their structural similarity. Healthy articular cartilage that contains synovial fluid is like a sponge impregnated with water (Figure 2.5). Indeed, the collagen fibrils are submerged in a gel of GAGs and water. In contrast, as a body gets older, the articular cartilage becomes unhealthy like a dried sponge without water. Since the ability of the cartilage matrix to retain synovial fluid decreases, the cartilage gets dehydrated. Eventually, the dehydrated cartilage causes poor lubrication in the joint, triggering arthropathia on the joint.

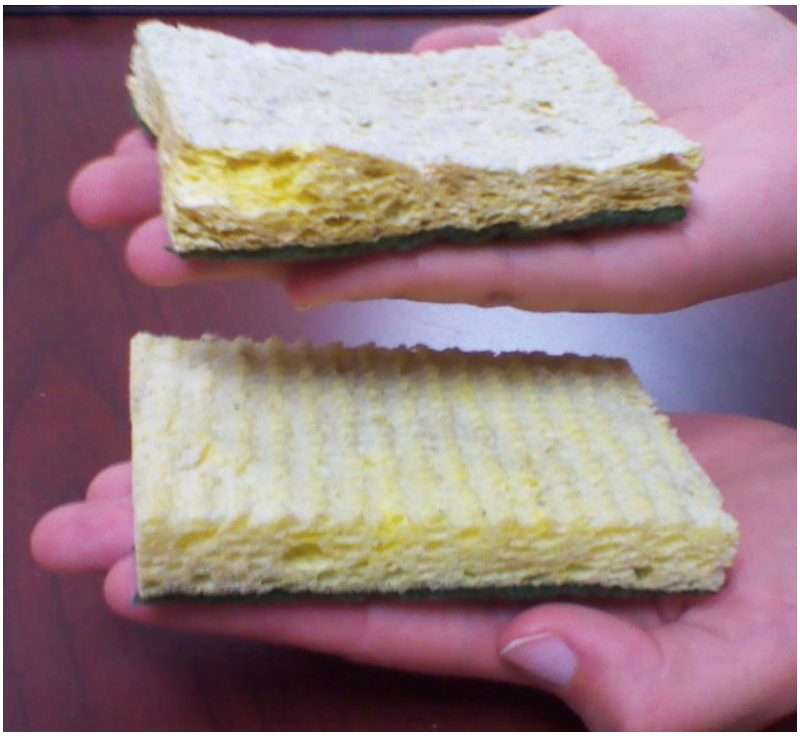

Figure 2.5: A dehydrated sponge and a sponge impregnated with water from top to bottom

The tissue is subdivided into four adjacent zones based on the chondrocytes and collagen orientation throughout the thickness: superficial (tangential), intermediate (transitional), deep (radiate), and calcified as shown in Figure 2.6. The highest density of chondrocytes that are arranged tangentially to the surface is found in the superficial zone. The long axes of the discoid

cells are parallel to the joint surface. The collagen here are also oriented parallel with the surface and are packed most densely. In the intermediate zone, larger and elliptical cells without the regular orientation are observed. The deep zone is characterized by the largest spheroidal cells that are oriented perpendicular to the surface. The calcified zone has mineralized cells and a matrix containing the calcium salts [29, 30].

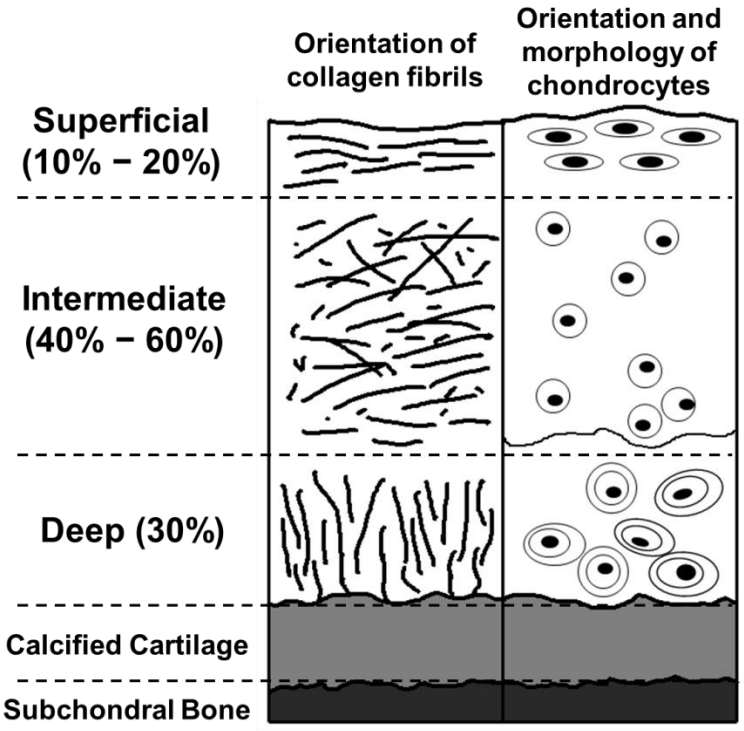

Figure 2.6: Zonal classification of the articular cartilage by the predominant orientation of collagen fibrils and chondrocytes

2.2. Basic theories for the cartilage mechanism

Based on the idea that the articular cartilage consists of the cartilage matrix and synovial fluid, Mow and his coworkers [39-41] had established the biphasic theory. It is both a basic and popular theory to explain the cartilage system. According to the biphasic theory, cartilage is

divided into two principal phases: a solid and fluid phase as shown in Figure 2.7. The solid phase is the mesh which consists predominantly of collagens with the tangled proteoglycans. The fluid phase consists of the interstitial fluid which is mainly water flowing through the solid phase. The mechanical properties of cartilage are characterized by this multiphasic nature based on the assumption that the cartilage matrix behaves linear elastically and is isotropic homogeneous.

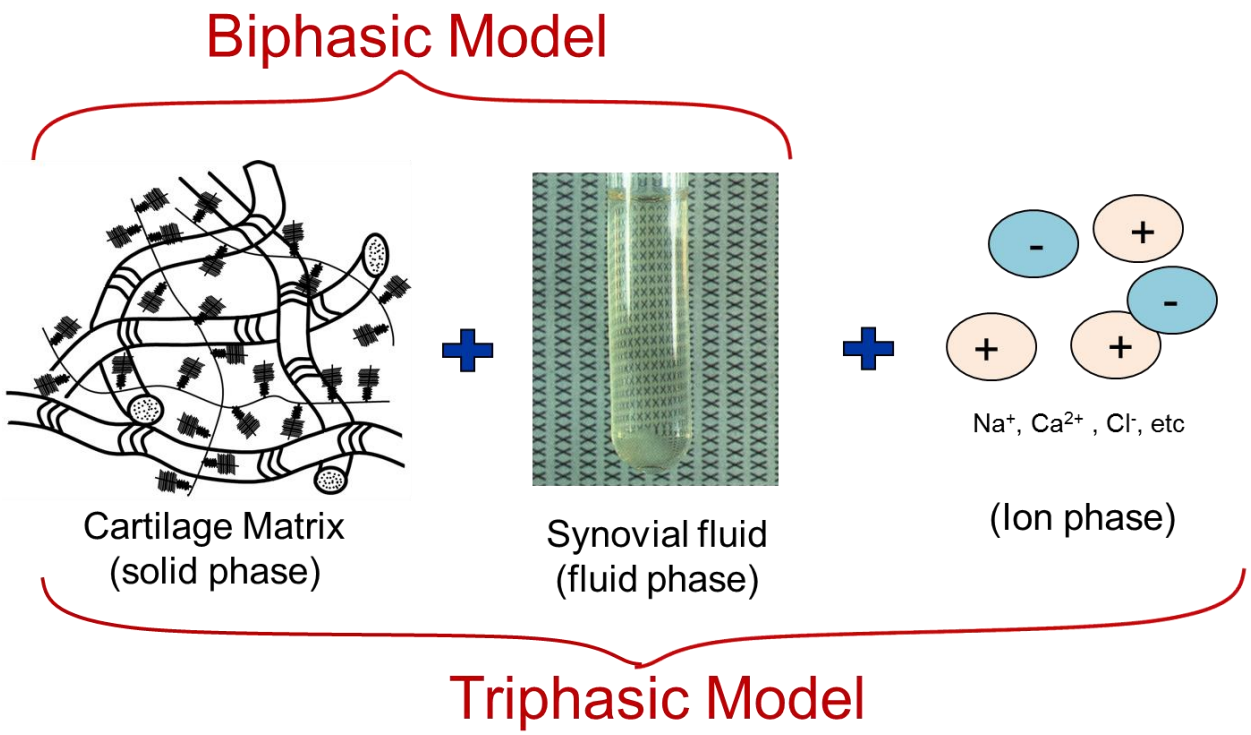

Figure 2.7: Cartilage matrix and synovial fluid (courtesy of Dr. Hanson) are considered as two phases forming the articular cartilage in the biphasic theory. Triphasic theory considers an ion phase additionally based on the biphasic theory

Recently, triphasic theory emerged as another popular model since the Donnan osmotic pressure attributed to high charge density caused by negatively charged sulfates in the cartilage matrix can enhance the load carrying capacity. As mentioned in section 2.1 above, the

proteoglycans are rich in the chondroitin and keratin sulfates. These charges and carboxyl groups in the tissues bring about a high charge density (called Fixed Charge Density, FCD), generating an imbalance of mobile ions in the articular cartilage. It gives rise to a pressure difference between the solutions inside and outside of the cartilage matrix, producing a high load carrying pressure in the fluid [35, 36, 42]. To describe this effect, Lai and coworkers supplemented the biphasic theory with an ion phase term and developed the triphasic theory [43] .

Viscoelastic models have also been employed to account for the behavior of cartilage. These are popular because the viscoelastic response combines the material behavior of an elastic solid and a viscous fluid that can describe the function of a solid matrix and interstitial fluid in cartilage [44-48]. The viscoelastic behavior and properties are obtained through creep and stress-relaxation tests on cartilage. It can be explained with the conventional knowledge of time dependent material behavior. The weak point of this model, however, is that the electrical characteristics described by the activities of ions in the electrolyte and the pressure resulting from these characteristics cannot be accounted for. The fluid flow in the cartilage also could not properly be described in this model.

2.3 Lubrication theories for the articular cartilage

There have been many theories that account for the mechanism of the articular cartilage resulting from the continuous efforts to understand the system of synovial joints for the past 7 decades (Table 2.1). Most theories that have been proposed mainly attempt to describe the cartilage lubrication from the mechanical and rheological perspectives. They also contain a presumption that friction on the cartilage surface is almost zero. Wear is not considered in these

models, though there has been work on the wear of cartilage. These models ignore the complexity caused by structure, composition, biochemistry, and the living nature of cartilage. Despite these general observations on many theories, they are grouped into approximately fifteen fundamentally different models [32]. Among the models, several basic models were briefly covered on this section.

Table 2.1: History of proposed lubrication theories for the articular cartilage [32]

Mechanism		Authors	Date
1.	Hydrodynamic	MacConnail	1932
2.	Boundary	Jones	1934
3.	Hydrodynamic	Jones	1936
4.	Boundary	Charnley	1959
5.	Weeping	McCutchen	1959
6.	Floating	Barnett and Cobbold	1962
7.	Elastohydrodynamic	Tanner	1966
		Dowson	1967
8.	Thixotropic/elastic fluid	Dintenfass	1963
9.	Osmotic (boundary)	McCutchen	1966
10.	Squeeze-film	Fein	1966
		Higginson et al.	1974
11.	Synovial gel	Maroudas	1967
12.	Thin-film	Faber et al.	1967
13.	Combinations of hydrostatic, boundary, & EHL	Linn	1968
14.	Boosted	Walker et al.	1968
15.	Lipid	Little et al.	1969
16.	Weeping + boundary	McCutchen and Wilkins	1969
		McCutchen	1969
17.	Boundary	Caygill and West	1969
18.	Fat (or mucin)	Freeman et al.	1970
19.	Electrostatic	Roberts	1971
20.	Boundary + fluid squeeze-film	Radin and Paul	1972
21.	Mixed	Unsworth et al.	1974
22.	Imbibe/exudate composite model	Ling	1974
23.	Complex biomechanical model	Mow et al.	1974
		Mansour and Mow	1977
24.	Two porous layer model	Dinnar	1974
25.	Boundary	Reimann et al.	1975
26.	Squeeze-film + fluid film + boundary	Unsworth, Dowson et al.	1975
27.	Compliant bearing model	Rybicki	1977
28.	Lubricating glycoproteins	Swann et al.	1977
29.	Structuring of boundary water	Sokoloff et al.	1979
30.	Surface flow	Kenyon	1980
31.	Lubricin	Swann et al.	1985
32.	Micro-EHL	Dowson and Jin	1986
33.	Lubricating factor	Jay	1992
34.	Lipidic component	LaBerge et al.	1993
35.	Constitutive modeling of cartilage	Lai et al.	1993
36.	Asperity model	Yao et al.	1993
37.	Bingham fluid	Tandon et al.	1994
38.	Filtration/gel/squeeze film	Hlavacek et al.	1995
39.	Surface-active phospholipid	Schwarz and Hills	1998
40.	Interstitial fluid pressurization	Ateshian et al.	1998

2.3.1 Boundary lubrication

Between two cartilage surfaces, various substances in synovial fluid work like additives in lubricating oil on practical applications. Hyaluronan and lubricin (a mucinous glycoprotein encoded by the *PRG4* gene) are absorbed to interacting surfaces, providing boundary lubrication in a diarthrodial joint [30]. Linear molecules of glycoprotein align themselves normally to the contacting surfaces to form a lubricating and protective layer shown in Figure 2.8. Although the boundary lubrication is sometimes considered as the primary mechanism to reduce friction between articulating surfaces, it is also regarded to be relatively ineffective on forming the frictionless condition [30]. This is an ongoing debate about the lubricating mechanisms of cartilage.

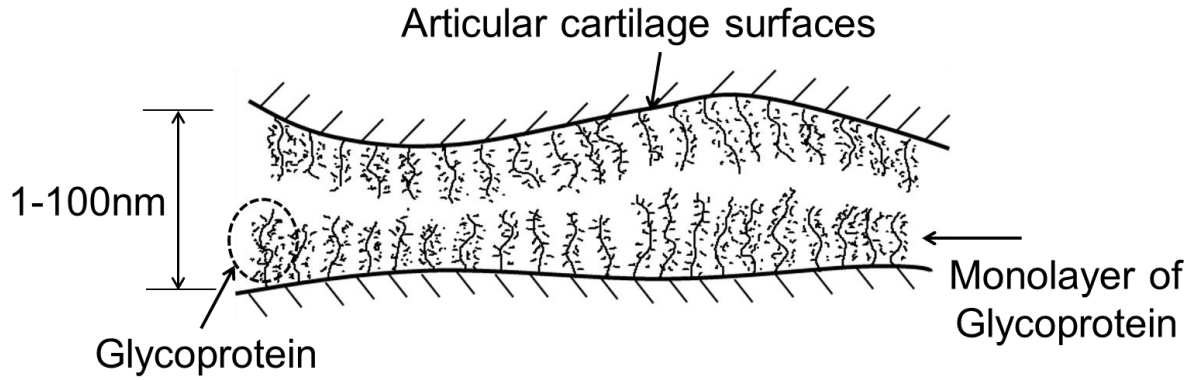

Figure 2.8: Boundary lubrication of the articular cartilage

2.3.2 Hydrodynamic lubrication

In hydrodynamic lubrication, two articular cartilages do not make contact so that the load is transmitted via the synovial fluid. A transversely moving surface with high speed is needed between two surfaces to drag a layer of viscous fluid for hydrodynamic pressure to bear external

load (Figure 2.9). However, continuous high speed is required for enough high pressure. It cannot always be satisfied because most activities in daily life result in low speed motions [49].

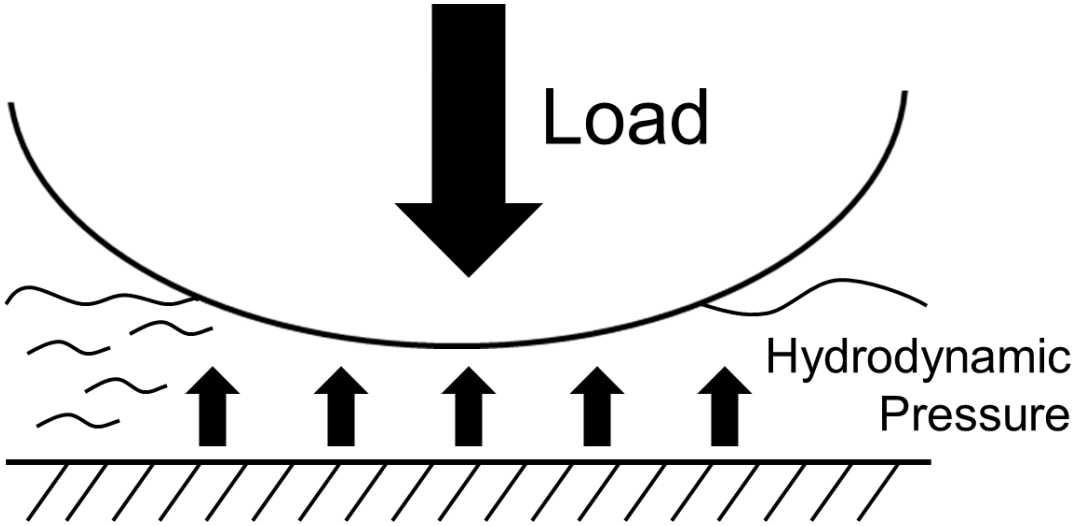

Figure 2.9: Hydrodynamic lubrication model

2.3.3 Elastohydrodynamic lubrication (EHL)

In this model, elastic deformation of the surface by high pressure plays a role in boosting hydrodynamic action. The EHL model is believed to be the best representation of the lubrication mechanism of articular cartilage. The mechanism operates due to the softness of cartilage that allows it to deform. In high pressure caused by loading, the cartilage deforms and the viscosity of the synovial fluid increases. This results in significant enhancement of hydrodynamic action in the joint (Figure 2.10).

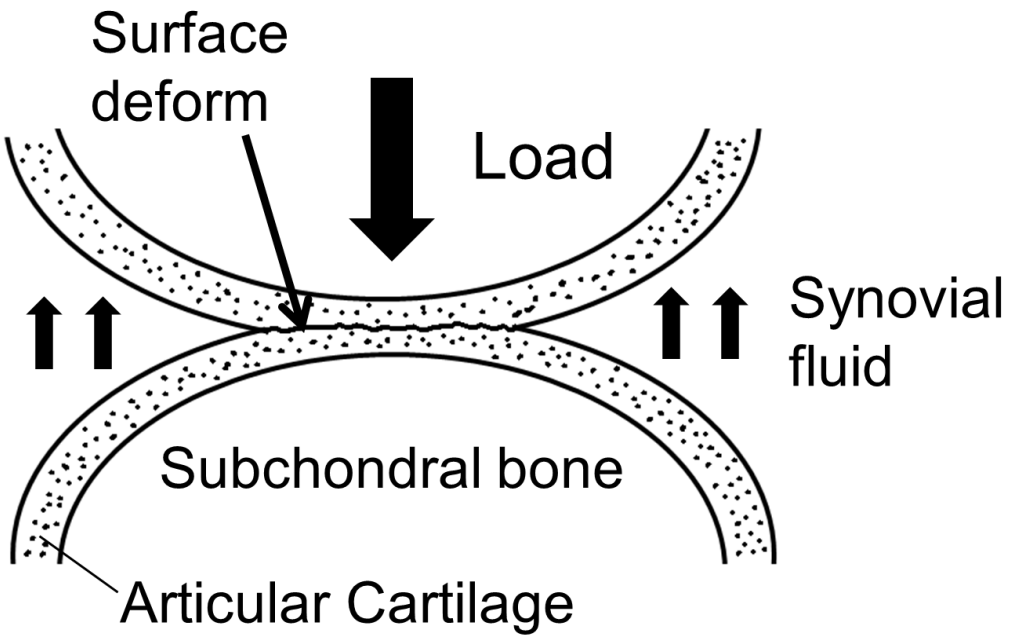

Figure 2.10: Elastohydrodynamic lubrication model of the articular cartilage

2.3.4 Mixed lubrication

Various mixed lubrication models have been developed to overcome the limitations of a single model for cartilage. The mixed lubrication model depicted on Figure 2.11 describes both the boundary and fluid-film lubrication simultaneously. The boundary condition occurs when the film thickness of the synovial fluid is on the same order as the roughness of the cartilage surfaces, while fluid-film lubrication occurs at the other areas [49].

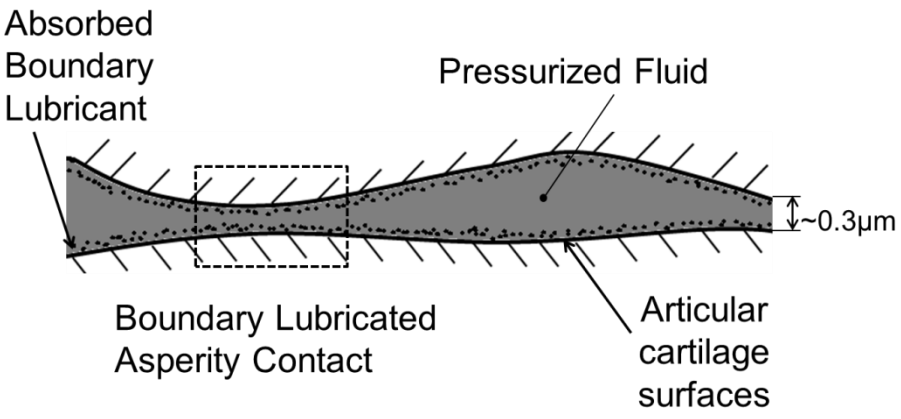

Figure 2.11: Mixed lubrication model of the articular cartilage

2.3.5 Squeeze-film lubrication

As two articulating surfaces are squeezed, a viscous resistance arises because the synovial fluid cannot be immediately squeezed out from the interspace between the surfaces. It generates a pressure supporting an external load as shown in Figure 2.12.

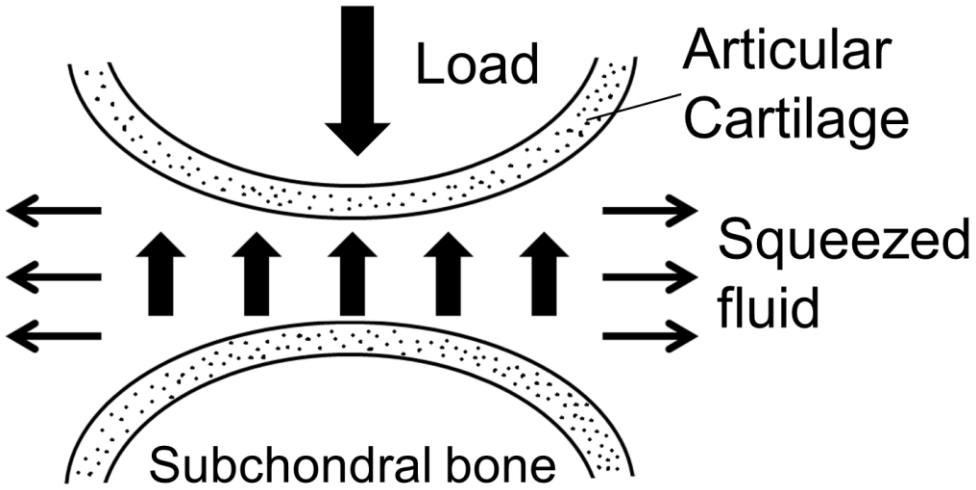

Figure 2.12: Squeeze-film lubrication model of the articular cartilage

2.4 Previous research methodology and current trend

The compression [14, 40, 50-52] and indentation tests are widely used to characterize the material properties of articular cartilage [36, 42, 43]. The behavior of a material in an space without lateral walls is observed under compression in the unconfined compress testing, while the material is in a space with walls in the confined compress testing as shown in Figure 2.13. In the compression tests, a whole sample is compressed by an indenter. Thus, the cross-sectional area of the sample corresponds to the contact area in the tests. In contrast, only part of a sample is loaded by an indenter during the indentation test. The indenters and bottom plates used in these tests are typically nonporous. However, some research groups prefer porous indenters and bottom plates to improve correlation with their theoretical models [40, 53] P.K.Korhonen et al. compared the behavior of articular cartilage between the unconfined compression, confined compression and indentation tests [54]. They found the elastic properties (Young's modulus, aggregate modulus, and Poisson's ratio) of bovine articular cartilage were statistically different in the three tests. M.R.DiSilvestro et al. developed the biphasic poroviscoelastic model of articular cartilage curve fit to the unconfined compression, confined compression, and indentation to validate the model [55]. Nonetheless, the indentation test is the most popular test to obtain the mechanical properties for biomaterials. The indentation test has been widely used and the analysis method has been refined to determine the elastic properties of metallic materials such as elastic modulus, and hardness [56, 57]. The indentation test, however, is now employed broadly in medical applications as well [13, 58, 59] because special specimen preparation is not required, the test can be performed on the intact sample tissue on the bone, and a sample is not destroyed due to the test [35]. In addition, the fact that various tip sizes and shapes of the employed indenter influence the determined properties should be considered when using the

indentation test [60, 61]. Specifically, a research showed that the elastic modulus of cartilage increases as the tip size of the indenter decreases.

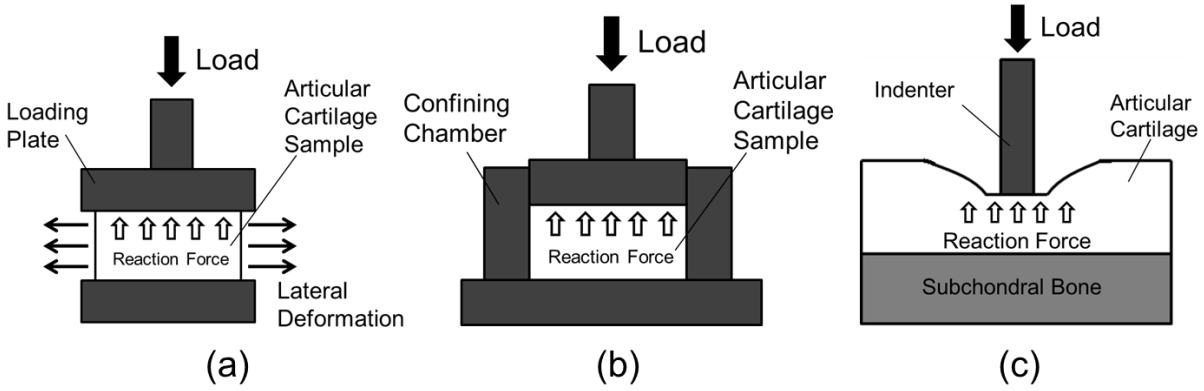

Figure 2.13: Schematic of the (a) unconfined compression, (b) confined compression, and (c) indentation tests

Either a creep (force is held constant) or relaxation (displacement is held constant) test is used to characterize the material properties of the cartilage [62, 63]. As another option besides the creep and relaxation tests, Park et al. [64] used a dynamic compression of cartilage to measure cartilage properties that are believed to better represent those of cartilage in actual physiological situations. Theoretically, this results in properties that are more realistic for cartilage actively being loaded in an animal, as a typical gate may be much shorter than the duration of a creep or relaxation test. Other recent studies have made use of this method, but some claimed mixed results [65-67].

There have been reasonable achievements in the mathematical and numerical analysis for how the articular cartilage responds in a test. A mathematical model was developed for the indentation test on articular cartilage using the plane-ended cylindrical and the spherical indenter

[68]. In addition, a theoretical solution for the rolling contact of articular cartilage was derived by Ateshian's group [69]. Also, Boschetti et al. created a computational method to mimic the test of confined and unconfined compression [53]. Lu and his fellows formulated a linearized triphasic theory which can be applied to describe the practical behavior of articular cartilage in a simpler way than the original triphasic theory using a regular perturbation method, and developed a finite difference method to calculate the mechanical properties of cartilage with the theory [70].

There are some groups who study articular cartilage from a tribological perspective. One group was interested in measuring the roughness of articular cartilage surface in different equine joints and comparing them, and observed different surface roughness values in different joints [71, 72]. Others demonstrated that the friction coefficient is low at high sliding speeds and the contact area is strongly affected by the probe radius and sliding speed [73]. They showed that the coefficient of friction is influenced by the loading time in indentation; the coefficient of friction slowly rises as the stationary loading time increases. Plainfossé et al. discussed the mechanical and frictional properties of a tissue-engineered cartilage matrix considering the relationship between composition, structure, and friction.

Another important property of articular cartilage is permeability. The permeability, or a resistance to flow through the cartilage matrix helps indicate the measure of fluid transport in a material. The permeability values obtained through the attempt of early works with various measurements are quite similar to those from recent works [74, 75].

There have been studies where the contact area, pressure distribution and loading of the synovial joint were investigated considering an animal or a human's movement to study the load

carrying mechanism. Some researchers observed the change of the contact area on cartilage surfaces in different loading condition [76, 77] and some found that the pressure distribution varies depending on the specific site on a same cartilage surface [78]. Petrtyl and his coworkers analyzed the flexion angle of the lower limb and load distribution during a human's simulated walk [79].

Recently, many researchers are focusing more on both the accurate measurement of properties of the synovial fluid and the formulation of a model for the mechanism of the fluid. This is because most people agree that the fluid plays a pivotal role in load support as mentioned previously. A change of the characteristics of the fluid leads to a change of the function of the whole joint. Some studies have concentrated on the role of load carrying pressurization of the fluid [34, 37], while others have measured the biomechanical properties of the fluid such as viscosity [79, 80]. However, it is still difficult to explain the function of the fluid correctly because of its complicated features. More efforts to understand the synovial fluid and its interactions with the solid matrix in the cartilage are needed.

3. The Equine Model for Cartilage Research

Since there is clearly a limitation on the harvesting of human articular cartilage, animal models have been employed by many researchers [34, 36, 37, 40-42, 46, 60, 61, 69, 71-74, 76, 77, 81, 82]. In this work, the equine model was selected as the alternative to the human articular cartilage model. The equine model and anatomy is introduced in this chapter, as well as the reasons why equine cartilage is a good model.

3.1 Comparison of equine model with the others

Generally, articular cartilage research uses with a smaller animal model such as a rat and rabbit because it is easier to handle and it costs much less than a larger animal model. However, a larger animal model is more appropriate as an alternative to the human model in terms of the size and structure of joints.

3.1.1 Size of joint

Sizes of distal femurs between a rat, goat, and human were compared in Chu et al.'s work, as shown in Figure 3.1. A dime and quarter were put beside the joints to place the comparison into context. The sizes of the joints on the different species were obviously different; the size of the human joint is significantly larger than the other species. In the same manner, the equine distal femur was compared with a quarter in our laboratory as shown in Figure 3.1. According to our observation, human and equine distal femurs are similar in size, while there is a significant difference in size between other three species. Thus, the human and equine joint would show similar mechanics, and provide a closer description of the human joint model.

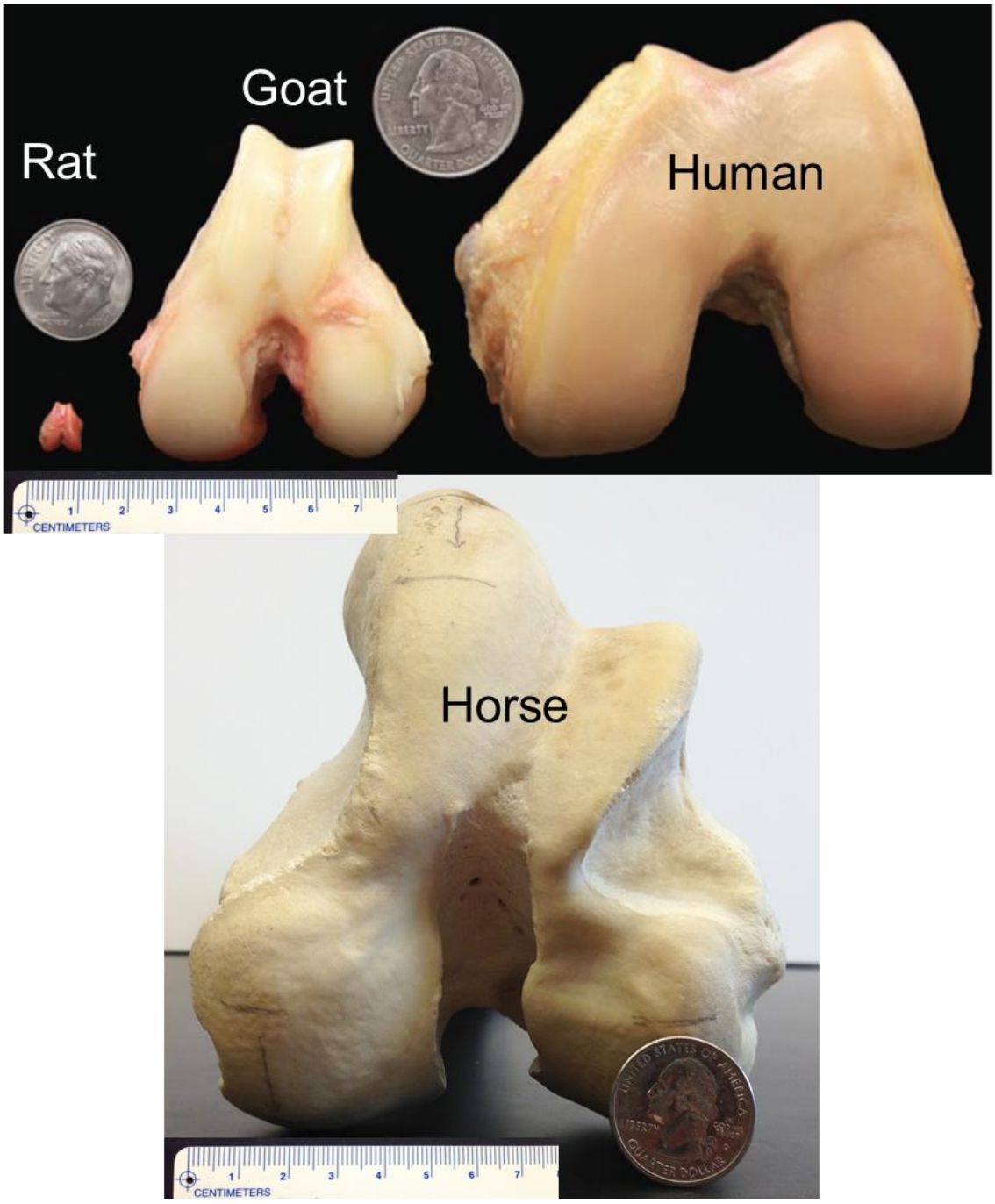

Figure 3.1: Comparative size of distal femurs between a rat, a goat, and a human from left to right with coins (top) and the equine distal femur with a quarter (bottom) at the same scale

3.1.2 Thickness of the articular cartilage

The thickness of the cartilage is a very important parameter in determining the material properties of the cartilage. In other words, if the thickness used in the mechanical model of the cartilage is not correct, then the other parameters could also have significant errors. There is a comparison of the cartilage thickness between several species. Frisbie et al. measured the thicknesses of the articular cartilage in different species on different locations as shown on Table 3.1. The equine articular cartilages on five different locations showed the closer average value of the thickness to that of the human articular cartilages, while other species obviously have much thinner cartilage thicknesses. Thus, the equine articular cartilage model is more structurally similar and could have similar mechanical behavior such as strain rate or failure under given conditions.

Table 3.1 Mean articular cartilage thicknesses in different species on different locations (PMT: proximal medial trochlear, LT: lateral trochlear, DMT: distal medial trochlear, PMC: proximal medial condyle, DMC: distal medial condyle) [82]

Species/Location	PMT	LT	DMT	PMC	DMC
Dog	524 ± 30	530 ± 30	530 ± 30	771 ± 30	731 ± 30
Equine	1832 ± 30	2162 ± 30	1761 ± 30	2215 ± 30	2203 ± 30
Goat	799 ± 30	699 ± 30	786 ± 30	1279 ± 30	1510 ± 30
Human	2596 ± 43	2877 ± 33	2461 ± 43	2411 ± 30	2523 ± 30
Rabbit	221 ± 30	314 ± 30	306 ± 30	341 ± 30	271 ± 30
Sheep	559 ± 30	707 ± 30	559 ± 30	542 ± 30	609 ± 30

3.1.3 Choice of equine model

The equine model provides a closer approximation for human pre-clinical studies because the joint size and the thickness of the human and equine articular cartilage are very similar as mentioned in previous sections. There are more studies that demonstrate the appropriacy of employing the equine model for human pre-clinical studies [82-84]. Moreover, it appears that very little work has been performed on equine cartilage, which could provide a viable model for human cartilage in some joints. For these reasons, this study focuses on the determination of the mechanical behavior and structure, stiffness and thickness of the equine cartilage from different joints.

3.2 Different joint types

There are many joints in the bodies of both humans and animals. The joints are of different joint types. Seven representative joint types are shown in Figure 3.2. From type A to G, Figure 3.2 displays the following joints: plane joint with articular processes of equine cervical vertebrae, hinge joint with equine fetlock, pivot joint with bovine atlantoaxial joint, condylar joint with canine femorotibial joint, ellipsoidal joint with canine carpus, saddle joint with canine distal interphalangeal joint, and spheroidal joint with canine hip joint, respectively. Since there are various joint types, each joint type should be fully studied to characterize how the articular cartilage might be adapted for different loads and motions. This is especially needed so that design of artificial joint can be tailored to each single joint because one design cannot represent all different types of joints. With this perception of the significance of the differences between joints, different equine synovial joints were studied and compared in this study.

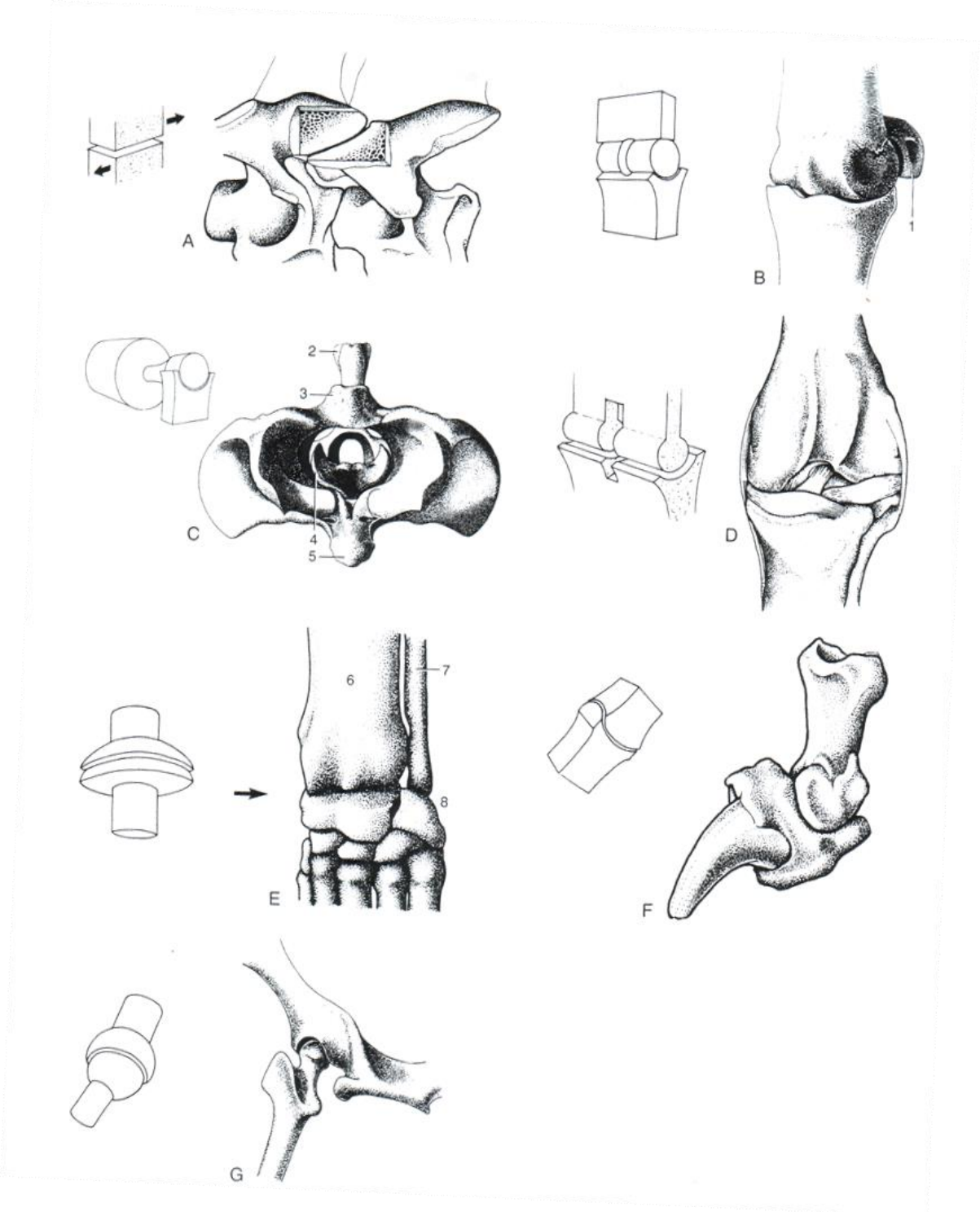

Figure 3.2: Types of joints with examples [85]

3.3 The studied joints

Prior to implementing this work, a basic knowledge of equine anatomy was required to choose the proper joints to be studied and the methodology to be employed. In this work, three different equine joints were studied: Fetlock, Carpus, and Stifle. The stiffness values of the fetlock, carpal, and stifle joints were determined and compared. In addition, the thickness of the fetlock, carpal and stifle joints were measured.

3.3.1. The fetlock

A horse has two fetlock joints in its forelimbs and two in its hind limbs (Figure 3.3). This joint belongs to the hinge joint type, similar to the human knuckle. The joint has a wide range of motion (110 degrees). The cartilage surfaces of distal metacarpus III from the fetlock were used for this work. The distal metacarpus III is called the fetlock for convenience in this work.

Figure 3.3**:** The location of the fetlock joints (left) and a radiograph of the fetlock (right, courtesy of Dr. Hanson)

The fetlock articular cartilage surfaces considered in this work were divided into two parts consisting of the lateral and medial sides, as shown in Figure 3.4.

The area along the horizontal axis of the fetlock (indicated by arrows) in Figure 3.4 is the weight bearing area that supports and carries most of the weight of the horse. In this study, the fetlock is classified as four surfaces: forelimb lateral metacarpus III condyle, forelimb medial metacarpus III condyle, hindlimb lateral metacarpus III condyle, and hindlimb medial metacarpus III condyle. These four surfaces were labeled front lateral fetlock, front medial fetlock, rear lateral fetlock, and rear medial fetlock for convenience, respectively. Not only is the stiffness values of each surface measured, but the overall stiffness of the fetlock was also obtained by averaging the stiffness values of these four fetlock surfaces. In addition, the overall thickness of the fetlock was measured.

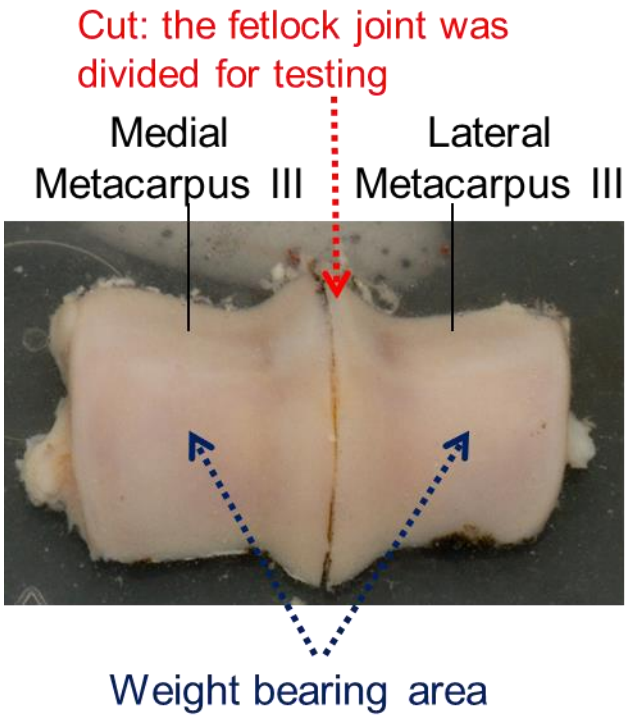

Figure 3.4: Distal metacarpus III articular cartilage surface divided into two sections: medial and lateral metacarpus III condyle

3.3.2 The carpus

There are two carpi that are located only on the forelimbs in a horse, unlike the fetlock (Figure 3.5). The carpal joint is composed of three subdivided joints: radiocarpal, midcarpal, and carpometacarpal.

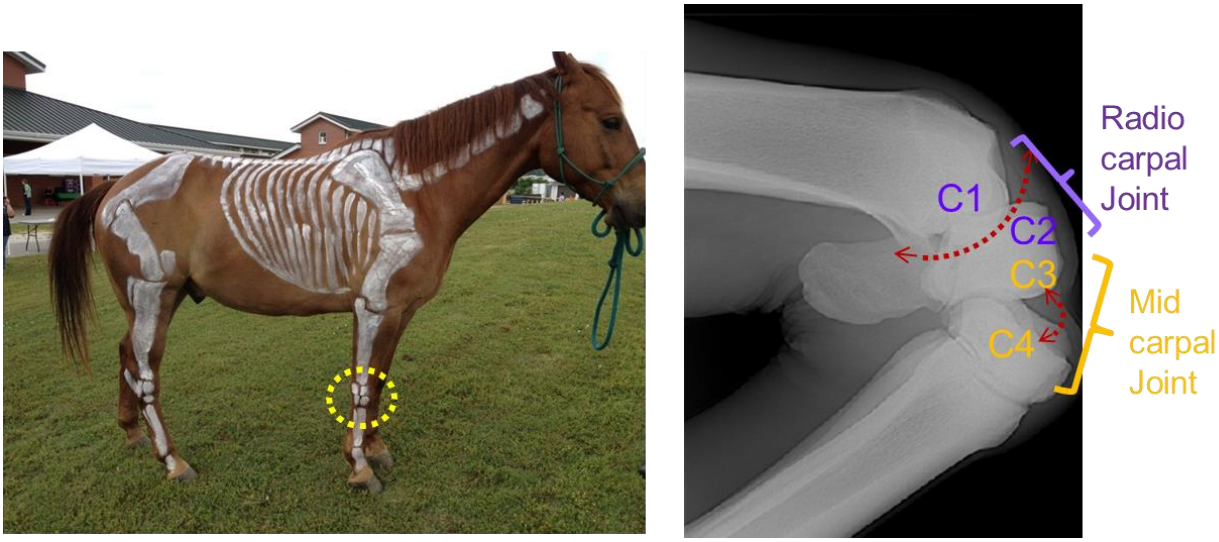

Figure 3.5: The location of the carpus (left) and a radiograph of the carpus showing three subjoints (right, courtesy of Dr. Hanson)

The carpometacarpal joint is the lowest set of surfaces in the carpal joint and was excluded from the study while the other two surfaces were investigated. This is because carpometacarpal joint remains stationary under plane axial and torsional loading [86], and is useless for the aims of the study, which deals with the mechanical properties related to loading and motion. The medial aspects of the radiocarpal and midcarpal joint were investigated because most of the weight is carried here and movement occurs on the medial side in the carpus [85, 87, 88]. The radiocarpal joint that is a condylar joint type is composed of the distal radius and proximal radial carpal bone. The surfaces of these two bones were labeled C1 and C2

respectively for simplicity in this work. C1 and C2 interact each other when carrying load and they conform to each other, as shown in Figure 3.6. Below C1 and C2, there are the distal radial carpal bone and proximal third carpal bone in the midcarpal joint that belongs to an ellipsoidal joint type (See Figure 3.7). The surfaces of these two bones were labeled C3 and C4 respectively. C3 and C4 are also conforming surfaces as well and shown in Figure 3.7. Different motions are observed in the radiocarpal and midcarpal joints. The radiocarpal joint shows a range of sliding and rolling motion of 90 to 100 degrees, while the midcarpal joint bends like a hinge over 45 degrees under various loading when a horse is standing, walking, and running [85, 87, 88]. All these surfaces from the carpus were tested to determine the stiffness and thickness.

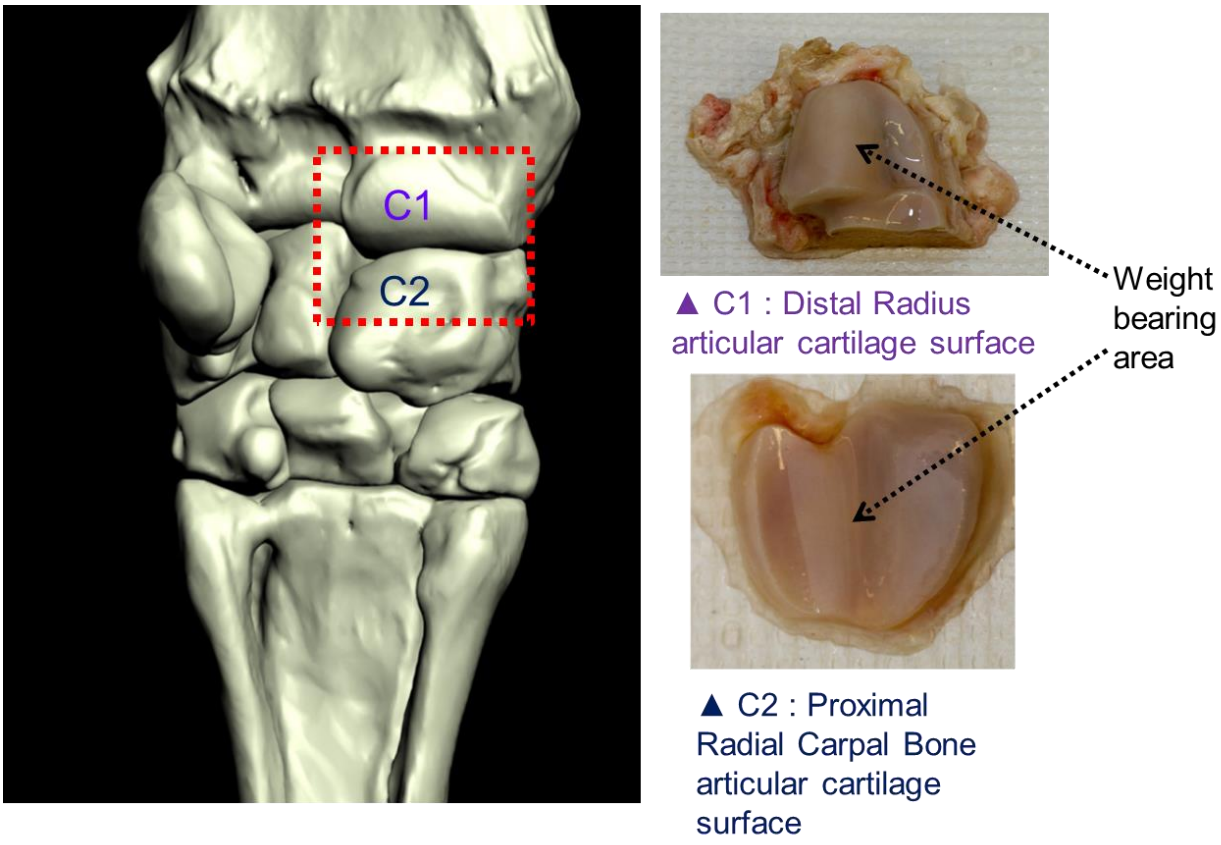

Figure 3.6: The radiocarpal joint of the carpus (left, courtesy of Dr. Hanson) and distal radius (C1) and proximal radial carpal bone (C2) articular cartilage surfaces from the joint

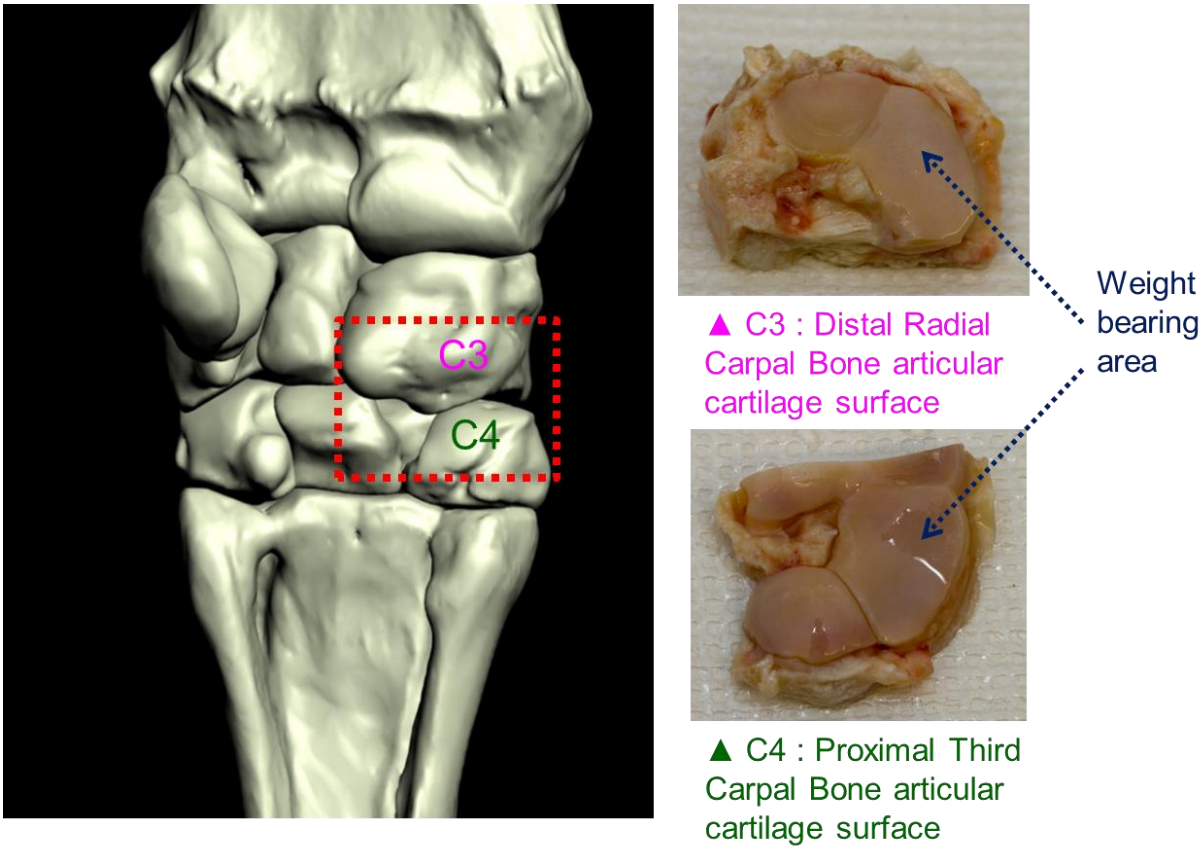

Figure 3.7: The midcarpal joint of the carpus (left, courtesy of Dr. Hanson) and distal radial carpal bone (C3) and proximal third carpal bone (C4) articular cartilage surfaces from the joint

3.3.3 The stifle

The last joint handled in this study is the medial femoral condyle or stifle. Two stifle joints are from two hind limbs in a horse as shown in Figure 3.8.

Figure 3.8: The location of the Stifle (left) and a radiograph of the stifle (right, courtesy of Dr. Hanson)

The stifle is generally the largest and most complex joint in a body. It shows a complicated combination of flexion, extension, rotation and sliding motions. This joint has been most often studied for cartilage clinical treatment because it is the largest weight bearing diarthrodial joint [89], and is very similar to the human knee. Thus, this joint is a more popular research object than the joints for human preclinical study [89, 90]. The joint is a condylar type (Figure 3.9). The stiffness and thickness of the stifle is measured as described by the methodology in chapter 4. More precisely, the medial femoral condyle was used for this work among articular cartilage surfaces in the stifle. However, the medial femoral condyle was called the stifle for convenience because it is the only surface from the stifle joint in this work.

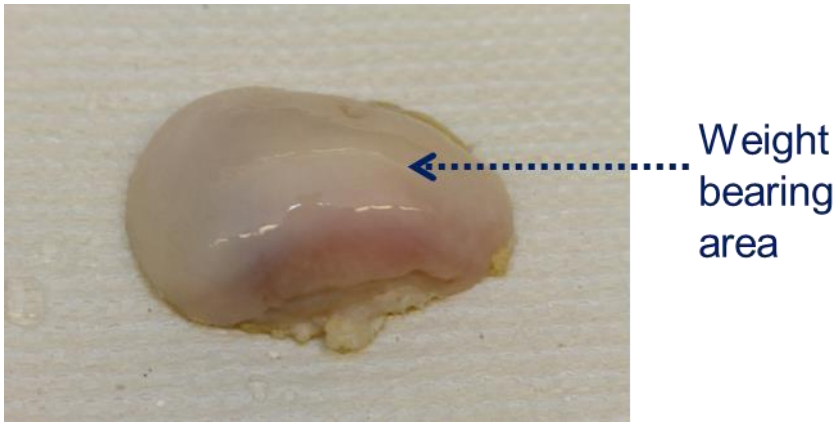

Figure 3.9: Medial femoral condyle (Stifle) articular cartilage surface

3.3.4 Difference between the three joints

The fetlock, carpal, and stifle joints show different geometries and motions. The shapes and sizes of the surface also vary between the joints (Figure 3.10). The length of the fetlock, C2, and stifle are approximately 4.8cm, 3cm, and 6cm, respectively as shown in Figure 3.10. Therefore, they will have different contact area and pressure distributions when in contact. Palmer et al. and Brama et al. studied the contact areas and pressure distributions on the cartilage surfaces in different equine joints [76, 77]. They characterized the different contact areas and pressure distributions on different joints, such as different pressure distribution patterns and percentage between contact and non-contact area.

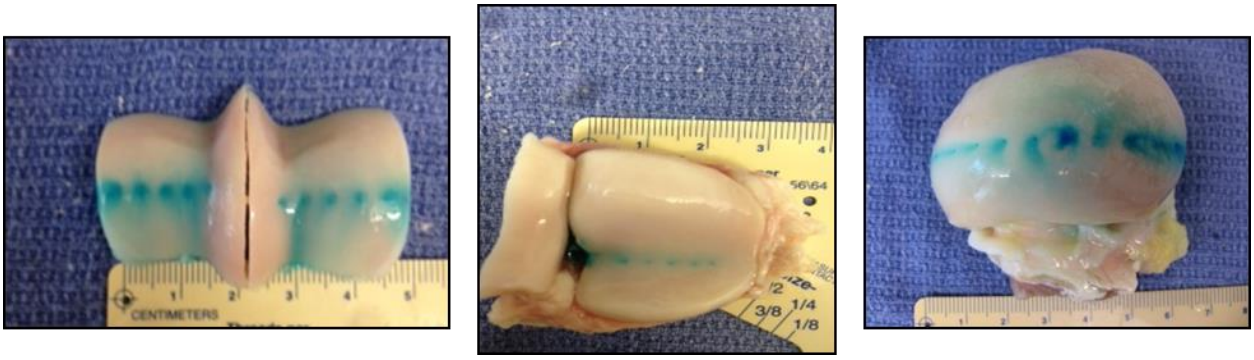

Figure 3.10: Distal metacarpus III (fetlock), proximal radial carpal bone (C2), medial femoral condyle (stifle) articular cartilage surfaces from left to right, respectively

Furthermore, each joint has a different motion as described in each subsection of 3.3. The movements and motions of the three joints were compared in Table 3.2. In the carpus, for example, the radiocarpal joint shows sliding and rolling motions, while the midcarpal joint bends like a book. The fetlock acts like a sliding hinge joint, and the stifle has a complex combination of various motions. If the equine articular cartilages on joints are adapted to different conditions, their properties will vary depending on the differences of mechanism resulting from geometry and motion.

Table 3.2: Comparison of movements and motions in the three joints

Joint	Joint Type	Movements	Motions
Fetlock	Hinge joint	Flexion, Extension, and Overextension	Sliding and rolling (110º)
Carpus	Combination of multiple joints	Flexion, Extension, Adduction, and Abduction	Sliding, rolling (90-100º), and ‘book’ like motion
Stifle	Condylar joint	Flexion, Extension, Rotation, and Sliding	Rolling and gliding

4. Experimental Methodology

4.1 Material acquisition

The fetlock, carpal, and stifle joints were harvested from 24 deceased horses. The horses were humanely euthanized for reasons unrelated to the study. They had no history of lameness or joint surgery. From these horses, 65, 48, and 7 articular cartilage surfaces were collected from the fetlock, carpal, and stifle, respectively, for stiffness measurements. In half of these horses, 40, 37, and 10 articular cartilage surfaces were harvested from the fetlock, carpal, and stifle joint, respectively, for thickness measurements. Articular cartilage surfaces damaged by injury or an operators' mistake during dissection were filtered from the test samples. The joints from the same horse were surgically obtained from the Auburn Laboratory at the Thomson Bishop Sparks State Diagnostic Laboratory within 4 hours of euthanasia. The articular cartilage samples harvested through this process do not lose their original properties, being much fresher than frozen samples or samples from butcher houses used in many studies [36, 42, 55, 73, 91, 92]. After the necropsy, the joint were transported to the Multiscale Tribology Laboratory at Auburn University for articular cartilage thickness measurement; the right paired joint was transported directly to the Multiscale tribology laboratory for stiffness measurement. The process of the material acquisition is displayed in Figure 4.1. All experimental procedures of the stiffness measurements and thickness measurements were performed at the College of Engineering at Auburn University.

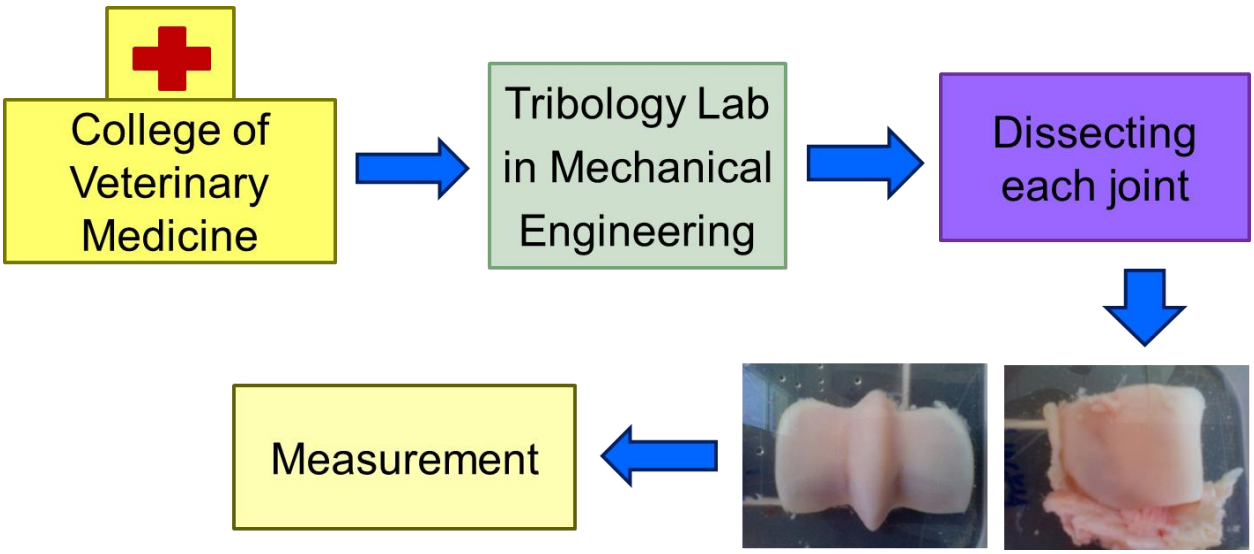

Figure 4.1: Flow chart of the material acquisition

After approximately three minutes of exposure to air during dissection, all cartilage samples were preserved in a saline solution for testing. The samples which are whole articular cartilage on subchondral bone were removed by dissection of the surrounding and associated structures and sized for measurement by a band saw. Tests on plug or cylindrical samples are advantageous because ideally a uniform stress distribution will result in the cartilage. In our work, however, the cartilage surface surrounding the test location was left untouched, while many researchers have used plugs for testing [34, 55, 91-93]. This is because the cartilage can be damaged and its properties may vary from cartilage in situ by extracting a plug from the cartilage. Anderson et al. showed the importance of extreme care on sample preparation because they observed that the articular cartilage surface is damaged by wiping with a latex glove [94]. In the current work, operators did not touch the surfaces on which the measurements were performed and the surfaces were kept hydrated by sprayed saline. Immediately upon removal from the joint

capsule, the samples were preserved in a saline bath to prevent air-drying. Once testing is completed, all samples were labeled, frozen in saline, and stored.

A total of four fetlock samples were harvested from a horse for stiffness measurements. These samples - the front lateral, front medial, rear lateral, and rear medial - were taken from the fetlock on the right side limbs. The surfaces were at the level of the subchondral bone. The four surfaces from the left fetlock joints were harvested for the thickness measurements. A total of four samples from right carpus (C1, C2, C3, C4) were collected from a horse for measurements, while the four surfaces from the left carpus were collected for the thickness measurements. One surface of the stifle from the right rear limb is harvested from each horse for the stiffness measurements, while one from the left stifle is harvested for the thickness measurements. The samples were handled with great care during dissection and measurement.

4.2 Experimental equipment

The Bruker UMT-3 Tribometer (Figure 4.2) was used to perform the indentation test to measure the mechanical stiffness of the cartilage and to perform the needle thickness tests. The UMT-3 is a versatile modular machine that measures the vertical displacement of the indenter into the cartilage at a resolution of 1 micrometer. Also, it is equipped with a high-sensitivity force sensor (1mN of resolution).

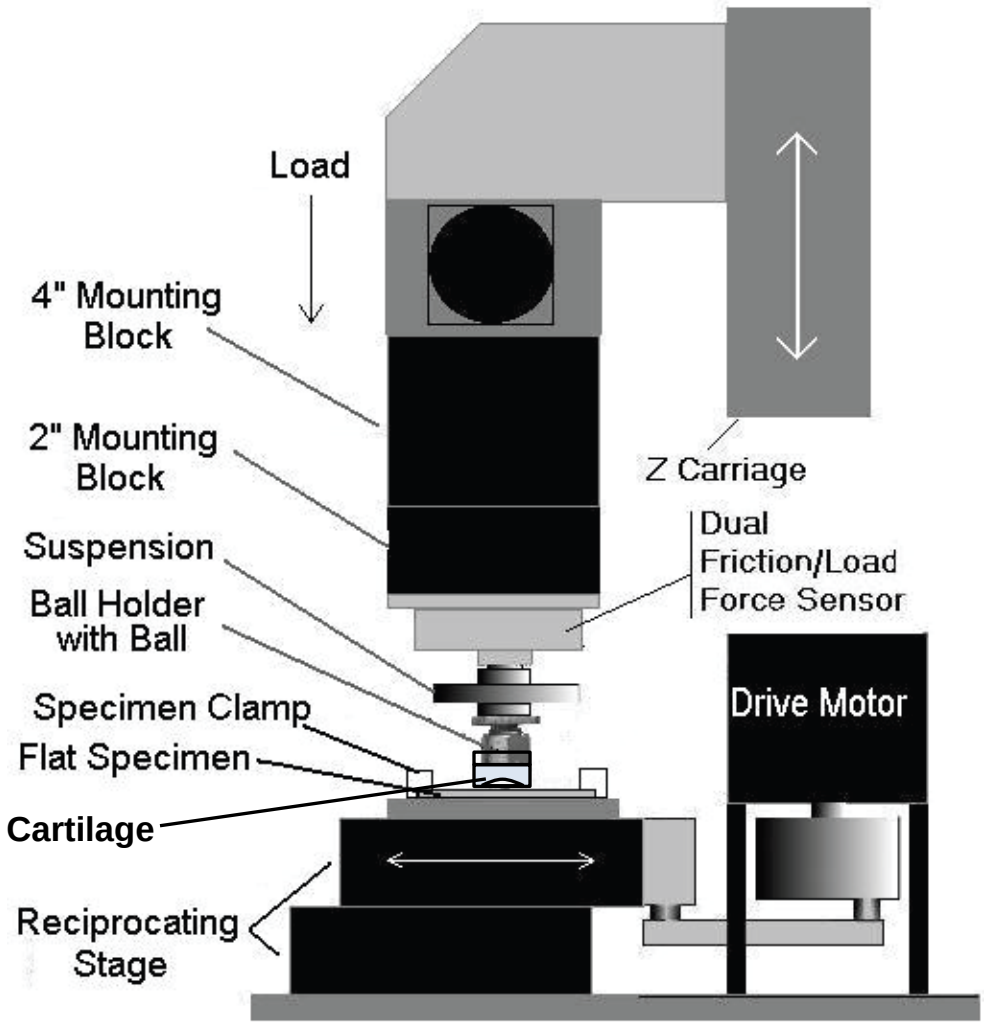

Figure 4.2: Schematic of Bruker UMT-3 test apparatus configured for indentation tests

4.3. Experiments

4.3.1 Indentation test

The indentation test was chosen because special sample preparation is not needed and the sample is not damaged in the indentation testing. Also, the Bruker UMT-3 Tribometer (Appendix B) is capable of implementing the indentation test. For these reasons, the indentation test was selected to determine the stiffness of equine articular cartilage in this study.

Figure 4.3: UMT-3 performing indentation tests of articular cartilage submerged in saline

A flat-ended cylindrical aluminum probe was fixed to the machine (Figure 4.3). This is similar what is widely used by many research groups [36, 39-41, 60] although the indenter has flaws: the possibility of incomplete contact and high pressure resulting from stress concentration on the edge of the indenter. The diameter of the indenter is 5mm. The indenter was brought into contact with the cartilage at a constant rate of 10μm/s while force and displacement are measured (Figure 4.4). The designed indenting velocity of 10μm/s provides a constant strain rate of 0.01/s that are used in experiments with a viscoelastic material based on the assumption that the articular cartilage thickness is 1mm [82, 89]. When it comes to the indentation depth, previous research have proposed that a maximum strain rate between 5% and 30% should be used during the test [34, 39-41, 61, 95]. Thus, the indentation depth of 0.2mm was set because it is in the range of the proposed strain rate. The indenter lowers until it approaches 0.2mm (loading), and then it ascends back immediately after it reaches the designated indentation depth (unloading).

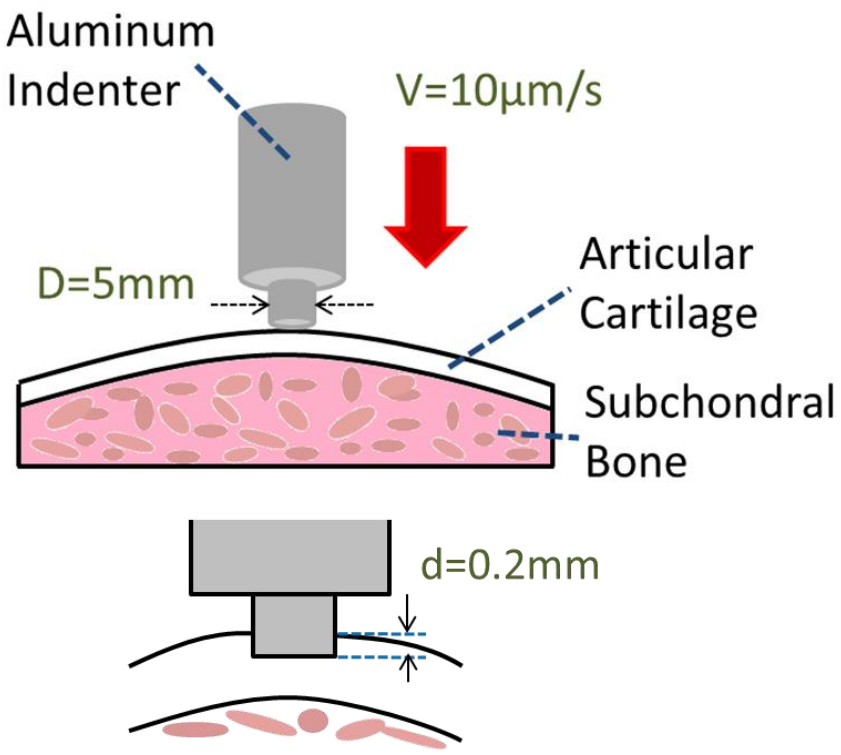

Figure 4.4: Schematic of the indentation test setup

The test was performed three times at different spots on the same articular cartilage surface. The test points were on the weight bearing area that bears and carries the most external load as shown in Figure 4.5. The distance between them was 5mm. The second measured point was on the center of the surface. The indentation test was conducted on four articular cartilage surfaces from the fetlock and four from the carpus.

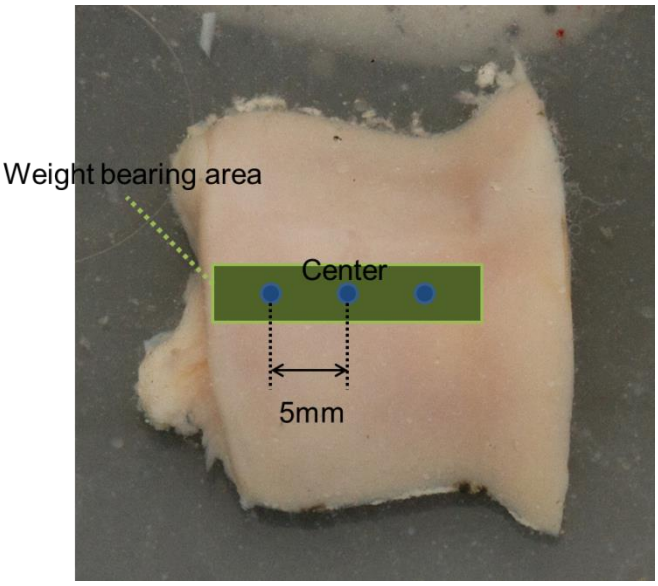

Figure 4.5: Example of tested points on a front medial fetlock articular cartilage surface

4.3.2 Needle probe test

As mentioned in Chapter 3, the cartilage thickness is very important in study of biphasic behaviors of the cartilage. Several methods are available to measure tissue thickness such as ultrasonic measurement, microscopic measurement, and needle probe measurement. There are studies that make comparisons of these methods [96, 97]. Among these techniques, the needle probe test was selected for measurement of the articular cartilage thickness in this study. This is because the technique does not require any special equipment or sample preparation. All that is needed is an apparatus with a carriage moving in the vertical direction and a needle as shown in Figure 4.6. In addition, the methodology for conducting a needle probe test to measure the cartilage thickness is already established [97].

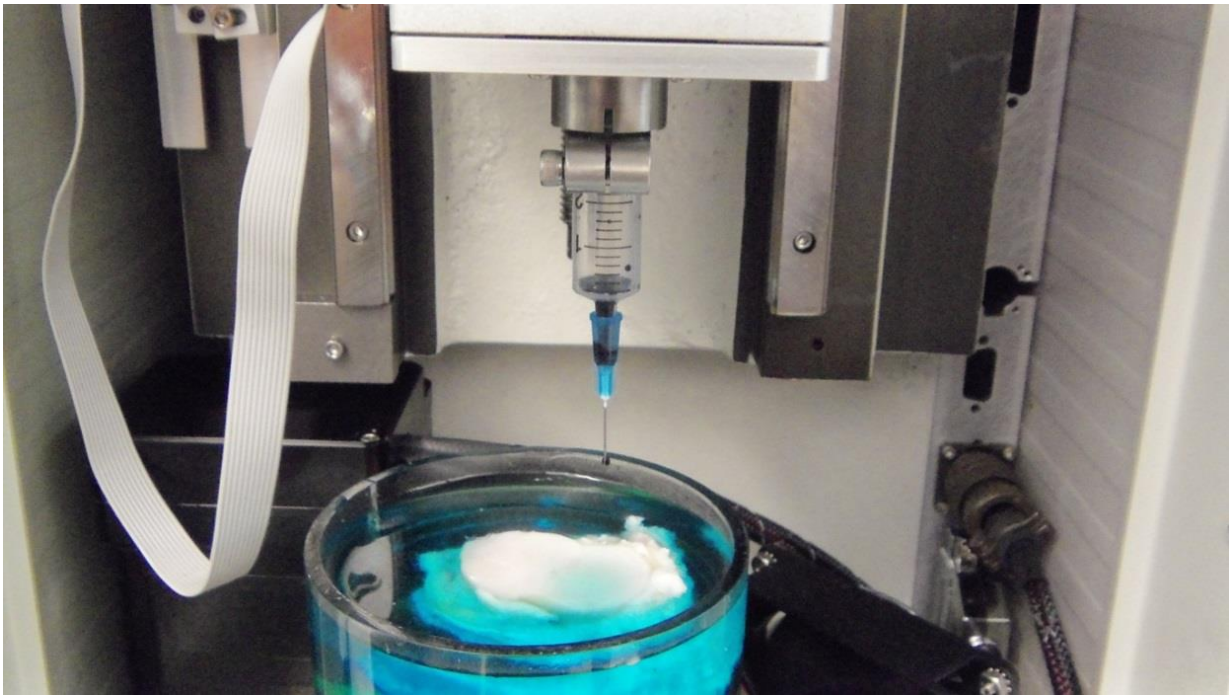

Figure 4.6: Needle probe test setup

Samples from the left side limb were brought to the engineering laboratory immediately after imaging for needle thickness testing. The 25gauge needle was used because it is thinner, and therefore less affected by friction and short enough to not bend (Appendix B). By fitting the needle into the indenter mount of the UMT-3 device, thickness measurements of the cartilage were also conducted for the various joints. The needle used is attached to a syringe. The syringe, additionally, is loaded with a dye so that the location of each test can be mapped.

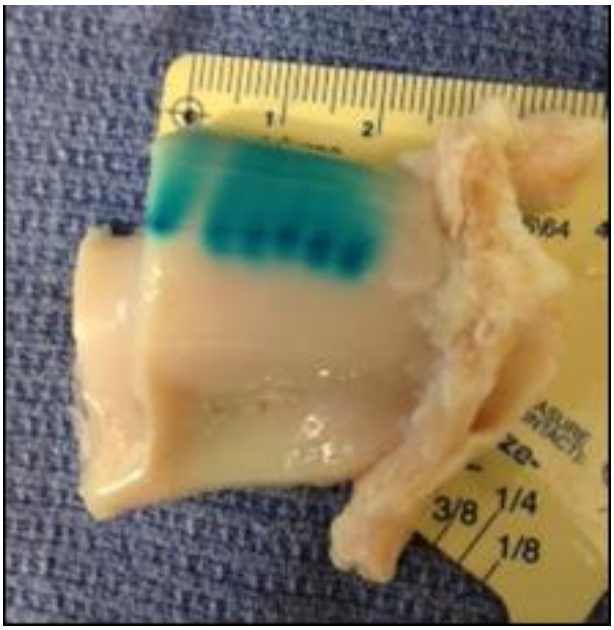

Figure 4.7: Marked points on a surface of C1 on which the needle probe tests were performed

The dye created the blue dots clearly visible in Figure 4.7, representing the spots where the needle has punctured the cartilage. The force was measured as a function of displacement. The needle is lowered at a velocity of 20 μm/s until the measured force exceeds 2.5N. The used needle was replaced with a new one on each test day. Just as with the indentation samples, the needle depth samples were frozen in saline, labeled and stored. The thickness was measured at five points on the same articular cartilage surface. The interval between points is 3mm. The third point is on the center of the surface.

5. Data Analysis

5.1. Indentation test

Plotting the force versus displacement allowed the prediction of the cartilage stiffness. The slope of the indentation curve of this force versus displacement is stiffness (Figure 5.1), i.e. the response load per unit deformation.

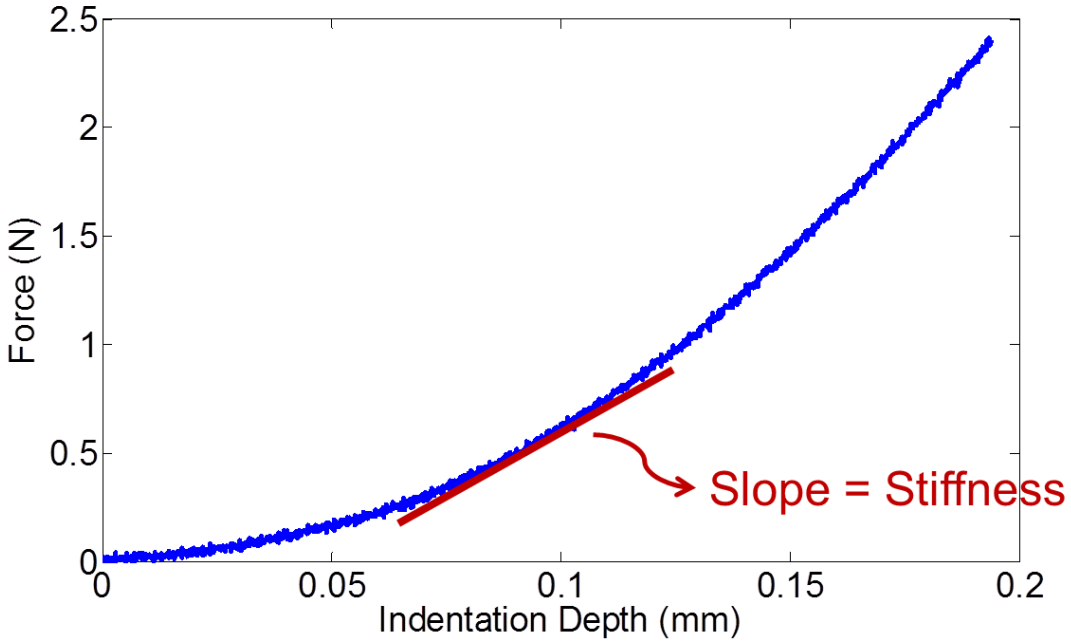

Figure 5.1: A raw data of an indentation test on a surface of C2

The proposed process in Figure 5.2 is followed to pursue the stiffness with a sample size of over one hundred samples of each surface. Cubic equations are fitted to the obtained indentation curves (force versus displacement curves) using the curve-fitting function of MATLAB 7.10.0. The cubic equation was chosen as the best way to express the curves (average

R^2>0.998) after multiple trials and with various types of equations. The measured force, *F*, was expressed as a function of displacement, *d* by Eq. 5.1.

$$F = Ad^3 + Bd^2 + Cd + D \text{ [N]} \tag{5.1}$$

where A, B, C, and D are the coefficients from curve-fitting, *F* is the force, and *d* is the indentation depth or displacement.

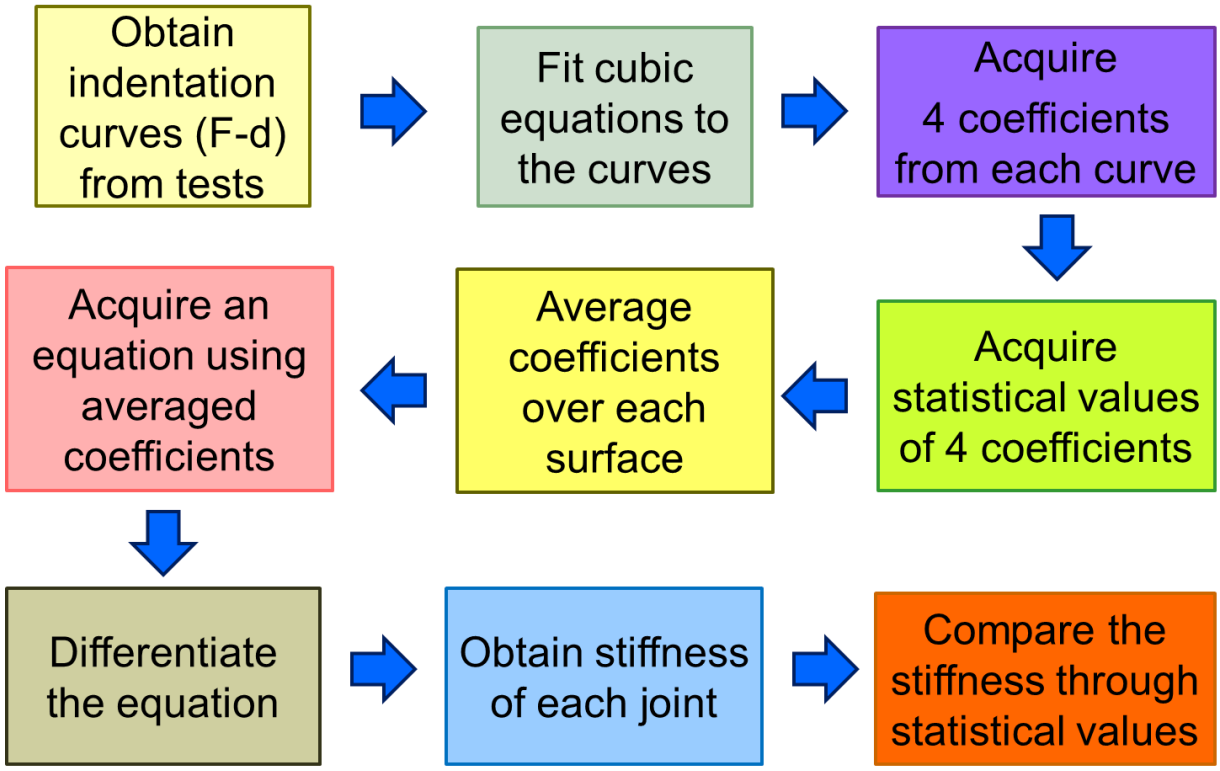

Figure 5.2: The flow chart of the analysis of experimental data

Four coefficients (A, B, C, and D) from each curve are acquired during the fitting. These four coefficients are averaged over each surface. Thus, four averaged coefficients for each nine different articular cartilage surfaces are gained. These values are statistically evaluated to confirm the significance of the differences between joints using student's t-test. P-values

between two objectives were obtained through the student's *t*-test. If a p-value is smaller than 0.05, the difference between the objectives is "significant." For the p-value smaller than 0.01, the difference is "highly significant." If a p-value is smaller than 0.001, the difference is "very highly significant." With the averaged coefficients, the new updated equations for each surface are acquired. They are the averaged force versus displacement curves representing the indentation characteristics of each surface. Afterwards, the equations obtained by differentiating the averaged indentation curves are the stiffness equations of each joint, as given by

$$k = 3Ad^2 + 2Bd + C \text{ [N/mm]} \tag{5.2}$$

where *k* is the stiffness.

The stiffness curves of different articular surfaces in the fetlock were compared. The stiffness values of different articular surfaces in the carpus were compared as well. The stiffness of the fetlock itself was determined by differentiating the averaged indentation curve of four different averaged indentation curves of each surface in the fetlock joint. The stiffness of the carpus and stifle itself was determined in the same manner.

5.2 Needle probe test

The changes in the slope of the curve were used to predict the thickness of the cartilage (following existing methods [98, 99]). The thickness was determined as the distance between the points where the curve has positive slope and where the slope increases dramatically in Figure 5.3. following existing methods [98, 99]. The two points marking the top and bottom of the cartilage are shown as an 'x' with a vertical line in Figure 5.3. The first positive slope means that the needle made contact on the cartilage surface and the force also suddenly drops when the

surface is pierced. The skyrocketing slope at the second ‘x’ means that the needle met the hard subchondral bone. The thickness is clearly determined because the two points can be found precisely. In this particular test of the left lateral fetlock joint, the predicted cartilage thickness was 0.85 mm. The thickness of each articular cartilage surface from the fetlock, the carpus and the stifle surface was measured and averaged. The averaged thicknesses of each surface were compared in the fetlock, carpus, and stifle. The results using the analysis methods described in this chapter are presented and discussed in chapter 6 and 7.

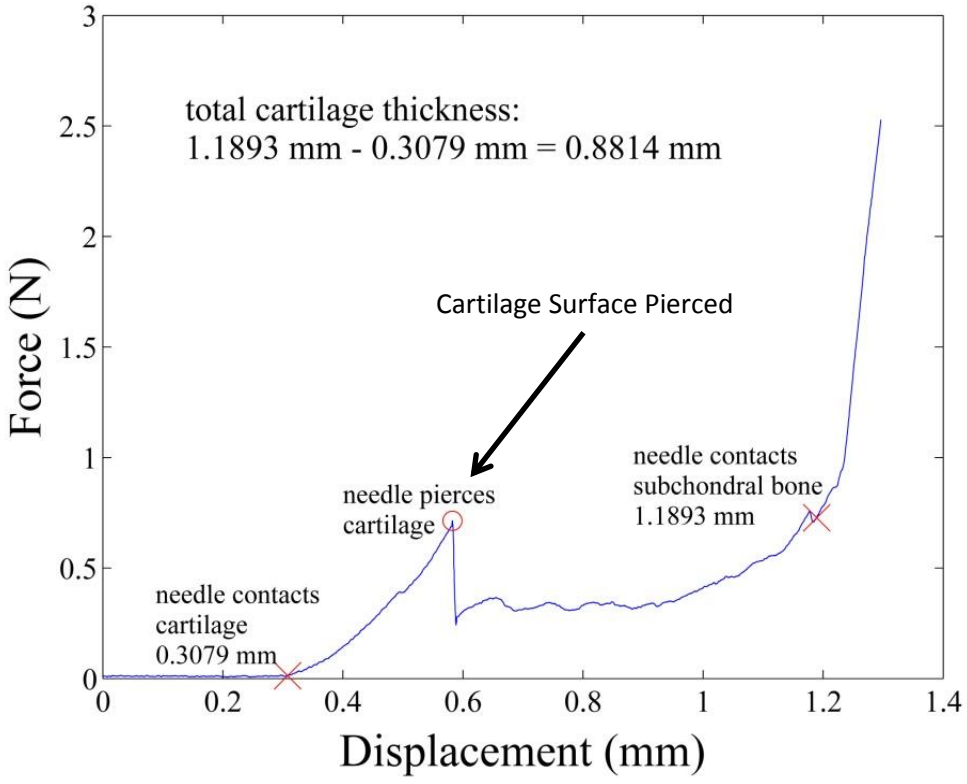

Figure 5.3: Example needle cartilage measurement on the left lateral fetlock

6. Results

6.1 Stiffness measurement (indentation test)

6.1.1. Comparison between the fetlock, carpus, and stifle

The applied forces and stiffness values of the fetlock, carpus, and stifle are compared following the analysis method described in chapter 5. Four coefficients (A, B, C, and D) from a curve are different from each other. Thus, the coefficients from a test on a sample are unique values representing the mechanical behavior of the sample. In other words, the coefficients reflect the unique reacting force of each sample under loading. Hence, the derivative of the force equation with the coefficients represents the unique material property of stiffness (Eq. 5.2). The magnitudes of most coefficients of the fetlock are greater than the coefficients of the carpus and stifle, indicating that overall a greater force was applied on the fetlock joint (Table 6.1).

Table 6.1: Average coefficients of the fetlock, carpus, and stifle

Joints	Average coefficients			
	A [N/mm^3]	B [N/mm^2]	C [N/mm]	D [N]
Fetlock	813.8	7.182	12.12	0.023
Carpus	252.1	25.77	5.262	0.020
Stifle	15.10	1.681	1.785	0.009

Table 6.2: Statistical comparison of four coefficients between the fetlock, carpus, and stifle with p-values

Compared joints		P-value			
		A	B	C	D
Fetlock	Carpus	7.75×10^{-7}	0.378	1.70×10^{-6}	0.755
	Stifle	4.86×10^{-11}	0.761	1.37×10^{-11}	0.111
Carpus	Stifle	4.78×10^{-7}	0.031	3.04×10^{-6}	0.012

A P-value that is smaller than 0.05, 0.01, and 0.001 indicates that a difference between two compared objectives is "significant," "highly significant," and "very highly significant," respectively. The p-values of the coefficients A and C are low (<<0.001). Differences cannot be completely explained with only these two coefficients. However, it is evidence showing that the statistical differences between all three joints are highly significant (Table 6.2). Hence, the difference of coefficients between the three joints indicated that applied forces on the three joints were statistically different. P-values were obtained using Microsoft Excel 2010. Using the averaged coefficients, the new equation of force was developed and plotted in Figure 6.1. The trends of the curves look very similar to the established literature [34, 42, 56, 57, 60, 61, 81]. The overall measured force on the fetlock joint is greater than on the carpal and stifle joint through the entire indentation procedure. When the indenter reached the designated indentation depth (0.2mm), the force on the fetlock is approximately 2.5 times and 10 times greater than the force on the carpus and stifle, respectively.

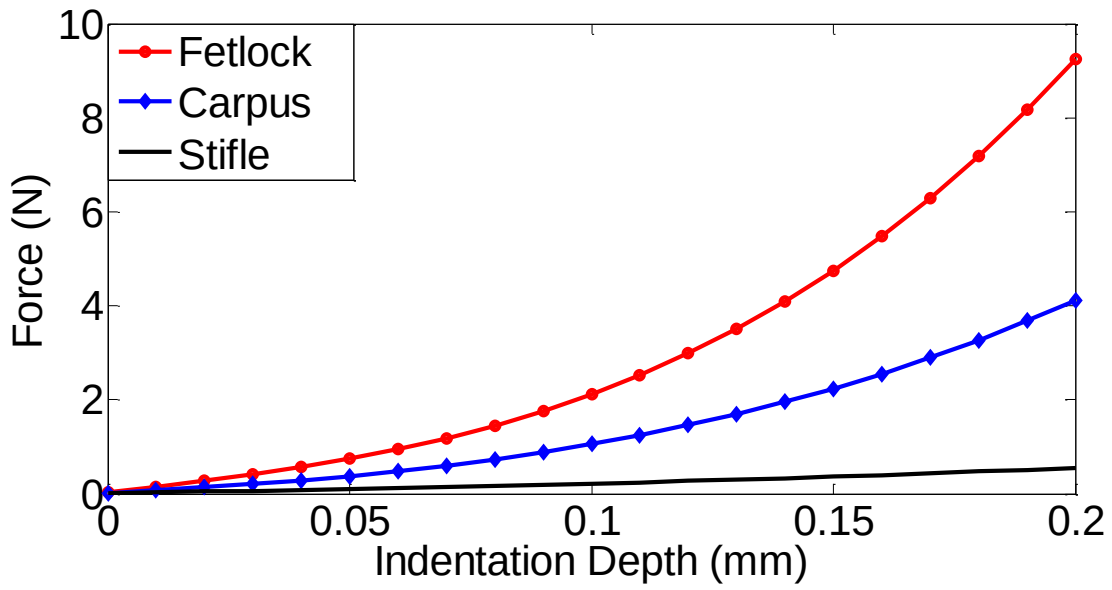

Figure 6.1: Comparison of the force throughout the indentation depth between the fetlock, carpus, and stifle

The coefficients (3A, 2B, and C) of the stiffness equation (Equation 5.2) were acquired by differentiating the force equation. Equations for stiffness of the fetlock, carpus, and stifle were established using the average coefficients and plotted in Figure 6.2. The overall stiffness of the fetlock is greater than the carpus and stifle through the indentation. There is a three folds difference between the stiffness values of the fetlock and the carpus at the end of the indentation process, while the stiffness of the stifle is very low. The stiffness values were not zero at the point of initial contact and increased from the start point. The stiffness values most likely increase due to the fluid being squeezed out of the cartilage. The stiffer cartilage matrix carries more loads. There is a possibility is that the cartilage becomes less permeable due to the closing of interfacing gaps as it is compressed.

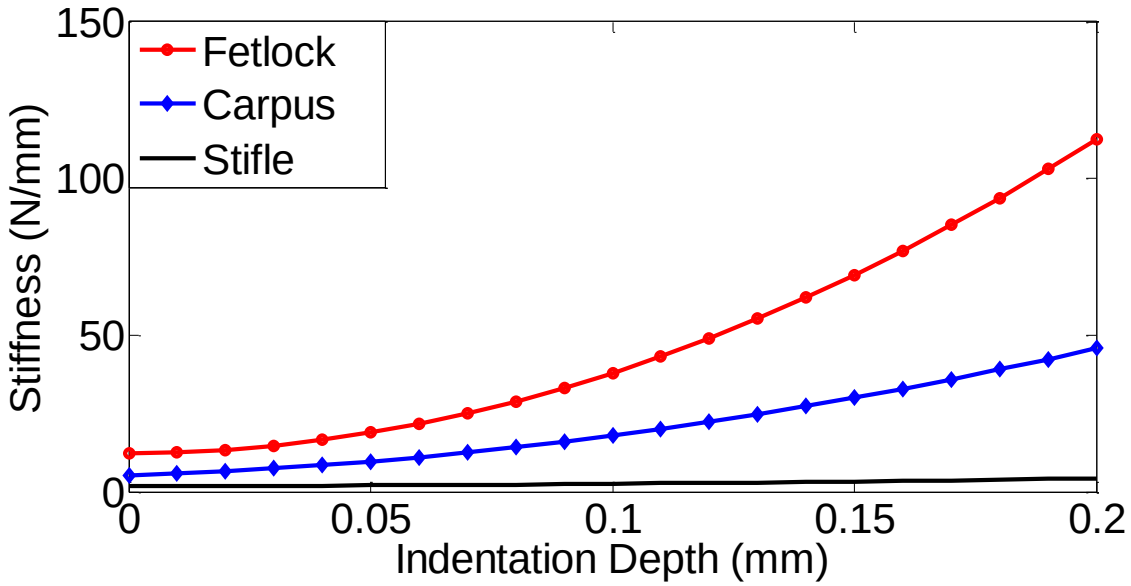

Figure 6.2: Comparison of the stiffness throughout the indentation depth between the fetlock, carpus, and stifle

The average stiffness values of the fetlock, carpus, and stifle through the test are determined as 46.11N/mm, 20.50N/mm and 2.725N/mm respectively by

$$k_{ave} = \frac{\int_0^{d_{max}} k\partial d}{d_{max}} \; [N/mm] \tag{6.1}$$

where $d_{\max}$ is designated indentation depth, 0.2mm

6.1.2 Comparison of stiffness between the surfaces in the fetlock

The stiffness values of articular cartilage surfaces in the fetlock introduced in section 3.3 were compared as well. The coefficients of the stiffness equation were obtained in the same

manner explained in chapter 5. The equations representing the stiffness of each surface from the fetlock were plotted (Figure 6.3) using the coefficients as shown in Table 6.3.

Table 6.3: Average coefficients of the articular cartilage surfaces in the fetlock

Joints	Average coefficients			
	A [N/mm^3]	B [N/mm^2]	C [N/mm]	D [N]
Front lateral fetlock	819.2	0.947	9.187	0.018
Front medial fetlock	738.2	57.73	11.80	0.045
Rear lateral fetlock	984.3	1.135	14.03	0.015
Rear medial fetlock	711.2	-30.42	13.73	0.013

As shown in Figure 6.3, the stiffness values of each fetlock surface are different. However, no statistically significant difference between them was observed. This is shown by most of the p-values are above 0.05 between the coefficients A, B, C, and D (see table 6.4.) Generally, it is believed that approximately 55% and 45% of total load are supported by the front and the rear limbs, respectively [100]. Also, it is believed that 60% and 40% of total load are supported by the medial and lateral side, respectively [76-78]. Regardless of the fraction of the weight distribution, however, the articular cartilage surfaces from the fetlock showed no statistically significant differences in the stiffness.

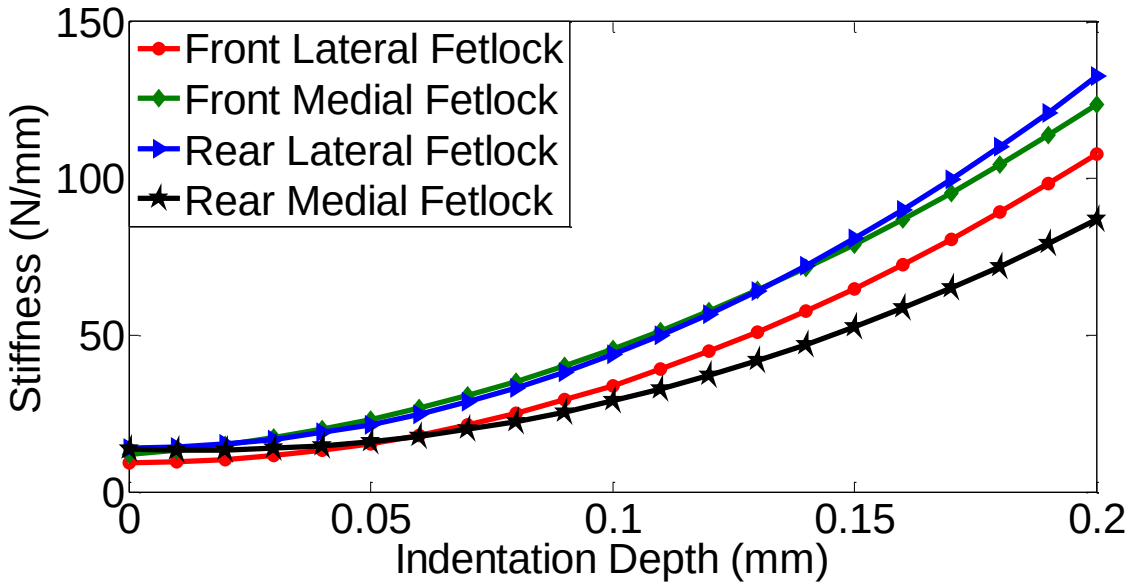

Figure 6.3: Comparison of the stiffness throughout the indentation depth between the articular cartilage surfaces from the fetlock joint

Table 6.4: Statistical comparison of three constants between the articular cartilage surfaces from the fetlock joint with p-values

Compared joints		P-value			
		A	B	C	D
Front lateral	Front medial	0.676	0.044	0.256	0.090
	Rear lateral	0.472	0.994	0.716	0.792
	Rear medial	0.570	0.243	0.074	0.716
Front medial	Rear lateral	0.232	2.21×10^{-8}	0.868	0.0003
	Rear medial	0.866	3.54×10^{-13}	0.494	4.16×10^{-5}
Rear lateral	Rear medial	0.179	3.22×10^{-9}	0.982	0.768

6.1.3 Comparison of stiffness between the surfaces in the carpus

The articular cartilage stiffness values of different surfaces in the carpus were compared. In the same manner used above, the coefficients of the stiffness equation were determined. The stiffness equations for each joint using the average coefficients were acquired (Table 6.5) and plotted (Figure 6.4). Contrary to the difference between cartilage surfaces in the fetlock, the stiffness of the distal radius is significantly greater than the stiffness of the other three surfaces in the carpus. The distal radius and the proximal radial carpal bone have visually different stiffness values from other surfaces while the distal radial carpal bone and proximal third carpal bone have similar stiffness values. In addition, it is observed that the stiffness values of the surfaces in the radiocarpal joint are greater than those in the midcarpal joint. Many p-values reflecting the difference between the distal radius and other surfaces in the first three rows are lower than 0.05 (Table 6.6). It shows that the distal radius is statistically different from other surfaces in terms of stiffness.

Table 6.5: Average coefficients of the articular cartilage surfaces in the carpus

Joints	Average coefficients			
	A [N/mm^3]	B [N/mm^2]	C [N/mm]	D [N]
Distal radius (C1)	414.5	47.13	7.552	0.022
Proximal radial carpal bone (C2)	237.2	17.09	4.044	0.024
Distal radial carpal bone (C3)	112.1	24.24	3.908	0.023
Proximal third carpal bone (C4)	173.4	3.761	4.650	0.010

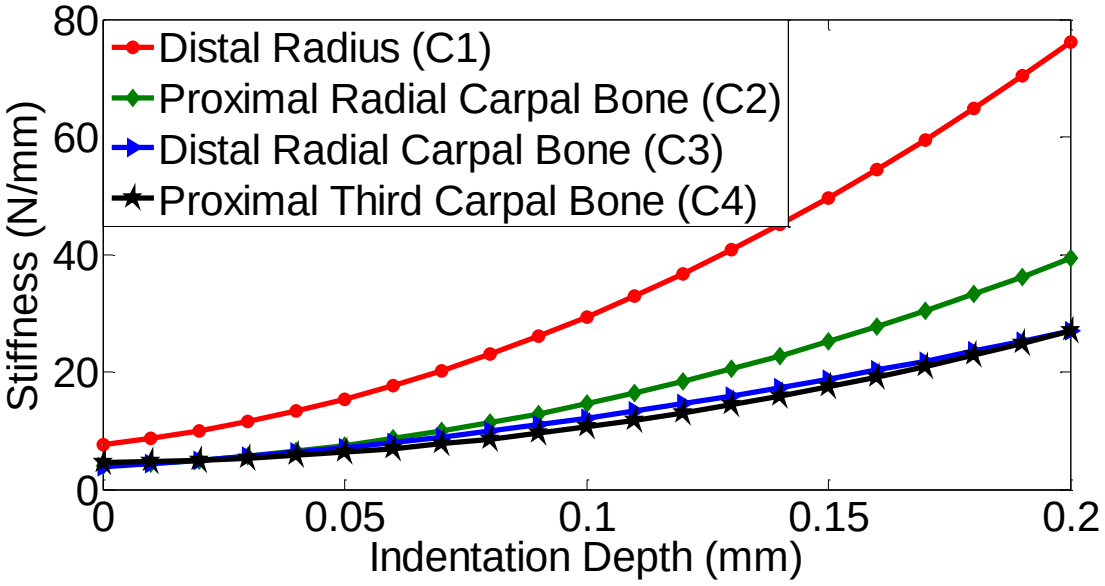

Figure 6.4: Comparison of the stiffness throughout the indentation depth between the articular cartilage surfaces from the carpal joint

Table 6.6: Statistical comparison of three constants between the articular cartilage surfaces from the carpal joint with p-values

Compared joints		P-value			
		A	B	C	D
Distal radius (C1)	Proximal radial carpal bone (C2)	0.113	0.358	0.038	0.825
	Distal radial carpal bone (C3)	0.002	0.445	0.038	0.925
	Proximal third carpal bone (C4)	0.040	0.161	0.100	0.331
Proximal radial carpal bone (C2)	Distal radial carpal bone (C3)	0.119	0.749	0.906	0.865
	Proximal third carpal bone (C4)	0.995	0.980	0.657	9.15×10^{-64}
Distal radial carpal bone (C3)	Proximal third carpal bone (C4)	0.476	0.295	0.557	0.186

6.2 Correlation between stiffness & weight and stiffness & age

The possible correlations between the stiffness and the weight, and the stiffness and the age of horses were studied. The results were displayed from in Figs 6.5 - 6.7. Each dot represents an individual horse in the graphs. In Figure 6.5, it appears that there is some evidence of an increase in these plots. However, there are still no clear trends of each correlation. Thus, more data is needed to make a valid conclusion. For the carpus, the trends of the plots (Figure 6.6) are ambiguous like those for the fetlock joint. Thus, more data is needed here as well to perform a conclusive analysis. There is far fewer data for the correlations on the stifle than the other two joints (Figure 6.7). Thus, more data of stifle joints is definitely needed.

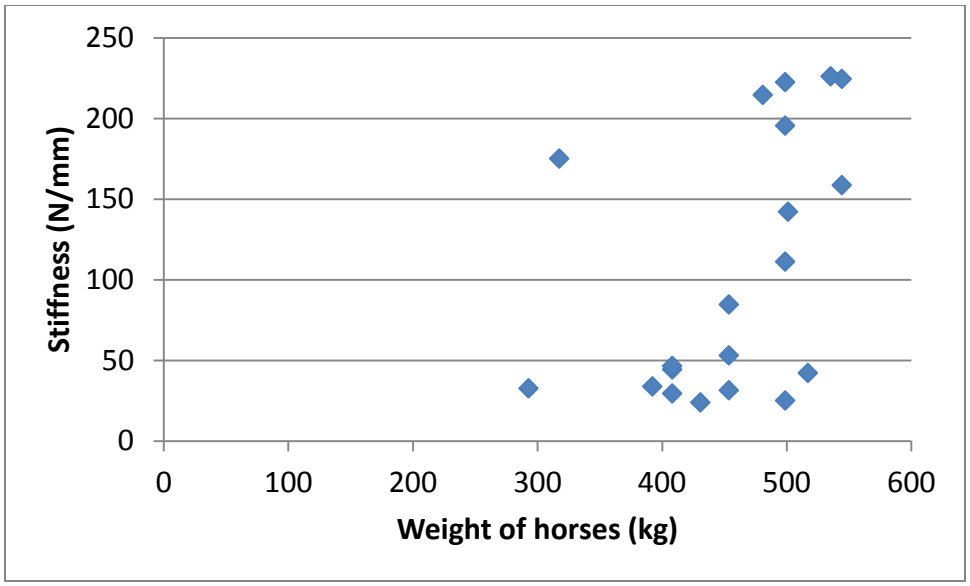

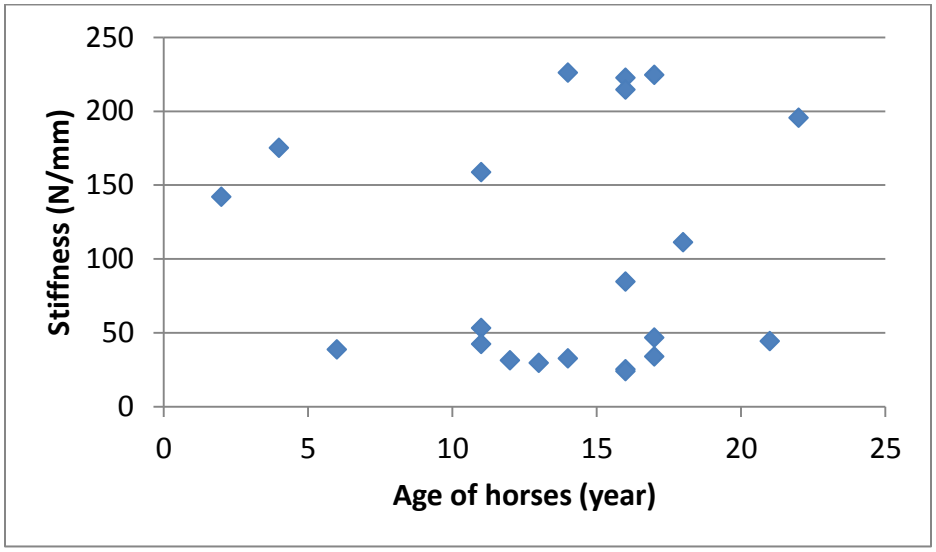

Figure 6.5: Correlation between the stiffness and the weight of horses (top) and between the stiffness and the age of horses (bottom) on the fetlock

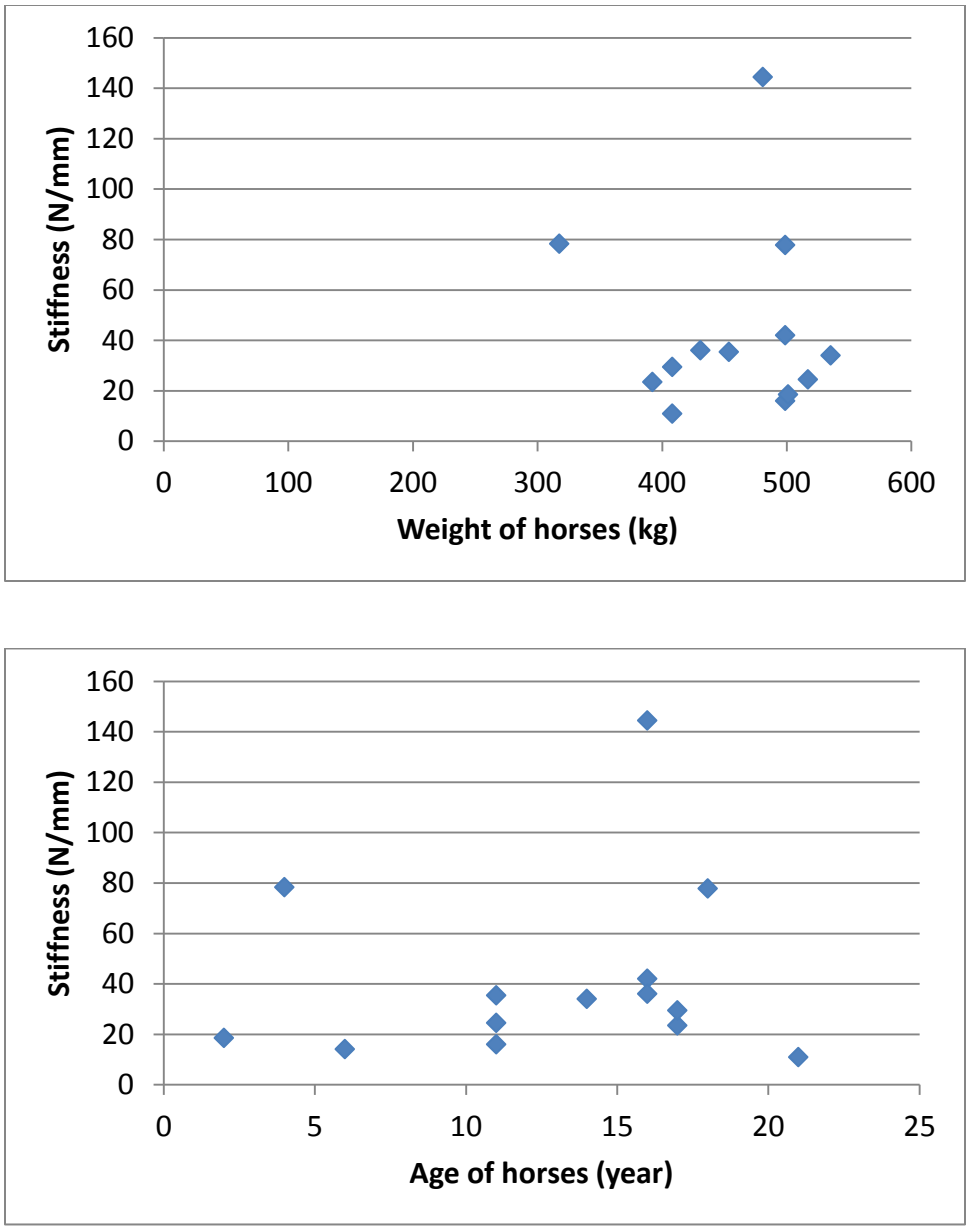

Figure 6.6: Correlation between the stiffness and the weight of horses (top) and between the stiffness and the age of horses (bottom) on the carpus

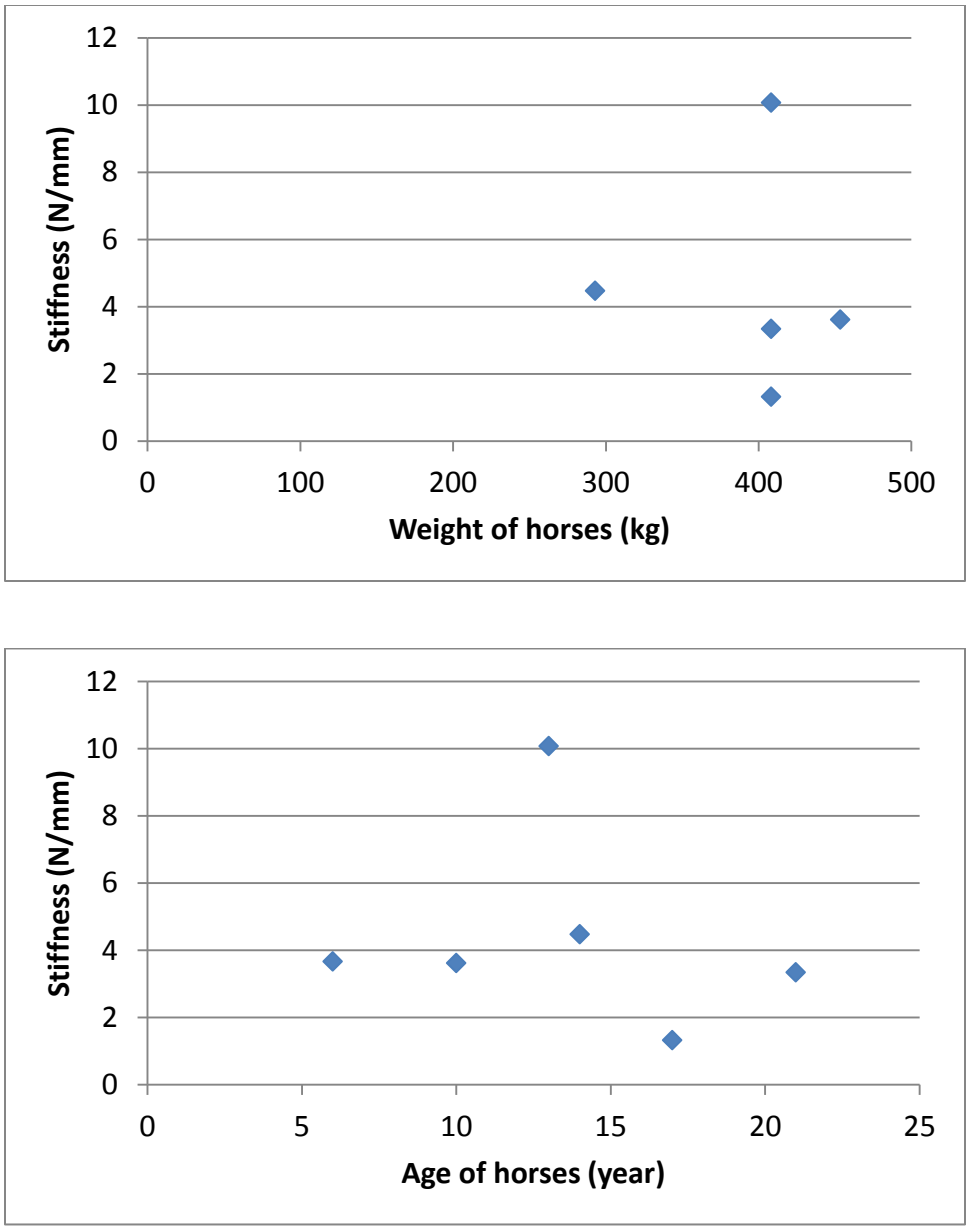

Figure 6.7: Correlation between the stiffness and the weight of horses (top) and between the stiffness and the age of horses (bottom) on the stifle

6.3 Thickness measurement (needle probe test)

6.3.1 Comparison between the fetlock, carpus, and stifle

The needle probe test was performed following the methodology described in chapter 4. The thicknesses of the fetlock, carpus, and stifle were compared. The average cartilage thickness of the fetlock and carpus were approximately 0.83mm, while the thickness of the stifle was more than twice that amount, approximately 2mm as shown in Figure 6.8 and Table 6.7. According to the previous studies, the measured thickness of the equine articular cartilage of a stifle joint is similar to the thickness of articular cartilage on a human knee [82, 83]. Therefore, the results here are in good agreement with previous works and may also provide a good model for a human knee joint.

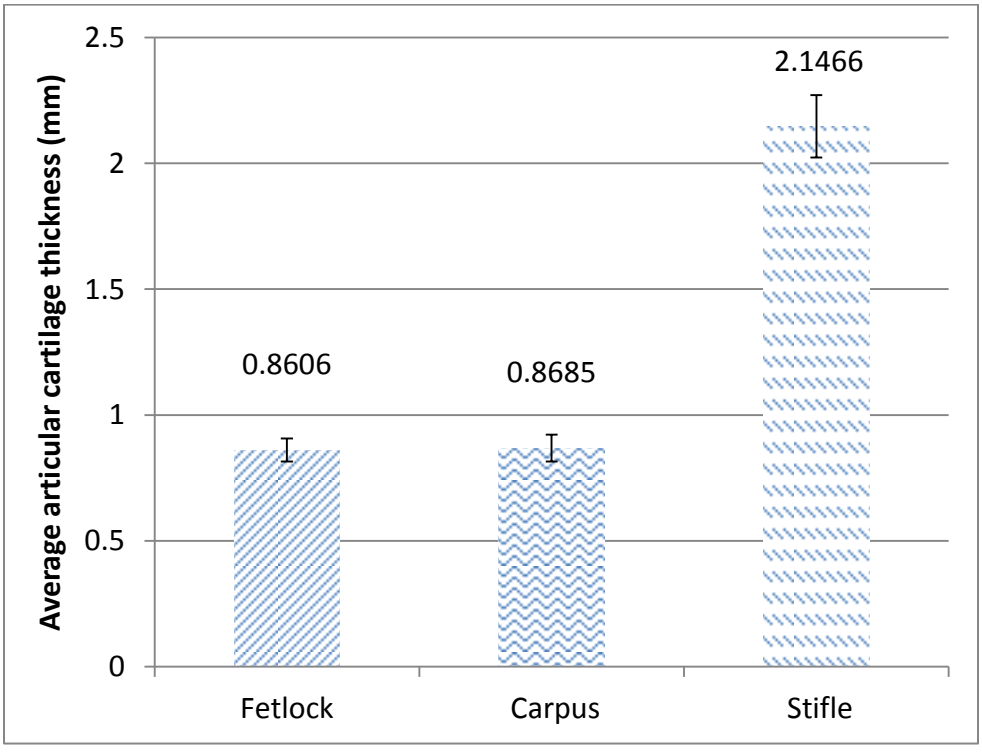

Figure 6.8: Comparison of the articular cartilage thickness between the fetlock, carpus, and stifle

Table 6.7: Comparison of the average thickness of articular cartilage and standard error between the fetlock, carpus, and stifle

Joints	Average thickness (mm)	Standard Error
Fetlock	0.8606	0.0459
Carpus	0.8685	0.0536
Stifle	2.1466	0.1239

Table 6.8: Statistical comparison of the articular cartilage thickness between the fetlock, carpus, and stifle with p-values

Compared joints		P-value	Difference
Fetlock	Carpus	0.913	No significant difference
	Stifle	3.09×10^{-9}	Very highly significant
Carpus	Stifle	1.26×10^{-9}	Very highly significant

The statistically analyzed data showed that the articular cartilage thickness of the stifle is significantly thicker than the thickness of the fetlock and carpus, while the fetlock and the carpus have a statistically equal thickness (Table 6.8).

6.3.2 Comparison of thickness between the surfaces of the fetlock

The thicknesses of different articular cartilage surfaces in the fetlock were compared (Figure 6.9). The p-values of each relation were greater than 0.05, showing that the four surfaces do not have significantly different thicknesses (Table 6.9). Front medial and rear medial surfaces have approximately the same cartilage thickness as their p-values were close to 1.

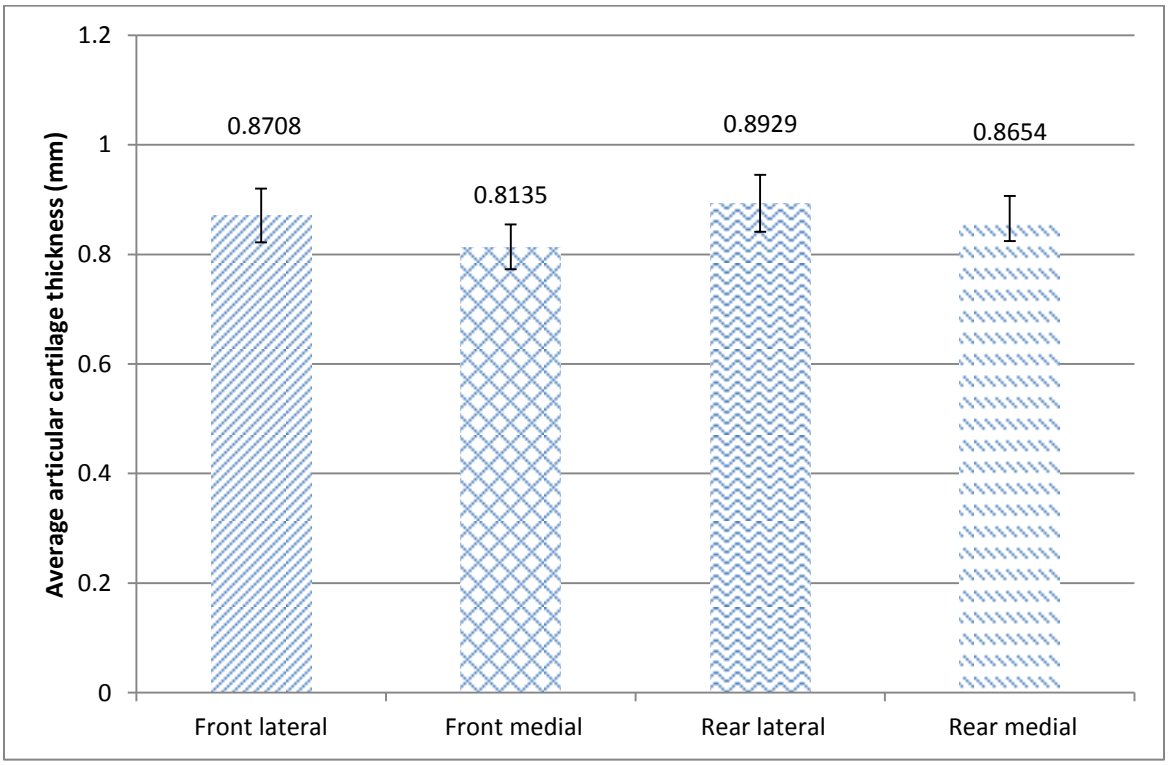

Figure 6.9: Comparison of the articular cartilage thickness between the surfaces from the fetlock

Table 6.9: Statistical comparison of the thickness between the articular cartilage surfaces from the fetlock joint with p-values

Compared joints		P-value
Front lateral	Front medial	0.381
	Rear lateral	0.762
	Rear medial	0.972
Front medial	Rear lateral	0.595
	Rear medial	0.703
Rear lateral	Rear medial	0.851

6.3.3 Comparison of thickness between the surfaces of the carpus

It is observed that there are differences not only among each of the four surfaces but also between the two joints (Figure 6.10). The proximal radial carpal bone is the thickest surface. In addition, the surfaces in the radiocarpal joint have thicker articular cartilage than those in the midcarpal joint.

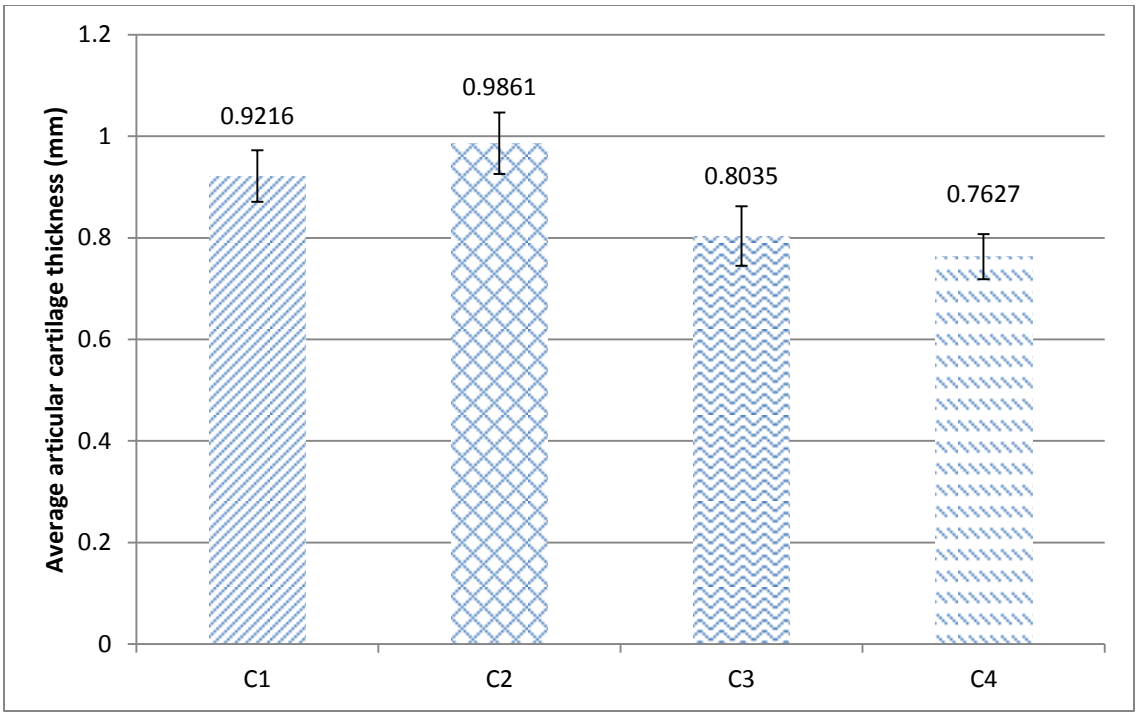

Figure 6.10: Comparison of the articular cartilage thickness between the surfaces from the carpus

Table 6.10: Statistical comparison of thickness between the articular cartilage surfaces from the carpal joint with p-values

Compared joints		P-value	Difference
Distal radius (C1)	Proximal radial carpal bone (C2)	0.424	•
	Distal radial carpal bone (C3)	0.144	•
	Proximal third carpal bone (C4)	0.030	Significant
Proximal radial carpal bone (C2)	Distal radial carpal bone (C3)	0.042	Significant
	Proximal third carpal bone (C4)	0.008	Highly significant
Distal radial carpal bone (C3)	Proximal third carpal bone (C4)	0.586	•

According to a statistical comparison, the thickness of the proximal radial carpal bone (C2) is different from the distal radial carpal bone (C3) and the proximal third carpal bone (C4), while the distal radius (C1) is different from the proximal third carpal bone (C4) as shown on Table 6.10. The thickness of articular cartilage varied on the surfaces of the carpal joint, while articular cartilage surfaces in the fetlock showed similar thicknesses.

6.4 Correlation between the stiffness, thickness, and curvature of the articular cartilage surfaces

The average stiffness, average thickness, and the radius of curvature of the cartilage surface between the three joints were compared (Table 6.11). The radius of curvature was measured manually and is not precise. This showed a correlation between the radius of curvature and thickness. The fetlock and carpus, whose radii of curvature were similar showed virtually the same thicknesses. Moreover, the stifle, whose radius of curvature was approximately twice as large as the fetlock and carpus, was approximately twice as thick as the fetlock and carpus. For the relation between the stiffness and thickness, and the stiffness and the radius of the curvature, there was some evidence that thinner cartilage and/or cartilage possessing a smaller radius of curvature was stiffer. However, significant correlations were not observed between the stiffness and thickness, or the stiffness and the radius of curvature. For example, the fetlock and carpus had approximately the same values of thickness and radius of the curvature, while the fetlock was twice as stiff as the carpus.

Table 6.11: The average stiffness, average thickness, and radius of curvature of the articular cartilage surface on each joint

Joints	Average Stiffness (N/mm)	Average Thickness (mm)	Approximate Radius of Curvature (mm)
Fetlock	46.11	0.8606	14.5
Carpus	20.50	0.8685	15.5
Stifle	2.725	2.1466	30

7. Discussion

For the stiffness measurements, the articular cartilage stiffness of the fetlock was greater than that of the carpus and stifle. The articular cartilage of the rear lateral fetlock and the articular cartilage of the distal radius were stiffest between surfaces in the fetlock and in the carpus, respectively. The articular cartilage surfaces of the carpus showed visually different stiffness values, while the stiffness values of the articular cartilage surfaces in the fetlock were similar - although they are not exactly the same. In addition, articular cartilage of the radiocarpal joint was stiffer than the midcarpal joint in the carpus.

There have been many efforts to quantify the elastic characteristics of the articular cartilage by determination of stiffness or aggregate modulus using the indentation method [36, 39, 40, 61, 93]. However, there are only few studies [101] about the stiffness measurement of different articular cartilage surfaces from different joints, specifically in the horse. Moreover, the studies were interested in different stiffness values depending on the different usage of the horse instead of the different joint as was examined in the current work. Some works also showed interest in different properties on different locations in the same joint, and in cartilage having different states of health. Mow's group performed a creep indentation test on three different cartilage surfaces in bovine knee joints to determine some properties [41]. They focused on testing not cartilage surfaces in different joints, but different cartilage surfaces in the same joint: lateral condyle, medial condyle, and patellar groove. Bae et al. implemented indentation testing on the cartilage surfaces from the human knee [93]. In their work, the cartilage surfaces harvested from the lateral femoral condyle and medial femoral condyle in human were classified into five groups: young-age normal, middle-age normal, middle-age degenerate, old-age normal,

and old-age degenerate. Samples were studied to find correlations between properties and age, and properties and degradation.

It is clear that most researchers focus on only the stifle or knee joint. This is because the stifle is the best joint to investigate as it is the most similar to the human knee, the most damaged joint in the human body. Through study of the stifle joint, people aim to obtain knowledge for human pre-clinical study. It also costs more when only one joint, rather than several different joints are, purchased at the same time though study of only one joint still require large funds. These possible reasons may explain why it is difficult to find research on the different properties of different joint. Nonetheless, the common point observed in all different studies is that the articular cartilage exposed to different conditions, such as different loading, showed different properties. Hence, the hypothesis that the equine articular cartilage properties vary on different joints in relation to different loading and motion appears to uphold as true. The hypothesis was validated through the results of this research. The results showed that the articular cartilage stiffness values in different joints are statistically different. In addition, it is observed that the articular cartilage stiffness values of the medial and lateral condyles are not significantly different, as an existing study also showed that the medial and lateral condyle cartilage of the bovine knee joint had similar aggregate moduli [41]. In Mow et al.'s work, other mechanical properties of lateral and medial condyle were very similar aside from the aggregate modulus, while those of the patellar groove were significantly different from the other two surfaces.

A 0.2mm indentation depth was employed to reach 20% strain of the articular cartilage in the longitudinal direction during indenting. This was done with the assumption that the cartilage thickness of the fetlock, carpus, and stifle is 1mm when the samples are considered as a regular specimen for the general compression test. After the thickness measurement, it was found that

the cartilage thicknesses of the three joints were different from each other. This means that the strain of cartilage surfaces from each joint was different, even though the indentation depth was the same. With the thickness measurement results, the stiffness values of the three joints were compared at the same level of strain. The articular cartilage surfaces from the fetlock, carpus, and stifle reach the 20% strain during indenting when the 0.1721mm, 0.1737mm, and 0.4293mm indentation depths were applied. These values were employed to calculate the average stiffness values of the articular cartilage surfaces from the three joints using equation 6.1 when the strain of each surface is 20%. As a result, the surfaces of the fetlock, carpus, and stifle had stiffness values of 37.46N/mm, 17.34N/mm, and 5.289N/mm, respectively. There was no considerable difference between these values and the average stiffness values shown in Chapter 6. In this case, however, the gap between the joints was smaller in stiffness. The stiffest and least stiff joints were the fetlock and stifle, respectively, as they were compared by same indentation depth in Chapter 6.

The correlations between stiffness and weight, and stiffness and age were investigated. The proteoglycan is the major factor in determining the elastic characteristic of the articular cartilage. Change in the structure of the proteoglycan molecules affects the mechanical properties of the articular cartilage. The structure of proteoglycan subunits changes markedly with increasing age. With aging, the proteoglycan content decreases while the keratin sulfate content increases relative to chondroitin sulfate in the cartilage matrix. Due to the change of proteoglycan in concentration, size, and charge, the articular cartilage loses the ability to retain water within itself, causing a decrease of its elastic characteristics, as well as degradation of the articular cartilage [102]. A previous study also showed that failure occurred on older cartilage samples at lower cycles than on younger samples in the fatigue test [103]. Because of these facts,

it would be expected that older horses have stiffer articular cartilage. It appears that there is some evidence of an increase in the relation between stiffness and age, but a clear trend was not found in the current work. A clear correlation is expected with the addition of more data in future work.

When it comes to the relation between stiffness and weight, there are complicated factors that should be considered. First, the breed of the investigated horses should be considered. The articular cartilage surfaces harvested from in this work were from 10 different breeds. They also have different ranges of weight. For example, the Welsh Pony is a smaller breed of horse than others. An adult of the breed typically weighs 320kg, while AQH (American Quarter Horse) usually weighs over 500kg. It is possible that two horses that have similar weights and different ages (one is young and the other is old) while have comparable cartilage properties. Since two horses could have differing cartilage health, the properties of their cartilage cannot be simply compared by weight. Furthermore, each horse has a different constitution. It is possible, therefore, that the health of the articular cartilage in the compared horses is different, regardless of their weight. In other words, the horses' articular cartilage can have different conditions due to their constitutions rather than their weight. In this situation, it is difficult to measure the effect of weight alone on the cartilage properties. Hence, the correlations between properties and the various parameters should be investigated considering these factors.

For the thickness measurements, the articular cartilage in the stifle joint was the thickest among the fetlock, carpus, and stifle. The thickness of the articular cartilage of the fetlock and the carpus are very similar. Within the carpus, the cartilage of the proximal radial carpal bone was the thickest and the radiocarpal joint showed to possess thicker cartilage than the midcarpal joint. Furthermore, there was no significant difference in the thickness of the articular cartilage

of the medial and later condyles in the fetlock as the thicknesses of the medial and lateral fetlock cartilage surfaces are not significantly different.

The thickness of the equine articular cartilage has been the focus of attention in many studies because it is an extrinsic property which can be easily compared with the cartilage in humans. Thus, the articular cartilage thicknesses of the stifle in the literature [82-84, 89] was validated by the measurements in this study. The articular cartilage thickness of the distal medial condyle measured in Frisbie et al.'s work was 2.203mm [82]. This value virtually agreed with the determined cartilage thickness of 2.147mm on the equine stifle in this work. Though there are unfortunately no comparison targets for the fetlock and carpus, the agreement of the stifle validated the accuracy of the data of the measurement technique and all the resulting data.

Different properties between the various joints could be attributed to the different mechanisms of each joint, as mentioned previously. Possible reasons for the different mechanisms, including the geometry of the articular cartilage surface and the motion of the different joints (mentioned previously in Chapter 3), were discussed.

First, different joint types can cause the variation of the articular cartilage properties on different joints. For instance, the radiocarpal joint is a type of condylar joint, while the midcarpal joint is an ellipsoidal joint type in spite of the fact that they are in the same joint assembly, the carpus. These different types of joints show different motions in various movements of flexion, extension, adduction, and abduction. The radiocarpal joint shows sliding and rolling motion with a wide range of 90 or 100º of articulation, while the midcarpal joint shows a 'book' like motion of only 45º. The difference between the two joints in motion could be a likely reason for the different mechanisms and therefore different mechanical properties of the joints.

Second, the different pressure distributions on the forelimb and hindlimb can result from the fact that the front limbs generally carry more weight and under larger impacts, while the rear limbs act as a forward-propelling force. Clayton et al. studied the ground reaction force and the fetlock kinematics in the horse [100]. In their work, various normalized forces were measured besides the ground reaction force when horses were trotting. The result showed that forelimb and hindlimb carry approximately 55% and 45% of the total load, respectively. The carpus is in the forelimb and the stifle is in hindlimb. According to the measurements of Clayton et al.'s work, the two joints carry and bear different magnitude of load. This difference could be the reason for different mechanisms and mechanical properties in the joints. For the fetlock, the joints are in both the forelimb and hindlimb. Though the joints are classified the same, the articular cartilage surfaces in the fetlock from the forelimb and hindlimb had different stiffness and thickness values. It could be the result of the different mechanisms due to the different load carry capacities in the forelimb and hindlimb.

Furthermore, the different composition of the components in different articular cartilage surfaces (e.g. the stifle is the only one of the three joints with a meniscal component) can bring about the different weight bearing characteristics. Brama et al. evaluated topographical differences between the biochemical composition of articular cartilage surfaces [104]. The biochemical properties of the cartilage matrix in the fetlock were investigated. The results demonstrated that the water and the GAG contents are significantly different in the right and left fetlock joints as well as on different sites on the same surface. Water is the most predominant component in the cartilage and plays a major role in the lubrication and supply of nutrients to the cartilage. The GAGs are also important ingredients because they are the major components forming the proteoglycan that determine the mechanical characteristics of the cartilage as

described earlier in this chapter. Hence, the different contents of these crucial components in different joints would bring about different mechanisms and properties in various joints.

Moreover, proximity to the body could be the reason of the difference denoted by distal and proximal. For example, the radiocarpal and midcarpal joints that are sub-joints in the carpus have different proximities. As described in Chapter 3, the midcarpal joint is located lower than the radiocarpal joint in position although they are in the same carpus joint assembly. It is observed that the properties of the articular cartilage surfaces from the joints were different. The fetlock and carpus have different proximities as well. The fetlock is closer to the ground, while the carpus is closer to the body. The two joints carry the same amount of load because they are in the same leg. However, it is possible that there are geometrical and kinematic factors causing the loads to change from joint to joint in the limb, bringing about the different characteristics between the joints.

Finally, different geometries of the articular cartilage surfaces and joints such as their sizes and shapes, can give rise to the different pressure distributions [85, 105]. The different sizes and shapes of the various articular cartilage surfaces were already displayed and discussed in Chapter 3. Surfaces of different sizes show different pressure distributions even if they are under the same magnitude of load because the contact areas carrying the load are different. Different shapes also causes different mechanisms of load carrying with different motions. Thus, this could result in the difference of mechanisms and properties in different joints.

An investigation to find correlations between these possible explanations and the difference of material properties is needed as a future work to make possible the tailored design

of artificial biomimetic joints and cartilage surfaces. In addition, it is important to select the optimal methodology among those available for more realistic testing and analysis.

8. Conclusions

Ceaseless research of the articular cartilage has been conducted to understand and describe the characteristics of articular cartilage for the past 7 decades. Although some groups conducted measurements on human articular cartilage samples [91-93], most researchers still perform measurements on the articular cartilage from animals, instead of humans due to the difficulty in obtaining human cartilage samples. Furthermore, national institutions may not be willing to authorize new research of cartilage treatments applied directly to humans without a validated model or supportive data. Hence, the alternative cartilage model for a human preclinical study is needed and many researchers have investigated the possibility of various models using different animals.

Although the articular cartilage from small animals has been widely used in research due to the relatively high cost for large animals, many studies show the advantages of the equine model. The equine model is a large animal model providing the closest approximation to humans [82, 84, 89, 90]. In other words, the equine model has been acknowledged as, while not perfect, the best alternative model to humans. Unfortunately, as yet, there are no models describing the behavior of the equine articular cartilage. Thus, more clinical studies of the well-established equine articular cartilage model, having high human applicability, are urgently needed. The characterization of material properties has to proceed the initiation of the model establishment because the properties are fundamental indicators of the unique behavior of the material. This must also be accompanied by the study of the equine articular cartilage on the different joints because of the different properties of different joints mentioned in this work. It will lead to the establishment of the best fit of a model to the equine articular cartilage in each joint. However,

there are only a few studies which focus on the variation of mechanical properties between different equine articular cartilage surfaces in different joints in the horse. Therefore, this study was conducted to characterize the stiffness and thickness of the equine articular cartilage in different joints as the first step, heeded for modeling of the equine articular cartilage.

As shown, most equine articular cartilage from joints showed a statistically different stiffness and thickness from each other. For the stiffness, the articular cartilage in the fetlock was stiffer than the cartilage in the carpus. The rear lateral articular cartilage surface and the distal radius surface were the stiffest in the fetlock and in the carpus, respectively. In addition, it was observed that the cartilage stiffness of the radiocarpal joint was greater than that of the midcarpal joint in the carpus. For the thickness, the stifle joint showed the thickest articular cartilage of all three joints. Although the articular cartilage of the fetlock and the carpus showed very similar thicknesses, the cartilage in the carpus was slightly thicker than that in the fetlock. The cartilage of the proximal radial carpal bone was thickest in the carpal joint. Moreover, the cartilage surfaces in the radiocarpal joint were thicker than those in the midcarpal joint.

The mechanical properties were measured not only for characterization but to also illuminate the difference between different joint surfaces. Thereby, this study became the initial point to the eventual quantitative understanding of equine cartilage performance in relation to the mechanical properties. Furthermore, it is expected that the properties of the articular cartilage should probably be tailored for different conditions to design effective biomimetic artificial cartilage joints. This knowledge with the proposed future work in the next chapter will eventually make it possible to develop and design optimal artificial joints that more closely mimic the biological loading properties. It will also contribute to the improvement of the replacement technologies that will radically surpass and outperform existing commercial

artificial joints, providing a transformative advancement to the field of the biomechanical engineering.

9. Future work

Multiple future works have been planned following this study for understanding cartilage performance in relation to measurable mechanical properties.

Mechanical properties other than stiffness will be determined via the indentation curve. The aggregate modulus, Poisson's ratio, permeability, and viscosity of the equine articular cartilage will be measured from the indentation test by employing the squeeze film model. In addition, another traditional method will be used: namely, the creep test where the change of the displacement is recorded in time while a constant force is applied to a sample. The mechanical properties will be double checked by comparison between those from the two test methods.

A different type of indenter, such as spherical one, will be employed for the next experiments to reduce the effect of the curvature of the articular cartilage. This will help to make a better contact between the indenter and samples. The stress concentration on the edge of the flat-ended indenter is not needed to be concerned using an indenter with different shape.

A fixed indenting velocity and indentation depth was applied in this work. In future tests, multiple indenting velocities and indentation depths will be employed to observe the effect on the mechanical behavior of the material. Afterwards, an indenting velocity and indentation depth providing a closer mimicking the actual loading situation eventually should be found.

A study of the load carriage mechanism in different joints will be implemented to discover the factors causing the different pressure distributions on each articular cartilage surface in relation to the different loads and motions of each joint.

The investigation of the correlation between stiffness and other parameters such as age and weight of horses will continue to be conducted.

The comparison of results of future tests on fresh and frozen samples will be an informative study because there are still many people who use frozen articular cartilage samples in their research without a clear check about the effect of freezing.

For cartilage thickness measurements, established MRI methods [106] will be performed to compare to the needle probe test results. Auburn University now houses a unique 7 Tesla (7T) Magnetic Resonance Imaging (MRI) machine dedicated solely to research. There are only eighteen 7T-MRI facilities available in the US and two in the Southeast US, so the new 7T-MRI provides a unique opportunity. Optimal imaging of samples in the 7T MRI will also require a custom coil designed to fit the shape and size of the equine joints. The Auburn MRI Research Center has fabricated a custom coil designed to image these joints. Not only will the coil and MRI sequencing routines be optimized, but the resolution will also improve with further coil and sequences testing.

With this study, the completion of the further works stated here will characterize the material properties of different articular joint cartilage surfaces and correlate them to the relative load and motion of each surface. This research will be very important for future work specifying design criteria for cartilage replacement and biomimetic technologies.

References

[1] Z. M. Jin, M. Stone, E. Ingham, and J. Fisher, "Biotribology," *Current Orthopaedics,* vol. 20, pp. 32-40, Feb 2006.

[2] F. C. Wang and Z. M. Jin, "Elastohydrodynamic lubrication modeling of artificial hip joints under steady-state conditions," *J. of Tribol. -Trans. of ASME,* vol. 127, pp. 729-739, Oct 2005.

[3] M. Hlavacek, "Squeeze-film lubrication of the human ankle joint subjected to the cyclic loading encountered in walking," *J. of Tribol. -Trans. of ASME,* vol. 127, pp. 141-148, Jan 2005.

[4] A. N. Suciu, T. Iwatsubo, and M. Matsuda, "Theoretical investigation of an artificial joint with micro-pocket-covered component and biphasic cartilage on the opposite articulating surface," *J. of Biomech. Eng. -Trans. of ASME,* vol. 125, pp. 425-433, Aug 2003.

[5] M. Hlavacek, "The thixotropic effect of the synovial fluid in squeeze-film lubrication of the human hip joint," *Biorheology,* vol. 38, pp. 319-334, 2001.

[6] D. Jalali-Vahid, N. Jagatia, Z. M. Jin, and D. Dowson, "Prediction of lubricating film thickness in a ball-in-socket model with a soft lining representing human natural and artificial hip joints," *Proc. of the Inst. of Mech. Eng. Part J-J. of Eng. Tribol.,* vol. 215, pp. 363-372, 2001.

[7] S. L. Graindorge and G. W. Stachowiak, "Changes occurring in the surface morphology of articular cartilage during wear," *Wear,* vol. 241, pp. 143-150, Jul 2000.

[8] T. Stewart, Z. M. Jin, and J. Fisher, "Analysis of contact mechanics for composite cushion knee joint replacements," *Proc. of the Inst. of Mech. Eng. Part H-J. of Eng. In Medicine,* vol. 212, pp. 1-10, 1998.

[9] Z. M. Jin, D. Dowson, and J. Fisher, "Analysis of fluid film lubrication in artificial hip joint replacements with surfaces of high elastic modulus," *Proc. of the Inst. of Mech. Eng. Part H-J. of Eng. in Medicine,* vol. 211, pp. 247-256, 1997.

[10] R. S. Fein, "Are Synovial Joints Squeeze-film Lubricated," *Proc. Inst. Mech. Eng. Part J,* vol. 18, p. 125, 1967.

[11] G. R. Higginson, "Elastohydrodynamic Lubrication in Human Joints," *Engineering in Medicine,* vol. 7, pp. 35-41, 1978.

[12] J. Fisher and D. Dowson, "Tribology of total artificial joints," *Proceedings of the Institution of Mechanical Engineers, Part H: Journal of Engineering in Medicine,* vol. 205, p. 73, 1991.

[13] E. Poiré, "Advanced Surface Mechanical Testing of Materials for Medical Applications," 2009.

[14] L. Røhl, F. Linde, A. Odgaard, and I. Hvid, "Simultaneous measurement of stiffness and energy absorptive properties of articular cartilage and subchondral trabecular bone," *Proceedings of the Institution of Mechanical Engineers, Part H: Journal of Engineering in Medicine,* vol. 211, pp. 257-264, 1997.

[15] H. Bang, Y.-l. Chiu, S. G. Memtsoudis, L. A. Mandl, A. G. Della Valle, A. I. Mushlin, R. G. Marx, and M. Mazumdar, "Total hip and total knee arthroplasties: trends and disparities revisited," *American Journal of Orthopedics,* vol. 39, p. E95, 2010.

[16] E. S. Fisher, J. Bell, I. Tomek, A. Esty, D. Goodman, and K. Bronner, "Trends and regional variation in hip, knee, and shoulder replacement," *Dartmouth Atlas Surgery Report. Hanover, NH: The Dartmouth Institute for Health Policy and Clinical Practice,* 2010.

[17] S. M. Kurtz, K. L. Ong, E. Lau, M. Widmer, M. Maravic, E. Gomez-Barrena, F. de Pina Mde, V. Manno, M. Torre, W. L. Walter, R. de Steiger, R. G. Geesink, M. Peltola, and C. Roder, "International survey of primary and revision total knee replacement," *Int Orthop,* vol. 35, pp. 1783-9, Dec 2011.

[18] (April 24). Available: https://www.healthcarebluebook.com

[19] Z. M. Jin and D. Dowson, "Elastohydrodynamic lubrication in biological systems," *Proceedings of the Institution of Mechanical Engineers, Part J: Journal of Engineering Tribology,* vol. 219, pp. 367-380, 2005.

[20] T. Pylios and D. E. T. Shepherd, "Prediction of lubrication regimes in wrist implants with spherical bearing surfaces," *Journal of Biomechanics,* vol. 37, pp. 405-411, 2004.

[21] M. E. Freeman, M. J. Furey, B. J. Love, and J. M. Hampton, "Friction, wear, and lubrication of hydrogels as synthetic articular cartilage," *Wear,* vol. 241, p. 129, 2000.

[22] R. J. Covert, D. N. Ku, and R. D. Ott, "Friction characteristics of a potential articular cartilage biomaterial," *Wear,* vol. 255, pp. 1064-1068, 2003.

[23] L. Caravia, D. Dowson, J. Fisher, P. H. Corkhill, and B. J. Tighe, "Comparison of friction in hydrogel and polyurethane materials for cushion-form joints," *Journal of Materials Science: Materials in Medicine,* vol. 4, p. 515, 1993.

[24] Y. Sawae, T. Murakami, H. Higaki, and S. Moriyama, "Lubrication property of total knee prostheses with PVA hydrogel layer as artificial cartilage," *JSME International Journal, Series C,* vol. 39, p. 356, 1996.

[25] J. A. Stammen, S. Williams, D. N. Ku, and R. E. Guldberg, "Mechanical properties of a novel hydrogel for the replacement of damaged articular cartilage," *Annual International*

Conference of the IEEE Engineering in Medicine and Biology - Proceedings, vol. 2, p. 725, 1999.

[26] L. Caravia, D. Dowson, J. Fisher, P. H. Corkhill, and B. J. Tighe, "Friction of hydrogel and polyurethane elastic layers when sliding against each other under a mixed lubrication regime," *Wear*, vol. 181-183, p. 236, 1995.

[27] T. Murakami, H. Higaki, Y. Sawae, N. Ohtsuki, S. Moriyama, and Y. Nakanishi, "Adaptive multimode lubrication in natural synovial joints and artificial joints," *Proceedings of the Institution of Mechanical Engineers, Part H: Journal of Engineering in Medicine*, vol. 212, p. 23, 1998.

[28] N. A. Steika, M. J. Furey, H. P. Veit, and M. Brittberg, "Biotribology: The wear resistance of repaired human articular cartilage," Washington, D.C., United States, 2005, p. 619.

[29] M. A. R. Freeman, *Adult articular cartilage*: Grune & Stratton, 1974.

[30] D. Frisbie, "Synovial joint biology and pathobiology," *Equine Surgery, 3rd ed. Auer JA, Stick JA, eds. St. Louis, Mo: Elsevier, Saunders*, pp. 1036-1055, 2006.

[31] X. L. Lu and V. C. Mow, "Biomechanics of articular cartilage and determination of material properties," *Med Sci Sports Exerc*, vol. 40, pp. 193-9, Feb 2008.

[32] M. J. Furey, "Joint lubrication," *Biomechanics: Principles and Application*, 2000.

[33] F. G. Donnan, "The Theory of Membrane Equilibria," *Chemical Reviews*, vol. 1, pp. 73-90, 1924/04/01 1924.

[34] E. D. Bonnevie, V. J. Baro, L. Wang, and D. L. Burris, "Fluid load support during localized indentation of cartilage with a spherical probe," *Journal of Biomechanics*, vol. 45, pp. 1036-1041, 2012.

[35] X. Lu and V. Mow, "Biomechanics of articular cartilage and determination of material properties," *Medicine+ Science in Sports+ Exercise,* vol. 40, p. 193, 2008.

[36] X. L. Lu, D. N. Sun, X. E. Guo, F. Chen, W. M. Lai, and V. Mow, "Indentation Determined Mechanoelectrochemical Properties and Fixed Charge Density of Articular Cartilage," *Annals of Biomedical Engineering,* vol. 32, pp. 370-379, 2004/03/01 2004.

[37] G. A. Ateshian, "The role of interstitial fluid pressurization in articular cartilage lubrication," *Journal of Biomechanics,* vol. 42, pp. 1163-1176, 2009.

[38] A. W. Pearsall, J. A. Tucker, R. B. Hester, and R. J. Heitman, "Chondrocyte viability in refrigerated osteochondral allografts used for transplantation within the knee," *The American Journal of Sports Medicine,* vol. 32, pp. 125-131, 2004.

[39] A. Mak, W. Lai, and V. Mow, "Biphasic indentation of articular cartilage—I. Theoretical analysis," *Journal of Biomechanics,* vol. 20, pp. 703-714, 1987.

[40] V. Mow, "Biphasic creep and stress relaxation of articular cartilage in compression," *J. Biomech. Eng.,* vol. 102, pp. 73-84, 1980.

[41] V. Mow, M. Gibbs, W. Lai, W. Zhu, and K. Athanasiou, "Biphasic indentation of articular cartilage—II. A numerical algorithm and an experimental study," *Journal of Biomechanics,* vol. 22, pp. 853-861, 1989.

[42] X. Lux Lu, C. Miller, F. H. Chen, X. Edward Guo, and V. C. Mow, "The generalized triphasic correspondence principle for simultaneous determination of the mechanical properties and proteoglycan content of articular cartilage by indentation," *Journal of Biomechanics,* vol. 40, pp. 2434-2441, 2007.

[43] W. Lai, J. Hou, and V. Mow, "A triphasic theory for the swelling and deformation behaviors of articular cartilage," *Journal of biomechanical engineering,* vol. 113, p. 245, 1991.

[44] W. Hayes and A. Bodine, "Flow-independent viscoelastic properties of articular cartilage matrix," *Journal of Biomechanics,* vol. 11, pp. 407-419, 1978.

[45] A. Mak, "The apparent viscoelastic behavior of articular cartilage--the contributions from the intrinsic matrix viscoelasticity and interstitial fluid flows," *Journal of biomechanical engineering,* vol. 108, p. 123, 1986.

[46] J. Parsons and J. Black, "The viscoelastic shear behavior of normal rabbit articular cartilage," *Journal of Biomechanics,* vol. 10, pp. 21-29, 1977.

[47] A. A. Spirt, A. F. Mak, and R. P. Wassell, "Nonlinear viscoelastic properties of articular cartilage in shear," *Journal of Orthopaedic Research,* vol. 7, pp. 43-49, 1989.

[48] S. Woo, B. Simon, S. Kuei, and W. Akeson, "Quasi-linear viscoelastic properties of normal articular cartilage," *Journal of biomechanical engineering,* vol. 102, p. 85, 1980.

[49] V. C. Mow and W. C. Hayes, *Basic orthopaedic biomechanics*: Lippincott-Raven Philadelphia, PA, 1997.

[50] M. D. Buschmann, J. Soulhat, A. Shirazi-Adl, J. S. Jurvelin, and E. B. Hunziker, "Confined compression of articular cartilage: linearity in ramp and sinusoidal tests and the importance of interdigitation and incomplete confinement," *Journal of Biomechanics,* vol. 31, pp. 171-178, 1997.

[51] K. M. Clements, A. P. Hollander, M. Sharif, and M. A. Adams, "Cyclic loading can denature type II collagen in articular cartilage," *Connective tissue research,* vol. 45, pp. 174-180, 2004.

[52] L. Li, M. Buschmann, and A. Shirazi-Adl, "Fibril stiffening accounts for strain-dependent stiffness of articular cartilage in unconfined compression," *Transactions of the Orthopaedic Research Society,* vol. 26, p. 425, 2001.

[53] F. Boschetti, G. Pennati, F. Gervaso, G. M. Peretti, and G. Dubini, "Biomechanical properties of human articular cartilage under compressive loads," *Biorheology,* vol. 41, pp. 159-166, 2004.

[54] R. Korhonen, M. Laasanen, J. Töyräs, J. Rieppo, J. Hirvonen, H. Helminen, and J. Jurvelin, "Comparison of the equilibrium response of articular cartilage in unconfined compression, confined compression and indentation," *Journal of Biomechanics,* vol. 35, p. 903, 2002.

[55] M. R. DiSilvestro and J.-K. F. Suh, "A cross-validation of the biphasic poroviscoelastic model of articular cartilage in unconfined compression, indentation, and confined compression," *Journal of Biomechanics,* vol. 34, pp. 519-525, 2001.

[56] W. C. Oliver and G. M. Pharr, "Improved technique for determining hardness and elastic modulus using load and displacement sensing indentation experiments," *Journal of materials research,* vol. 7, pp. 1564-1583, 1992.

[57] G. Pharr, W. Oliver, and F. Brotzen, "On the generality of the relationship among contact stiffness, contact area, and elastic modulus during indentation," *Journal of materials research,* vol. 7, pp. 613-617, 1992.

[58] R. C. Appleyard, M. V. Swain, S. Khanna, and G. A. Murrell, "The accuracy and reliability of a novel handheld dynamic indentation probe for analysing articular cartilage," *Physics in medicine and biology,* vol. 46, p. 541, 2001.

[59] J. Huyghe and J. Janssen, "Quadriphasic mechanics of swelling incompressible porous media," *International Journal of Engineering Science,* vol. 35, pp. 793-802, 1997.

[60] H. Jin and J. L. Lewis, "Determination of Poisson's ratio of articular cartilage by indentation using different-sized indenters," *Journal of biomechanical engineering,* vol. 126, p. 138, 2004.

[61] N. K. Simha, H. Jin, M. L. Hall, S. Chiravarambath, and J. L. Lewis, "Effect of indenter size on elastic modulus of cartilage measured by indentation," *Journal of biomechanical engineering,* vol. 129, p. 767, 2007.

[62] R. K. Korhonen, M. S. Laasanen, J. Toyras, J. Rieppo, J. Hirvonen, H. J. Helminen, and J. S. Jurvelin, "Comparison of the equilibrium response of articular cartilage in unconfined compression, confined compression and indentation," *J Biomech,* vol. 35, pp. 903-9, Jul 2002.

[63] M. R. DiSilvestro and J. K. Suh, "A cross-validation of the biphasic poroviscoelastic model of articular cartilage in unconfined compression, indentation, and confined compression," *J Biomech,* vol. 34, pp. 519-25, Apr 2001.

[64] S. Park, C. T. Hung, and G. A. Ateshian, "Mechanical response of bovine articular cartilage under dynamic unconfined compression loading at physiological stress levels," *Osteoarthritis Cartilage,* vol. 12, pp. 65-73, Jan 2004.

[65] S. Ronken, M. P. Arnold, H. Ardura Garcia, A. Jeger, A. U. Daniels, and D. Wirz, "A comparison of healthy human and swine articular cartilage dynamic indentation mechanics," *Biomech Model Mechanobiol,* vol. 11, pp. 631-9, May 2012.

[66] M. Stolz, R. Raiteri, A. U. Daniels, M. R. VanLandingham, W. Baschong, and U. Aebi, "Dynamic elastic modulus of porcine articular cartilage determined at two different levels

of tissue organization by indentation-type atomic force microscopy," *Biophys J*, vol. 86, pp. 3269-83, May 2004.

[67] R. C. Appleyard, M. V. Swain, S. Khanna, and G. A. Murrell, "The accuracy and reliability of a novel handheld dynamic indentation probe for analysing articular cartilage," *Phys Med Biol*, vol. 46, pp. 541-50, Feb 2001.

[68] W. Hayes, L. Keer, G. Herrmann, and L. Mockros, "A mathematical analysis for indentation tests of articular cartilage," *Journal of Biomechanics*, vol. 5, pp. 541-551, 1972.

[69] G. A. Ateshian and H. Wang, "A theoretical solution for the frictionless rolling contact of cylindrical biphasic articular cartilage layers," *Journal of Biomechanics*, vol. 28, pp. 1341-1355, 1995.

[70] X. L. Lu, L. Q. Wan, X. Edward Guo, and V. C. Mow, "A linearized formulation of triphasic mixture theory for articular cartilage, and its application to indentation analysis," *Journal of Biomechanics*, vol. 43, pp. 673-679, 2010.

[71] P. A. Smyth, R. E. Rifkin, R. L. Jackson, and R. REID HANSON, "A Surface Roughness Comparison of Cartilage in Different Types of Synovial Joints," *Journal of biomechanical engineering*, vol. 134, 2012.

[72] P. A. Smyth, R. E. Rifkin, R. L. Jackson, and R. Reid Hanson, "The Fractal Structure of Equine Articular Cartilage," *Scanning*, vol. 34, pp. 418-426, 2012.

[73] E. Bonnevie, V. Baro, L. Wang, and D. L. Burris, "In situ studies of cartilage microtribology: roles of speed and contact area," *Tribology letters*, vol. 41, pp. 83-95, 2011.

[74] J. M. Mansour and V. C. Mow, "The permeability of articular cartilage under compressive strain and at high pressures," *J Bone Joint Surg Am*, vol. 58, pp. 509-16, 1976.

[75] A. Maroudas, P. Bullough, S. Swanson, and M. Freeman, "The permeability of articular cartilage," *Journal of Bone & Joint Surgery, British Volume*, vol. 50, pp. 166-177, 1968.

[76] P. Brama, D. Karssenberg, A. Barneveld, and P. v. Weeren, "Contact areas and pressure distribution on the proximal articular surface of the proximal phalanx under sagittal plane loading," *Equine veterinary journal*, vol. 33, pp. 26-32, 2001.

[77] J. L. Palmer, A. L. Bertone, and A. Litsky, "Contact area and pressure distribution changes of the equine third carpal bone during loading," *Equine veterinary journal*, vol. 26, pp. 197-202, 1994.

[78] S. d. Hartog, W. Back, H. Brommer, and P. v. Weeren, "In vitro evaluation of metacarpophalangeal joint loading during simulated walk," *Equine veterinary journal*, vol. 41, pp. 214-217, 2009.

[79] M. Petrtyl, J. Lisal, and J. Danesova, "Biomechanical Properties of Synovial Fluid in/Between Peripheral Zones of Articular Cartilage."

[80] D. Davies, "Paper 7: Properties of Synovial Fluid," in *Proceedings of the Institution of Mechanical Engineers, Conference Proceedings*, 1966, pp. 25-29.

[81] L. Cao, I. Youn, F. Guilak, and L. A. Setton, "Compressive properties of mouse articular cartilage determined in a novel micro-indentation test method and biphasic finite element model," *Journal of biomechanical engineering*, vol. 128, p. 766, 2006.

[82] D. Frisbie, M. Cross, and C. McIlwraith, "A comparative study of articular cartilage thickness in the stifle of animal species used in human pre-clinical studies compared to

articular cartilage thickness in the human knee," *Veterinary and Comparative Orthopaedics and Traumatology,* vol. 19, p. 142, 2006.

[83] J. Malda, K. Benders, T. Klein, J. de Grauw, M. Kik, D. Hutmacher, D. Saris, P. van Weeren, and W. Dhert, "Comparative study of depth-dependent characteristics of equine and human osteochondral tissue from the medial and lateral femoral condyles," *Osteoarthritis and cartilage,* 2012.

[84] C. W. McIlwraith, L. A. Fortier, D. D. Frisbie, and A. J. Nixon, "Equine models of articular cartilage repair," *Cartilage,* vol. 2, pp. 317-326, 2011.

[85] K. M. Dyce, W. O. Sack, and C. J. G. Wensing, *Textbook of veterinary anatomy*: Saunders, 2009.

[86] O. R. Adams and T. S. Stashak, *Adams' Lameness in horses*. Philadelphia: Williams & Wilkins.

[87] J. F. Burn, B. Portus, and C. Brockington, "The effect of speed and gradient on hyperextension of the equine carpus," *The Veterinary Journal,* vol. 171, pp. 169-171, 2006.

[88] H. Clayton, D. Sha, J. Stick, and D. Mullineaux, "Three-dimensional carpal kinematics of trotting horses," *Equine veterinary journal,* vol. 36, pp. 671-676, 2004.

[89] C. R. Chu, M. Szczodry, and S. Bruno, "Animal models for cartilage regeneration and repair," *Tissue Engineering Part B: Reviews,* vol. 16, pp. 105-115, 2010.

[90] B. Ahern, J. Parvizi, R. Boston, and T. Schaer, "Preclinical animal models in single site cartilage defect testing: a systematic review," *Osteoarthritis and cartilage,* vol. 17, pp. 705-713, 2009.

[91] Y. Merkher, S. Sivan, I. Etsion, A. Maroudas, G. Halperin, and A. Yosef, "A rational friction test using a human cartilage on-cartilage arrangement," ed: Parma, 2006.

[92] G. Verberne, Y. Merkher, G. Halperin, A. Maroudas, and I. Etsion, "Techniques for assessment of wear between human cartilage surfaces," *Wear,* vol. 266, pp. 1216-1223, 2009.

[93] W. C. Bae, M. M. Temple, D. Amiel, R. D. Coutts, G. G. Niederauer, and R. L. Sah, "Indentation testing of human cartilage: sensitivity to articular surface degeneration," *Arthritis & Rheumatism,* vol. 48, pp. 3382-3394, 2003.

[94] R. Sayles, T. Thomas, J. Anderson, I. Haslock, and A. Unsworth, "Measurement of the surface microgeometry of articular cartilage," *Journal of Biomechanics,* vol. 12, p. 257, 1979.

[95] A. Kerin, M. Wisnom, and M. Adams, "The compressive strength of articular cartilage," *Proceedings of the Institution of Mechanical Engineers, Part H: Journal of Engineering in Medicine,* vol. 212, pp. 273-280, 1998.

[96] J. S. Jurvelin, T. Räsänen, P. Kolmonens, and T. Lyyra, "Comparison of optical, needle probe and ultrasonic techniques for the measurement of articular cartilage thickness," *Journal of Biomechanics,* vol. 28, pp. 231-235, 1995.

[97] A. Swann and B. Seedhom, "Improved techniques for measuring the indentation and thickness of articular cartilage," *Proceedings of the Institution of Mechanical Engineers, Part H: Journal of Engineering in Medicine,* vol. 203, pp. 143-150, 1989.

[98] J. S. Jurvelin, T. Rasanen, P. Kolmonen, and T. Lyyra, "Comparison of optical, needle probe and ultrasonic techniques for the measurement of articular cartilage thickness," *J Biomech,* vol. 28, pp. 231-5, Feb 1995.

[99] A. C. Swann and B. B. Seedhom, "Improved techniques for measuring the indentation and thickness of articular cartilage," *Proc Inst Mech Eng H,* vol. 203, pp. 143-50, 1989.

[100] H. M. CLAYTON, J. Lanovaz, H. Schamhardt, and R. v. Wessum, "The effects of a rider's mass on ground reaction forces and fetlock kinematics at the trot," *Equine veterinary journal,* vol. 31, pp. 218-221, 1999.

[101] R. Murray, C. Zhu, A. Goodship, K. Lakhani, C. Agrawal, and K. Athanasiou, "Exercise affects the mechanical properties and histological appearance of equine articular cartilage," *Journal of Orthopaedic Research,* vol. 17, pp. 725-731, 1999.

[102] P. J. Roughley and R. White, "Age-related changes in the structure of the proteoglycan subunits from human articular cartilage," *J Biol Chem,* vol. 255, pp. 217-224, 1980.

[103] J. M. Mansour, "Biomechanics of cartilage," *Kinesiology: the mechanics and pathomechanics of human movement,* vol. 2, pp. 66-79, 2004.

[104] P. Brama, J. Tekoppele, R. Bank, D. Karssenberg, A. Barneveld, and P. v. Weeren, "Topographical mapping of biochemical properties of articular cartilage in the equine fetlock joint," *Equine veterinary journal,* vol. 32, pp. 19-26, 2000.

[105] C. J. Pasquini, T. L. Spurgeon, and S. Pasquini, *Anatomy of Domestic Animals: Systemic and Regional Approach*: Sudz Publishing, 1992.

[106] R. C. Murray, M. V. Branch, C. Tranquille, and S. Woods, "Validation of magnetic resonance imaging for measurement of equine articular cartilage and subchondral bone thickness," *Am J Vet Res,* vol. 66, pp. 1999-2005, Nov 2005.

Appendix A: Student's *t*-test

Student's *t*-test compares the difference between two sets when the statistic follows a student's t distribution with the null hypothesis. Using this method, the actual difference between two means in variation of the data is determined. The procedure of the test is shortly described below.

First, calculate mean values of first and second set (m_1 and m_2). Then, calculate standard deviation (σ) and standard error (SE) of each set following equation A.1 and A.2.

$$\text{Standard Deviation: } \sigma^2 = \frac{1}{n}\sum_{i=1}^{n} {x_i}^2 - m^2 = \frac{1}{n}\sum_{i=1}^{n}(x_i - m)^2 \quad \text{(A.1)}$$

$$\text{Standard Error: } SE = \frac{\sigma}{\sqrt{n}} \quad \text{(A.2)}$$

where *n* is the number of replicate and *m* is the mean value.

Next, obtain combined standard deviation (σ_d) by equation A.3.

$$\text{Combined Standard Deviation: } \sigma_d = \sqrt{{SE_1}^2 + {SE_2}^2} \quad \text{(A.3)}$$

Calculate *t*-value with equation A.4.

$$t\text{-value: } t = \frac{|m_1 - m_2|}{\sigma_d} \quad \text{(A.4)}$$

Degree of freedom is calculated by equation A.5.

$$DOF = N_1 + N_2 - 2 \quad \text{(A.5)}$$

where N is the sample size.

With the degree of freedom, select a level of significance and read the tabulated t-value on the t-table that is available in literature. If the obtained t-value is greater than the tabulated one, the condition fulfills the requirement for the chosen level of significance. For example, if the selected level of significance is p=0.01 and the calculated t-value is greater than the tabulated number on the table, the difference between compared means is "highly significant." P-value is simply obtained using 'tdist' function in Microsoft Excel.

Appendix B: Equipment Specification

All stiffness and thickness measurements were performed by the Bruker UMT-3 Tribometer with a force sensor, DFM-2-1104. The available range and the resolution of the DFM-2 in force measurement are 0.2 to 20N (20g to 2kg) and 1mN (100mg), respectively. The information of company is provided below:

Center for Tribology Inc Bruker Nano Inc. 1717 Dell Ave., Campbell, CA 95008

Figure B.1: Bruker UMT-3 Tribometer

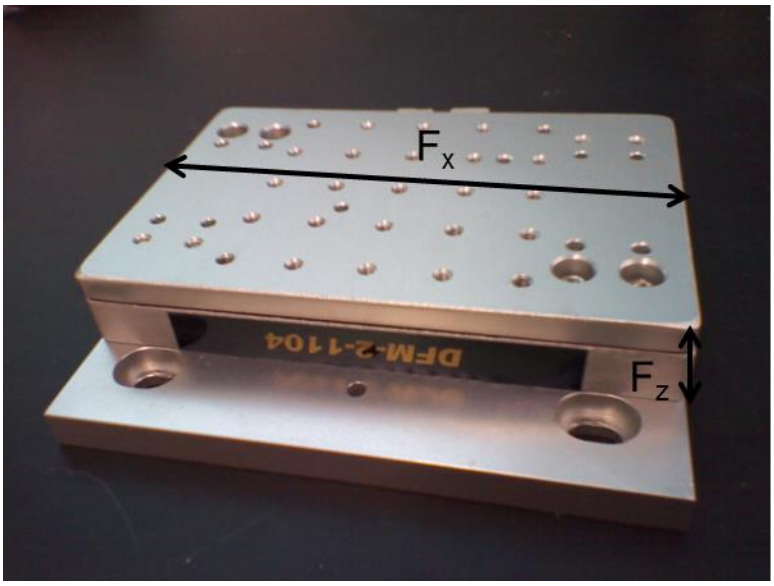

Figure B.2: DFM-2-1104 sensor

PrecisionGlide® 25 Gauge × 5/8 in. needle was used for the needle probe test. Its nominal outer diameter and inner diameter were 0.5144mm (0.02025in.) and 0.260mm (0.01025in.), respectively. Its length was15.88mm (0.625 in.).

Figure B.3: PrecisionGlide® 25 Gauge × 5/8 in. needle

For sample preparation, some equipment was employed. G0513P 17 Bandsaw was used for cutting the equine cartilage surface into sample size. The information of company is provided below:

Grizzly Industrial®, Inc. Bellingham Washington, 1821 Valencia St. Bellingham, WA 98229.

Figure B.4: Grizzly G0513P 17 Bandsaw

Stealth™ Safety Scalpels were used during entire dissection process. After dissection process, all samples were preserved in Irrigation Sodium Chloride 0.9% Solution manufactured by Baxter Healthcare.

Figure B.5: Stealth™ Safety Scalpels

Figure B.6: 0.9% Sodium Chloride Irrigation, USP

Appendix C: Horse Information

Table C.1: Information sheet of horses used in this work

No.	Date	Horse Name	Weight	Age
1	5/22/2012	Lucky	498.96kg	16
2	5/24/2012	Mel's Aristomatic	453.74kg	11
3	5/29/2012	Sunny	544.32kg	17
4	5/30/2012	GP	544.32kg	11
5	5/30/2012	TEX	535.248kg	14
6	6/7/2012	N/A	498.96kg	16
7	6/9/2012	Diamond	317.52kg	4
8	6/12/2012	Falkland	501.228kg	2
9	6/13/2012	Twisty	453.6kg	16
10	6/20/2012	Seven	498.96kg	18
11	6/20/2012	Generator	498.96kg	22
12	6/21/2012	Lacey	480.81kg	16
13	6/26/2012	Loki	453.6kg	12
14	9/5/2012	Rabbit	453.6kg	3
15	9/11/2012	Lizzie	408.24kg	17
16	9/20/2012	Splasy	517.1kg	11
17	10/3/2012	Dakota	453.6kg	10
18	10/5/2012	Shalia	408.24kg	13
19	11/28/2012	Cody	408.24kg	21
20	1/17/2013	Moheghan	392.36kg	17
21	1/30/2013	Chip	293kg	14
22	2/4/2013	A. Merose	N/A	6
23	2/12/2013	Judah	430.9kg	16
24	3/21/2013	Peppy Badger	408.24kg	17

Appendix D: Measurement Data

Table D.1: Raw data of stiffness measurement on the fetlock

Sample			**Coefficients**				**R-square**
Date	Joint	Test#	A	B	C	D	Fitting
5/24/2012 (Mel's)	RF Fetlock Lateral	2	82.36	12.51	1.272	0.01749	0.9977
		3	90.4	36.2	1.488	-0.01276	0.9997
5/29/2012 (Sunny)	RF Fetlock Lateral	1	1304	-118.9	11.09	-0.04419	0.9999
		2	1139	128.7	-3.183	0.06373	0.9998
		3	345.9	350.9	-2.238	0.0933	0.9999
5/30/2012 (GP)	RF Fetlock Lateral	1	339.6	-22.89	10.6	0.02534	0.9998
		2	671.2	32.48	6.127	0.04796	0.9998
		3	345.4	-7.816	10.22	0.02847	0.9998
5/30/12 (TEX)	RF Fetlock Lateral	1	1903	168.3	8.306	0.1164	0.9999
		3	4378	-118.1	4.092	0.2337	0.9992
6/7/2012 (Adult)	RF Fetlock Lateral	3	2057	-53.42	12.37	-0.04433	0.9999
6/7/2012	RF Fetlock Lateral	1	29.24	4.168	3.667	-0.00356	0.999
		3	145.9	6.178	4.53	0.03993	0.9997
6/9/2012 (Diamond)	RF Fetlock Lateral	1	2266	-255.5	16.17	-0.07173	0.9999
		2	2280	-307	17.49	-0.1332	0.9996
		3	2797	-213.4	12.11	-0.01331	0.9999
6/12/2012 (Falkland)	RF Fetlock Lateral	1	1496	-263.4	17.65	-0.08847	0.998
		2	1478	196.4	-12.7	0.2757	0.9995
		3	1972	-87.34	6.887	-0.01406	0.9999
6/13/2012	RF Fetlock Lateral	1	153.6	-11.47	1.973	0.009391	0.9987
		2	3828	-701.4	43.34	-0.4092	0.9912
		3	155	-6.149	5.958	0.04231	0.9996
6/20/2012 (Seven)	RF Fetlock Lateral	1	836.5	-168.3	21.17	-0.00045	0.9994
		2	439.1	-79.82	8.649	0.000266	0.9995
		3	283.7	-30.76	11.18	6.93E-05	0.9997

6/21/2012 (Lacey)	RF Fetlock Lateral	1	754.2	-51.02	17.5	0.0743	0.9999
		2	444.4	378.8	16.34	0.1553	1
		3	1914	-77.29	23.26	0.09789	0.9999
5/24/2012 (Mel's)	RF Fetlock Medial	1	279.7	40.97	6.68	-0.02383	0.9997
		2	825	-23.39	3.785	-0.01758	0.9999
		3	1065	-110.9	16.73	-0.1228	0.9989
5/29/2012 (Sunny)	RF Fetlock Medial	2	2112	-67.18	15.25	-0.01933	0.9998
		3	3474	-61.56	3.401	0.04673	0.9999
5/30/2012 (GP)	RF Fetlock Medial	3	120.9	51.35	7.74	0.02663	0.9999
5/30/12 (TEX)	RF Fetlock Medial	1	2375	-47.17	27.74	0.1478	0.9999
		2	1079	147.1	22.18	0.2148	0.9999
		3	272.5	-1.154	10.66	0.01606	0.9999
6/7/2012 (Adult)	RF Fetlock Medial	2	551.1	259.1	6.307	0.07718	0.9999
		3	441.2	132.5	5.8	0.04281	0.9999
6/7/2012	RF Fetlock Medial	3	331	91.43	15.36	-0.06045	1
6/9/2012 (Diamond)	RF Fetlock Medial	1	128.2	-21.82	2.026	-0.01525	0.9932
6/12/2012 (Falkland)	RF Fetlock Medial	1	2139	-327.5	19.2	-0.1217	0.9989
		2	964.4	-24.33	13.51	0.08405	0.9998
		3	228.1	18.87	9.494	-0.00701	0.9997
6/13/2012	RF Fetlock Medial	1	1216	-224.5	13.94	-0.1091	0.9857
		2	916.9	107.6	8.336	0.02021	1
		3	153.6	-11.47	1.973	0.009391	0.9987
6/20/2012 (Seven)	RF Fetlock Medial	1	1127	-193.8	18.32	0.000329	0.999
		2	1387	-235.2	20.31	-0.00056	0.9991
		3	998	-237	20.11	-0.00024	0.9987
6/21/2012 (Lacey)	RF Fetlock Medial	1	1551	105.4	69.78	0.1362	1
		2	324.3	440.2	28.56	0.2353	0.9999
		3	1671	131.6	26.43	0.1511	0.9999
5/22/2012 (Lucky)	RR Fetlock Lateral	1	118.1	4.798	1.753	-0.01246	0.9993
		3	208.7	-8.134	0.7276	-0.00442	0.999
5/30/2012 (GP)	RR Fetlock Lateral	1	1501	-46.58	8.456	0.01777	0.9999

		2	464.8	1082	-6.741	0.3872	0.9999
		3	3031	-149.5	13.78	0.02623	0.9998
5/30/12 (TEX)	RR Fetlock Lateral	1	695.8	159.2	5.4	-0.09082	0.9994
		2	2030	-34.97	44.52	0.01759	0.9996
		3	966.1	23.21	11.68	0.07009	0.9998
6/7/2012 (Adult)	RR Fetlock Lateral	1	3673	-645.1	82.49	-0.7089	0.9923
		3	1247	131.4	8.711	0.03532	1
6/7/2012	RR Fetlock Lateral	1	432.4	58.34	35.45	0.01647	0.9999
		2	461.6	205.4	17.63	0.0441	1
		3	217.9	-22.91	7.787	0.03622	0.9996
6/20/2012 (Generator)	RF Fetlock Lateral	1	941.6	305.1	8.192	0.001436	0.9999
		2	715.2	-6.933	27.1	-0.00112	0.9999
		3	1295	91.64	20.61	0.03146	0.9996
	RF Fetlock Medial	1	2146	136.9	21.13	0.000583	0.9998
		2	1788	531.9	-8.281	0.3367	0.9997
		3	257.9	812.2	7.844	0.2994	0.9999
	RR Fetlock Lateral	1	643.5	-83.56	17.72	-0.01988	0.9995
		2	2250	-403.6	25.79	0.01769	0.9998
		3	3884	-588.8	44.89	0.001089	0.999
	RR Fetlock Medial	1	1825	-375	31.14	0.00434	0.9989
		2	812.3	-198.4	21.02	0.000634	0.9949
		3	984	-224.1	24.41	-0.00065	0.9961
6/20/2012 (Seven)	RR Fetlock Lateral	1	2030	-245.7	25.3	0.003451	0.9999
		2	2352	-172	24.84	0.05851	0.9999
		3	1451	-10.45	23.18	0.000973	1
6/21/2012 (Lacey)	RR Fetlock Lateral	1	1750	-178	25.33	0.0486	0.9998
		3	3322	-105.7	32.72	0.0264	0.9999
5/22/2012 (Lucky)	RR Fetlock Medial	1	300.5	-19.59	1.801	0.00754	0.9995
		2	225	-43.28	8.419	-0.03561	0.9979
		3	191.7	16.51	7.702	-0.02012	0.9987
5/24/2012 (Mel's)	RR Fetlock Medial	3	329.5	-42.78	3.094	-0.02235	0.9981
5/30/2012 (GP)	RR Fetlock	1	2534	-145.9	25.65	0.03138	0.9999

	Medial						
		2	556.6	-21.42	11.83	0.0556	0.9999
		3	214	17.87	8.652	0.01182	0.9999
5/30/12 (TEX)	RR Fetlock Medial	1	6196	-959.5	55.45	-0.3407	0.9989
		2	1082	-140.5	16.04	-0.06911	0.9995
		3	750.1	-41.96	11.51	0.02128	0.9999
6/7/2012 (Adult)	RR Fetlock Medial	1	795.5	534.4	24.03	0.2935	0.9998
6/7/2012	RR Fetlock Medial	1	108.4	411.9	24.09	0.1325	1
		2	183.4	161.4	9.769	0.07656	0.9999
		3	352.9	78.66	9.071	0.1086	0.9999
6/9/2012 (Diamond)	RR Fetlock Medial	2	2021	-354.7	20.96	-0.1903	0.9944
		3	4252	-588.2	28.45	-0.1623	0.9994
6/20/2012 (Seven)	RR Fetlock Medial	1	1100	-151.8	26.13	0.007265	0.9999
		2	1350	-175	32.94	-0.00054	0.9998
		3	1611	-91.01	23.23	-0.00268	0.9999
6/21/2012 (Lacey)	RR Fetlock Medial	2	561.6	217.4	36.24	0.1591	1
		3	375.1	-24.3	14.67	0.07413	0.9999
6/26/12 (Loki)	RF Fetlock Lateral	1	117.7	-2.5	4.15	0.02824	0.9995
	RF Fetlock Medial	1	79.25	37.55	6.06	-0.01477	0.9998
		3	105.7	9.51	2.5	0.03892	0.9995
	RR Fetlock Lateral	1	470.8	7.249	-2.364	0.06108	0.9987
		2	589.9	-54.95	2.732	0.02273	0.9976
		3	320.2	-28.47	3.548	0.01438	0.9994
	RR Fetlock Medial	2	104.8	-3.962	2.632	0.01557	0.9989
9/20/12 (Splasy)	RF Fetlock Lateral	1	279	-26.59	3.49	-0.00437	0.9997
		2	-196.6	201.9	-1.096	0.09128	0.9998
		3	237.5	-3.995	8.113	0.00646	0.9999
	RF Fetlock Medial	1	-102.9	128.9	12.52	0.1028	0.9998
		2	-193	129.4	13.51	0.005593	1
		3	-159.4	117.8	14.12	0.007477	1
10/5/2012 (Shalia)	RF Fetlock Lateral	2	178.5	10.92	4.131	0.006775	0.9998

		3	80.67	4.294	4.756	0.016	0.9998
	RF Fetlock Medial	1	513.9	-43.38	2.394	0.02311	0.9987
		2	295	-21.59	4.046	-0.00067	0.9992
		3	5.352	45.84	1.835	0.01685	0.9999
	RR Fetlock Lateral	1	346.3	-19.63	1.824	0.02437	0.9987
		2	91.01	73.48	0.5738	0.04795	0.9998
	RR Fetlock Medial	1	116.5	2.417	2.472	0.009081	0.9998
		2	162.1	12.45	2.504	0.008695	0.9996
11/28/2012 (Cody)	LF Fetlock Lateral	1	-148.5	142	7.423	0.01174	1
		2	-405.2	206.9	22.84	-0.00864	1
		3	-277.4	179.1	9.852	0.0286	1
	LF Fetlock Medial	2	-104.9	117.5	7.079	0.03079	1
		3	61.19	34.81	3.405	0.01376	1
	LR Fetlock Lateral	1	-131.1	155.1	9.365	0.01619	1
		2	96.34	46.69	3.374	0.01603	1
		3	43.98	37.85	4.184	0.03981	0.9999
	LR Fetlock Medial	1	-93.33	123.6	15.67	0.03128	1
		2	-265	159.2	20.55	-0.00239	1
		3	71.29	96.73	2.099	0.05843	0.9999
1/17/13 (Moheghan)	LF Fetlock Lateral	1	159.5	12.44	5.1	0.01517	0.9999
		2	-89.12	128.6	3.473	0.05396	0.9999
		3	63.7	38.71	5.185	0.03741	0.9999
1/30/13 (Chip)	LR Fetlock Lateral	1	162.7	28.16	1.191	0.03916	0.9993
		2	-886.6	416.5	-3.221	0.09587	0.9998
		3	90.85	48.98	4.531	0.03106	0.9999
	LR Fetlock Medial	1	74.69	5.746	2.327	0.01708	0.9998
		2	263	-11.54	4.082	0.009233	0.9999
		3	315.7	-27.97	7.209	-0.00108	0.9999
		4	181.8	1.541	3.625	0.008241	0.9998
2/4/13 (A. Merose)	RF Fetlock Lateral	2	386.1	3.335	4.067	0.0117	0.9996
		3	327.4	-3.737	5.234	0.01137	0.9999
	RR Fetlock	1	10.2	115	0.918	0.05233	0.9998

	Lateral						
		2	-466.8	243.3	-1.17	0.06488	0.9997
	RR Fetlock Medial	1	124.1	-0.5707	1.37	0.01967	0.9997
		2	111.7	70.68	2.789	0.0226	1
		3	61.23	39.17	4.363	0.0239	0.9999
2/12/13 (Judah)	RF Fetlock Lateral	3	87.61	21.71	4.665	0.02424	0.9999
3/21/2013 (Peppy Badger)	RF Fetlock Medial	1	-221.9	249.9	-6.747	0.1773	0.9994
		2	-3.267	109	3.524	0.07511	0.9998
		3	69.38	31.52	5.289	0.02738	0.9999
	RR Fetlock Medial	1	-395.3	264.2	0.08199	0.09232	0.9999
		2	-60.02	108.4	11.58	0.05182	1
		3	126.8	26.44	8.197	0.03207	1
Average			818.84	7.1820	12.119	0.02318	0.999

Table D.2: Raw data of stiffness measurement on the carpus

Sample			**Coefficients**				**R-square**
Date	Joint	Test#	A	B	C	D	Fitting
5/22/2012 (Lucky)	Carpus1	1	798.3	443.4	25.44	-0.02285	1
		2	710.9	246.7	7.015	-0.07666	0.9997
		3	100.1	54.3	-2.92	0.03414	0.9992
5/30/2012 (GP)	Carpus1	1	4.867	19.11	-0.1216	0.000268	0.9964
		2	262.2	-24.89	3.213	0.0348	0.9989
		3	63.29	-0.0874	2.074	0.005313	0.9975
5/30/12 (TEX)	Carpus1	1	80.01	-4.721	2.244	-0.00756	0.9978
		2	129.1	-7.179	1.794	-0.00356	0.9985
		3	41.17	8.79	0.2219	0.000925	0.9956
6/7/2012 (Adult)	Carpus1	1	224.8	-32.09	4.042	0.006241	0.9984
		3	1065	-148.2	10.14	-0.04593	0.9992
		4	1310	-149	9.425	-0.02623	0.9998
6/9/2012 (Diamond)	Carpus1	1	1380	-48.93	18.68	-0.00071	0.9999
		2	841.4	278.1	-6.639	0.1758	0.9997
		3	1229	-159.3	9.496	-0.05374	0.9996

		4	1423	-107.6	4.599	0.02581	0.9997
6/12/2012 (Falkland)	Carpus1	1	235.8	-3.553	4.69	-0.00138	0.9997
		3	612.7	-11.71	8.649	-0.06278	0.9999
6/20/2012 (Seven)	Carpus1	1	693.7	-93	11.77	0.001817	0.9999
		2	998	-108.6	10.85	0.00157	0.9999
		3	726.2	-111.5	15.24	-0.00173	0.9999
6/21/2012 (Lacey)	Carpus1	1	398	-14.96	20.27	0.1118	0.9999
		2	552.2	652.8	38.26	0.1696	1
		3	1532	119.5	28.1	0.1445	1
5/24/2012 (Mel's)	Carpus2	3	250.9	20.3	8.208	-0.06492	0.9996
5/30/2012 (GP)	Carpus2	2	25.38	-0.725	0.7428	0.013	0.9828
5/30/12 (TEX)	Carpus2	2	1860	-70.03	-3.33	0.07481	0.9989
		3	59.17	10.09	2.813	0.0121	0.9993
6/7/2012 (Adult)	Carpus2	2	48.25	-5.733	1.905	0.006185	0.9954
6/9/2012 (Diamond)	Carpus2	1	146.9	-8.374	1.901	0.0124	0.9988
		2	797.2	-7.731	9.5	-0.00506	0.9999
		3	214.8	-5.286	4.227	0.007411	0.9997
6/12/2012 (Falkland)	Carpus2	1	61.77	-9.237	2.485	0.02377	0.9939
		4	80.91	-11.07	5.122	0.01061	0.9986
6/20/2012 (Seven)		2	581.6	508.3	0.6125	0.1833	0.9999
6/21/2012 (Lacey)	Carpus2	1	198.7	-9.205	7.452	0.05626	0.9997
		2	296.8	-7.453	10.15	0.05913	0.9999
		3	821.5	-17.9	17.36	0.04596	0.9999
5/22/2012 (Lucky)	Carpus3	2	379.2	12.71	-3.348	0.05749	0.9963
		3	568.2	-55.64	3.246	-0.00358	0.9996
5/24/2012 (Mel's)	Carpus3	1	276.5	34.71	4.183	0.0104	0.9999
		2	94.91	14.47	1.215	0.01548	0.9994
		3	170.4	11.35	0.6649	0.03129	0.9994
5/30/2012 (GP)	Carpus3	2	69.95	-6.118	2.149	0.0277	0.9968
		3	125.7	-7.954	3.481	0.01327	0.999
6/7/2012 (Adult)	Carpus3	2	159	-8.777	4.53	0.004424	0.9995
		4	165	-4.148	4.33	0.005114	0.9996
6/9/2012 (Diamond)	Carpus3	3	15.19	20.82	1.49	0.0186	0.9985
		4	285.1	-24.13	2.344	0.01781	0.9994
6/12/2012 (Falkland)	Carpus3	1	14.9	-0.2241	0.8957	0.01073	0.9823
		3	20.97	-1.063	0.594	0.01232	0.9764
6/20/2012 (Seven)	Carpus3	1	247.3	-16.06	7.625	2.56E-05	0.9998
		2	395.2	-53.8	14.34	0.001956	0.9998
		3	237	-39.38	10.54	-0.00035	0.9997
5/22/2012 (Lucky)	Capus4	2	1811	-208.8	15.11	-0.1295	0.9993
5/30/2012 (GP)	Carpus4	3	280.1	-9.507	12.04	0.02274	0.9997
5/30/12 (TEX)	Carpus4	1	175.3	-12.65	1.915	-0.00696	0.9977

		2	57.79	12.62	0.1515	-0.00307	0.9981
		3	4.719	6.908	-0.3795	0.002041	0.976
6/9/2012 (Diamond)	Carpus4	2	15.42	-1.819	0.8929	0.004701	0.9782
6/12/2012 (Falkland)	Carpus4	2	46.46	-3.797	1.861	0.02485	0.9954
		3	105.5	-6.162	3.823	0.02825	0.9992
		4	106.5	-1.408	3.433	-0.0027	0.9993
6/20/2012 (Seven)	Carpus4	3	372.2	-19.62	14.95	-0.00043	0.9998
9/20/12 (Splasy)	Carpus3	2	100.6	20.32	2.524	0.01516	0.9999
		3	79.24	37.07	1.779	0.0171	0.9998
11/28/2012 (Cody)	LCarpus1	1	194.6	-14.97	3.3	0.01219	0.9998
		2	148.1	-14.62	4.007	0.01543	0.9999
		3	24.1	51.44	4.279	0.03842	0.9999
	LCarpus2	2	16.72	0.2241	1.524	0.009117	0.9992
		4	28.41	4.343	2.238	0.008481	0.9998
	LCarpus3	1	35.77	-1.87	1.872	0.006771	0.9996
		2	27.32	-1.146	2.001	0.007525	0.9996
		3	10.94	0.5667	1.187	0.003571	0.9991
	LCarpus4	1	24.34	22.02	2.817	0.01747	0.9999
		2	19.77	4.034	2.225	0.008651	0.9998
1/17/13 (Moheghan)	LCarpus1	1	225.8	-24.12	3.111	0.009018	0.9979
		3	207.5	19.73	6.449	0.01708	1
	LCarpus2	3	242.6	6.228	3.143	0.02218	0.9998
	LCarpus3	3	44.85	-3.323	2.283	0.01206	0.9996
	LCarpus4	1	119.9	-6.134	2.176	0.01253	0.9997
		2	133.5	10.8	3.521	0.02652	0.9999
		3	57.05	39.17	2.756	0.02945	0.9999
2/4/13 (A Merose)	Carpus1	1	75.88	-3.17	7.822	0.003045	0.9998
		2	-119.4	82.79	6.179	0.02117	0.9999
		3	-117.8	82.03	6.286	0.02417	0.9999
	Carpus2	1	75.46	-8.983	1.991	0.006154	0.9996
		2	21.72	6.062	1.727	0.007992	0.9998
		3	20.84	1.1	1.365	0.004374	0.9994
2/12/13 (Judah)	LCarpus1	1	64.27	72.22	5.859	0.02539	1
		2	-121	139.2	11.22	0.0139	1
	LCarpus2	1	23.65	30.87	-0.2336	0.02651	0.9997
		2	110.8	15.71	2.461	0.01935	0.9999
	LCarpus3	1	-170.9	114.3	15.97	-0.01093	0.9998
		2	-211.8	217.8	-1.581	0.1212	0.9998
	LCarpus4	1	85.17	-3.227	4.87	-0.00435	0.9998
		2	23.71	26.16	6.833	0.01318	1
		3	68.25	20.86	8.342	0.02068	0.9999

	Carpus2	1	145.5	-17.39	3.873	0.002738	0.9976
		2	60.73	15.68	4.443	0.02016	0.9999
		3	81.55	21.19	4.422	0.02477	0.9999
	Carpus3	1	196.4	56.15	3.361	0.06028	0.9998
		2	-208.1	195.5	4.904	0.08026	0.9999
		3	-102.6	142.3	12.94	0.07599	0.9999
	Carpus4	1	-315.1	249.5	-0.5229	0.08691	0.9999
		2	261.3	14.9	8.239	0.0259	0.9999
		3	350.4	-42.03	3.33	0.02363	0.9992
3/21/2013 (Peppy Badger)	Carpus1	1	120.1	63.16	1.224	0.06689	0.9997
		2	-238.8	184.8	-1.167	0.0627	0.9999
		3	-537.1	307.9	-5.689	0.0818	0.9999
	Carpus2	1	118.9	-3.541	4.983	0.05014	0.9996
		2	115.1	6.961	7.369	0.02434	1
		3	135.1	14.14	4.782	0.01785	0.9999
	Carpus4	2	83.22	0.03374	5.179	0.01795	0.9999
		3	101.1	-5.359	3.369	0.01506	0.9999
Average			252.11	25.767	5.2617	0.02021	0.99842

Table D.3: Raw data of stiffness measurement on the stifle

Sample			**Coefficients**				**R-square**
Date	Joint	Test#	A	B	C	D	Fitting
10/3/12 (Dakota)	Rstifle	1	17	-3.722	2.285	0.005262	0.9977
		2	3.922	4.588	2.081	0.007347	0.9987
10/5/2012 (Shalia)	Rstifle	1	40.86	7.311	2.812	0.02091	0.9996
		2	18.77	8.247	3.948	0.02163	0.9997
11/28/2012 (Cody)	Lstifle	1	5.531	-2.453	1.552	0.00658	0.9978
		2	39.41	-0.9177	0.8332	0.01005	0.9979
		3	6.333	1.145	2.191	0.007188	0.9996
		4	7.001	-0.6603	1.591	0.007954	0.999
	Rstifle	1	13.73	2.848	1.254	0.009691	0.9994
		2	-8.18	9.571	0.8795	0.008843	0.9993
		3	0.1432	6.168	1.096	0.009963	0.9985
1/30/13 (Chip)	LStifle	2	23.55	-0.395	1.82	0.007601	0.9994
		3	23.19	-0.3316	1.81	0.007344	0.9993

2/4/13 (A Merose)	Rstifle	2	24.4	-2.072	1.798	0.006156	0.999
		3	19.4	-0.7816	1.409	0.006921	0.9988
3/21/2013 (Peppy Badger)	Rstifle	3	6.513	-1.651	1.198	0.001866	0.9979
Average			15.098	1.6808	1.7849	0.00908	0.99885

Table D.4: Raw data of thickness measurement on the fetlock

Sample		**LF Fetlock Lateral (mm)**	**LF Fetlock Medial (mm)**	**LR Fetlock Lateral(mm)**	**LR Fetlock Medial (mm)**
Horse Name	Test#				
Lucky	2	0.6185	0.5975	-	-
	3	0.8697	0.7260	-	-
Mel's	1	0.6289		-	-
	2	0.7260	0.7312	-	-
	3	0.8380	0.7193	-	-
	4	0.9454	0.6324	-	-
	5	0.7020	0.7633	-	-
Sunny	1	0.5888	0.6143	-	0.8394
	2	0.5866	0.6683	-	-
	3	0.7729	0.7612	-	0.7960
	4	0.8295	0.6206	-	1.0350
	5	0.5225	-	-	0.9101
TEX	1	-	0.6359	1.1284	0.5285
	2	0.6885	0.7460	0.7629	0.6576
	3	0.7015	0.7315		0.7831
	4	0.6618	0.7003	0.7705	0.4433
	5	-	0.9710	0.6234	0.9774
GP	1	1.2235	1.1264	0.6939	0.8394
	2	0.9775	1.3231	0.5576	0.7671
	3	0.9071	1.0439	0.8205	1.0204
	4	1.0060	-	0.9508	1.0118
	5	1.4819	-	1.3020	0.8546
Falkland	1	0.7429	0.9405	0.9719	-
	2	0.9330	0.9990	1.0034	1.2459
	3	1.2409	-	1.0472	1.2090
Skipper's	1	0.6207	0.8701	0.6207	0.8701
	2	0.6020	0.6698	0.6020	0.6698
	3	0.6198	0.9126	0.6198	0.9126
	4	0.6498	0.6038	0.6498	0.6038

	5	0.7066	0.8790	0.7066	0.8790
Splasy	1	0.7623	0.9292	-	-
	2	0.8709	0.9045	-	-
	3	0.8963	0.7943	-	-
	4	0.7929	0.7770	-	-
	5	0.7888	0.7632	-	-
Dakota	1	0.8730	0.8720	-	-
	2	1.0588	0.9082	-	-
	3	1.0701	0.8168	-	-
	4	0.9389	0.8604	-	-
	5	0.8640	0.9314	-	-
Shalia	1	1.1458	1.0052	0.9100	0.8870
	2	0.8572	0.7329	1.0015	0.9383
	3	0.7747	0.7025	1.0600	0.9867
	4	0.8512	0.7725	1.1338	0.9436
	5	0.9340	0.8289	1.2051	0.9333
Chip	1	1.1919	0.8553	-	-
	2	0.8172	0.8043	-	-
	3	0.6990	0.8455	-	-
	4	0.7110	0.8525	-	-
	5	0.8068	0.8429	-	-
Judah	1	0.9754	0.7683	0.7373	0.6745
	2	0.8115	0.6103	0.6483	0.5704
	3	0.8222	0.5521	0.6661	0.5585
	4	0.8146	0.5495	0.6479	0.6053
	5	0.7605	0.5365	0.7888	0.8955
Average		0.9216	0.9861	0.8035	0.7627

Table D.5: Raw data of thickness measurement on the carpus

Sample		**Carpus1 (mm)**	**Carpus2 (mm)**	**Carpu3 (mm)**	**Carpus4 (mm)**
Horse Name	Test#				
Lucky	1	0.5975	0.625	0.747	0.6651
	2	0.6861	0.7244	0.6313	-
	3	0.5267	0.493	0.5605	0.3606
Mel's	1	0.9084	0.9559	-	0.5805
	2	0.8244	0.9798	0.5560	0.4704
	3	1.0634	0.9774	0.9040	0.7162

	4	0.9841	1.4043	0.7070	0.5579
	5	1.3500	-	0.6739	0.6004
Sunny	1	1.0300	0.4559	0.4210	0.4459
	2	0.7258	-	0.6000	0.5729
	3	-	0.9655	0.5985	0.5016
	4	-	0.8190	-	0.4619
	5	0.7082	0.6601	0.7896	-
TEX	1	0.9829	0.7719	0.5670	-
	2	0.7675	0.8114	0.6275	0.6406
	3	0.7218	0.8360	0.6600	-
	4	0.6781	0.8351	0.5385	0.6072
	5	0.7575	0.8835	-	0.3725
GP	1	1.0310	1.0500	0.9215	0.9818
	2	1.0850	1.4979	-	-
	3	0.9585	1.4086	1.1519	-
	4	1.2506	1.2310	-	-
	5	-	1.0801	0.9664	0.8896
Falkland	1	-	0.8568	0.9141	-
	2	0.8009	0.6915	0.8754	0.7640
	3	0.9756	-	0.7487	-
	4	0.8977	-	0.8781	-
Skipper's	1	0.7998	0.7247	0.6346	0.8340
	2	0.6952	0.8118	0.6165	0.7843
	3	0.8317	0.6537	0.8854	0.5819
	4	0.7742	0.9837	0.7135	0.7084
	5	0.8592	0.5680	0.8918	0.4769
Splasy	1	0.8806	1.1358	0.7083	-
	2	0.9064	0.9940	0.6890	-
	3	0.8833	1.0565	0.7447	-
	4	0.7873	0.9523	0.8947	-
	5	0.7840	0.7913	0.6653	-
Shalia	1	1.1748	0.9845	0.8575	0.8483
	2	1.0038	1.0625	0.9225	0.9233
	3	0.6658	1.1028	-	0.9605
	4	0.9545	1.3494	0.9946	1.0198
	5	0.8664	1.5167	0.8314	1.0935
Judah	1	0.6750	0.9834	0.5908	0.9167
	2	0.6302	0.7714	0.5410	0.7889
	3	0.8141	0.5587	0.4673	0.9409
	4	0.8610	0.8219	0.3787	1.1244
	5	0.6917	1.2723	0.4873	1.3135
Average		0.8708	0.8135	0.8929	0.8654

Table D.6: Raw data of thickness measurement on the stifle

Sample		Stifle (mm)
Horse Name	Test#	
Lucky	1	1.8448
	2	1.3503
	3	2.0973
Mel's	1	2.4935
	2	2.8575
	3	2.6901
	4	2.7605
	5	2.6306
Sunny	1	2.1525
	2	2.4450
	3	1.9650
TEX	1	1.4788
	2	2.3550
	3	2.1582
	4	2.1973
	5	2.5797
GP	1	0.7869
	2	0.7373
	3	1.4765
	4	1.6985
	5	2.6586
Falkland	1	-
	2	2.5975
	3	1.3628
Skipper's	1	1.4381
	2	1.6308
	3	1.2146
	4	1.8711
	5	1.1673
Dakota	1	2.2678
	2	2.2385
	3	2.2540
	4	2.2114
	5	2.2560
Shalia	1	2.6181
	2	2.5265
	3	2.7490
	4	2.8159
	5	3.0288
Chip	1	2.0601

	2	2.5430
	3	2.7129
	4	2.6400
	5	2.4235
Average		2.1466